

University of Nottingham
UK | CHINA | MALAYSIA

Keeping the balance - importance of balanced hippocampal neural activity for attention and memory

Miriam Gwilt, BSc

Thesis submitted to the University of Nottingham for the degree of

Doctor of Philosophy

November 2020



Biotechnology and Biological Sciences Research Council



Boehringer Ingelheim

Thesis Abstract

Hippocampal neural disinhibition, i.e. decreased GABAergic control, has been implicated in neuropsychiatric disorders, including schizophrenia and age related cognitive decline, and cognitive impairments associated with these conditions. Previous work within our lab has demonstrated that infusion of the GABA-A antagonist picrotoxin into the ventral hippocampus causes marked increases in local multi-unit activity in anaesthetised rats, and causes both memory and attentional deficits akin to those seen in patients with schizophrenia and age-related cognitive decline (McGarrity et al. 2017). Alterations in normal neuronal oscillations are often seen in such clinical conditions, however the underlying pathology leading to such changes is still largely unknown (Schnitzler and Gross, 2005; Ulhaas and Singer, 2015). Furthermore, current pharmacological treatments for such disorders are limited in efficacy and, this leaves a large impact on patients (Maric et al. 2016; Breier 2005). Recently, the second-generation anti-epileptic drug levetiracetam has shown promise, at low doses, for ameliorating cognitive impairments related to hippocampal hyperactivity in both rodents and patients (Haberman et al. 2017; Koh et al. 2010, Bakker et al. 2012). Therefore, our two main aims were to assess the impact of our hippocampal disinhibition model on oscillatory activity within the brain, and to determine if low doses of levetiracetam are able to alleviate the neuro-behavioural impact of hippocampal disinhibition.

First, we analysed the hippocampal local field potential (LFP) data from within the vicinity of the infusion site, which was recorded in conjunction with the previously published multi-unit data in anesthetised rats (McGarrity et al. 2017). To this end, we developed a novel semi-automated routine to separate three distinct LFP states seen under anaesthesia (Burst, Suppression, and Continuous), so that frequency analysis could be run without interference from state-specific properties (see Chapter 2 for details). Overall, we showed that hippocampal picrotoxin infusion caused an increase in theta power, tended to decrease high beta/low gamma power, and decreased high beta/low gamma connectivity (Chapter 2). In a further study, we examined the impact

of hippocampal disinhibition on both the hippocampal LFP, frontal electroencephalogram (EEG) and heart rate variability (HRV) in unanaesthetised rats, by combining our hippocampal picrotoxin infusions with a telemetric-EEG (tEEG) protocol used by our industry partners at Boehringer Ingelheim (Chapter 3). These data revealed that, contrasting with our anaesthetised recordings (Chapter 2), hippocampal disinhibition had no effect on hippocampal theta power, but decreased hippocampal high beta/low gamma LFP power, confirming the trend seen previously. We saw limited effects on both the frontal EEG and the HRV. Overall, our studies assessing the oscillatory changes within the hippocampus after hippocampal disinhibition reveal a consistent decrease of power in the high beta/low gamma frequencies, which may be relevant to findings in schizophrenia and mild cognitive decline (Schnitzler and Gross, 2005).

Secondly, to see if levetiracetam could ameliorate the neuro-cognitive impact of hippocampal disinhibition, we examined if systemic levetiracetam treatment could ameliorate the electrophysiological and some of the cognitive/behavioural effects caused by hippocampal disinhibition (Chapters 4-6). Initially, using multi-unit recordings under anaesthesia, we replicated previous findings (McGarrity et al., 2017) that hippocampal picrotoxin (150ng) enhances hippocampal burst firing. Levetiracetam selectively attenuated the increased burst duration at 10mg/kg (i.p.), but not 50mg/kg; 50mg/kg slightly reduced the peak frequency in bursts under baseline conditions (Chapter 4). Furthermore, 10mg/kg, but not 50mg/kg, ameliorated the decreased high beta/low gamma hippocampal LFP power induced by hippocampal disinhibition (Chapter 5). Based on these findings, we used 10mg/kg for the behavioural studies. We replicated previous findings (Bast et al., 2001; McGarrity et al., 2017) of increased locomotor activity in the open field and decreased search preference in the DMP watermaze task following hippocampal picrotoxin infusion. Levetiracetam (10mg/kg) numerically attenuated both locomotor hyperactivity and search preference in the DMP watermaze, although these beneficial effects failed to achieve criteria of statistical significance (Chapter 6). Overall, a low dose (10 mg/kg) of levetiracetam showed a trend towards ameliorating electrophysiological changes

caused by hippocampal disinhibition; however, this was not sufficient to ameliorate the memory impairments and locomotor hyperactivity associated with hippocampal disinhibition.

We showed that hippocampal disinhibition causes a local decrease in high beta/low gamma frequencies in both anesthetised and unanaesthetised rats, and an increase in theta frequencies of anaesthetised rats only. Furthermore, levetiracetam 10mg/kg was able to restore normal high beta/low gamma frequencies, and the burst duration multi-unit parameter, with limited ameliorative effect on locomotor hyperactivity and memory impairment in the DMP watermaze.

Acknowledgements

The work within this thesis was funded by a BBSRC iCASE PhD studentship in collaboration with Boehringer Ingelheim, and conduced at the University of Nottingham and Boehringer Ingelheim (Biberach).

First and foremost, a huge thank you to Tobias Bast, the best PhD supervisor one could ask for! Thanks for all of the teaching, guidance and trust you gave me throughout my PhD, and thank you for creating such an enriching and relaxing research environment. Thank you also to Markus Bauer for the invaluable guidance on all things MATLAB and LFP analysis; thanks for your patience at the beginning as I found my feet, and for imparting a small portion of your knowledge!

Thanks also go out to the rest of team SMARTs: to Adam and Rebecca showing me the ropes, Stu being my coffee, pointless and thesis buddy, and to all three for keeping me just about sane enough to make it through (as well as all the help on the science side!). Also to our relatively newer recruits Charlie, Jacco and Joanna, thank you for helping when everyone else had abandoned me (!) and for providing me many different training experiences! A final team SMARTs shout out to Charlie (and on call Sara and Adam) for your help with the covid-induced-intensity of the final watermaze experiment, I honestly cannot thank you enough.

Thanks to everyone at Boehringer Ingelheim for welcoming me during my time in Biberach. Thanks to Boris Ferger for arranging everything and welcoming me to Germany. A particular thanks to Henrike Raith for showing me how everything worked, helping with the experiments and planning, and for making me feel welcome in a foreign country, all whilst writing her own thesis! Finally, thanks to Patrizia, Holger, Ting-Ting, and Virginia.

Additional thanks to the various other people who have made my work possible in Nottingham. Thanks to Dave Watson and Clare Spicer for looking after the ephys, behavioural and surgical suites, for providing help whenever I needed. Thanks to the

staff in the BSU for looking after all of the rats, particular thanks goes to Mark and Helen.

Finally, thanks to all the people in my life who supported me throughout these four and a bit years. Thanks to all my family for uplifting and believing in me, to the Fellowship of da Bling for giving me much needed relief in the form of board-games, and finally to Adam who is included far too much already but who really has been my rock throughout the thesis writing process!

Contents

Abstract ……..1

Acknowledgements …… 4

Chapter 1: Thesis Introduction …… 8

Aims of PhD project…….…… 18

Chapter 2: Frequency- and state-dependent effects of hippocampal neural disinhibition on hippocampal local field potential oscillations in anesthetized rats

Abstract ……20

Introduction ……..... 21

Methods …….. 27

Results …… 37

Discussion …….. 45

Chapter 3: Frequency- and vigilance state-dependent effects of hippocampal neural disinhibition on hippocampal local field potential and frontal EEG oscillations, and heart-rate variability, in freely moving rats

Introduction …… 55

Methods ……...59

Results ……..... 67

Discussion ……..… 76

Chapter 4: Can levetiracetam ameliorate the aberrant hippocampal neural activity induced by hippocampal disinhibition?

Introduction ……..…… 82

Methods ……..…. 85

Results …… 92

Discussion …….. 98

Chapter 5: Can levetiracetam ameliorate the LFP-changes induced by hippocampal disinhibition?

Introduction ……..…….. 107

Methods ……..…… 108

Results …… 109

Discussion …….. 115

Chapter 6: Can levetiracetam ameliorate the behavioural changes induced by hippocampal disinhibition?

Introduction ……..…….. 123

Methods ……..…… 124

Results……..…… 130

Discussion ……..…… 135

Chapter 7: General discussion and conclusions

Discussion ……..…… 140

Conclusions ……..…… 146

References ……..…….. 147

Appendices

Appendix 1: Published Work …… 175

Appendix 2: Additional Work …… 176

Chapter 1: General Introduction

Hippocampal neural disinhibition, i.e. reduced GABAergic inhibition, has been implicated in several clinical conditions, such as schizophrenia and age-related cognitive decline (see *Hippocampal disinhibition and schizophrenia* and *Hippocampal Disinhibition and Age-related cognitive decline/Alzheimer's Disease*) and causes attentional and memory deficits in rats (see *Disinhibition in the hippocampus*). Neural oscillations are driven in part by GABAergic signalling, and are often altered in such clinical conditions (see *Neural oscillations, as revealed by local field potentials and electroencephalogram*), therefore, establishing alterations in oscillations in rat disinhibition models provides greater translatability to clinical conditions. Furthermore, current treatments for such conditions are limited in efficacy, which combined with the time taken to develop novel compounds leaves a large impact on patients (Maric et al. 2016; Breier 2005). Recently, the second generation anti-epileptic drug levetiracetam has shown promise for reversing cognitive impairments associated with age-related hippocampal hyperexcitability (see *Levetiracetam: A potential ameliorative agent for neural disinhibition?*). This drug may also be suitable to ameliorate neuro-behavioural effects caused by hippocampal neural disinhibition.

Neural Disinhibition

Neural disinhibition, resulting from decreased inhibitory control, results in an imbalance of excitation and inhibition within the brain (McGarrity et al. 2017; Krystal et al. 2017). This balance is maintained mostly by glutamate, the primary excitatory neurotransmitter, and gamma-aminobutyric acid (GABA), the primary inhibitory neurotransmitter. During normal physiological conditions small fluctuations in balance allow for normal function; the excitation allows stimulus response in the brain while the inhibition drives selectivity of which stimuli to process (Letzkus et al. 2015). With a loss of GABAergic signalling, i.e. neural disinhibition, the excitation is more dominant and therefore there is a decrease in the selectivity of stimuli processed. Extreme neural disinhibition in cortical and subcortical brain areas can cause epileptic-like

seizure activity due to too much activity in the brain (Foss-Feig et al. 2017). However, subconvulsive neural disinhibition has been implicated in many disorders which feature cognitive impairments, such as schizophrenia and age-related cognitive decline, and has been suggested a contributing factor to the cognitive deficits (Heckers and Konradi 2015; Bast et al. 2017; McGarrity et al. 2017; Foss-Feig et al. 2017; Marín 2012; Murray et al. 2014).

Disinhibition in the hippocampus

The hippocampus plays an important role in memory and has also been linked to other cognitive and behavioural functions (Bast 2007; Bast 2011). Hippocampal GABA dysfunction has been implicated in disorders characterised by cognitive impairments, such as schizophrenia and age-related cognitive decline (Bast et al., 2017). More recently, studies using subconvulsive manipulations of hippocampal GABA, i.e. disinhibition by picrotoxin (PTX), a GABA-A antagonist, in rat models have provided some direct evidence that hippocampal GABA dysfunction can cause clinically relevant cognitive impairments (McGarrity et al., 2017).

Hippocampal disinhibition and schizophrenia

There is compelling evidence for dysfunction of the GABAergic system in the hippocampus in schizophrenia; post mortem studies have shown that the overall number of GABAergic interneurons in the hippocampus is decreased (Reynolds et al., 1990; Benes & Berreta, 2001; Konradi et al., 2011) and that various GAD genes, which are responsible for synthesizing GABA, are downregulated (Ruzicka et al. 2015; Zhang et al. 2009). Whereas, GABA-A receptors are upregulated, probably reflecting a compensatory effect (Benes & Beretta, 2001; Heckers & Konradi, 2015). Consistent with such hippocampal disinhibition, functional imaging studies have found increased hippocampal activity in patients with schizophrenia at rest, especially at early stages of the disorder (Lieberman et al. 2018; Schobel et al. 2009; Schobel et al. 2013; Heckers 2001). Additionally, magnetic resonance imaging (MRI) studies have consistently shown a marked decrease in hippocampus volume in patients with

schizophrenia (Lawrie & Abukmeil 1998), which may be as a result of excitotoxicity from increased glutamate levels (Schobel et al. 2013; Kraguljac et al. 2013). Furthermore, NMDA glutamate receptor dysfunction has been shown in schizophrenia (Gao et al. 2000). For example, post-mortem tissue from patients with Schizophrenia show various NMDA receptor markers are decreased in the hippocampus, and taking NMDAR antagonists leads to psychosis and other Schizophrenia like symptoms in humans and animals (Coyle 2012; Snyder and Gao 2013). The disruption of NMDA receptor function in the hippocampus may lead to decreased activation of the GABAergic interneurons, with in vitro evidence suggesting NMDA receptor blockage disrupts hippocampal inhibitory mechanisms (Grunze et al. 1996). This decreased activation results in reduced GABA release, causing decreased inhibition of the glutamatergic system leading to an overall increase in activity, a.k.a. disinhibition (Bast et al. 2017; Olney et al. 1999; Heckers & Konradi 2015; Lewis & Moghaddam 2006). This type of disruption has been linked to the cognitive deficits that are seen in Schizophrenia (Lewis & Moghaddam 2006; O'Donnell 2011; McGarrity et al. 2017; Lewis et al. 2012).

Hippocampal Disinhibition and Age-related cognitive decline/Alzheimer's Disease

The decrease in memory during age-related cognitive decline and early stages of Alzheimer's disease have been suggested to be partly due to an increase in excitatory signalling due to inhibitory interneuron loss (Nava-Mesa, 2014, Stanley et al. 2012). There are several studies, both in vitro and in vivo, which show that in the presence of amyloid-β plaques the hippocampus displays hyperexcitability due to altered GABAergic signalling and interneuron dysfunction, which correlates with decreased memory (eg. in watermaze studies) (Busche et al. 2012; Abramov et al. 2009; Busche et al. 2008; Lei et al. 2015; Hazra et al. 2013). Interestingly, in one study the hyperexcitability effects from amyloid-β, measured by increased amplitude of population spiking, were replicated with picrotoxin (Lei et al. 2015). Additionally, patients with epilepsy present with memory loss in mild cognitive impairment and

Alzheimer's Disease earlier than those without epilepsy, which has been suggested to be due to a reduction in GABAergic signalling (Vossel et al. 2013; Scharfman 2012). Although this evidence provides association between hippocampal GABA dysfunction and memory impairments, direct evidence of clinical hippocampal neural disinhibition is limited.

Picrotoxin - mechanism of action

PTX is a naturally occurring plant toxin that causes inhibition of GABA receptor currents by antagonising GABA-A receptors non-competitively. PTX is not a structural analogue of GABA so binds to a separate binding site within the pore of the channel. Once GABA is bound to the receptor it causes a conformational change which results in increased likelihood of PTX binding and exerting its blocking effect. PTX has been shown to leave unaltered the characteristics of the current that passes through the channel (i.e. amplitude, duration), causing only a decrease in frequency of openings (Yoon et al. 1993). In addition to PTX's main action on the GABA-A receptor, it has also been shown to inhibit other channels from within the ligand-gated ion-channel group, including Glycine and 5-HT3A, although PTX has 10-fold less affinity for these receptors than for GABA-A (Das & Dillon 2005). While 5-HT3A receptors are located on and inhibit hippocampal interneurons, glycine receptors are found on both interneurons and pyramidal cells where they cause inhibition in a modulatory function (Zhang et al. 2008). Therefore, antagonism at these receptors by PTX would not impact greatly on the GABA-A inhibition as either they occur upstream of the effect and are therefore negated, or they inhibit the same neurons in the same manner.

Neural oscillations, as revealed by local field potentials and electroencephalogram

The extracellular electrical currents generated within the brain are an accumulation of all ionic changes within the brain (eg. postsynaptic depolarisation, action potentials, gap junctions etc.) and can be detected using multiple methods (Schnitzler and Gross 2005; Buzsaki et al. 2012*)*. For example, the electroencephalogram (EEG) can non-invasively record such activity from the surface of the scalp, whereas local field

potentials (LFP), from electrodes situated within the brain itself, record activity more locally. The signal detected by the electrode depends on the overall amplitude of the ionic changes, and the distance from the electrode (i.e. signals directly next to the electrode will appear stronger than the same amplitude changes further away from the electrode). Thereby, LFP recordings can detect activity within more precise regions as the electrode sits closer to the source, whereas the EEG recordings are limited to recording from the surface alone (Schnitzler and Gross 2005; Buzsaki et al. 2012*)*. Therefore, any regions deeper within the brain will contribute less to the signal than superficial regions due to their distance from the recording electrode. Oscillations within these recordings arises from the synchronous activity of the neurons within the network. Oscillations within the brain are often characterised into different frequency bands that, in general, are reflective of their various functions within the brain. The main oscillations within the human brain are Delta (1-3Hz), Theta (4-7Hz), Alpha (8-13Hz), Beta (14-30Hz), Gamma (30-80Hz) (Schnitzler and Gross, 2005). The frequency ranges of these oscillations in rodents is shifted slightly so that the frequencies of the different bands can be defined as follows: Delta (1-4Hz), Theta (4-10Hz), Beta (10-30Hz), and Gamma (30-80Hz) (Buzsaki & Draguhn, 2004).

Many neuropsychiatric disorders are associated with abnormal EEG measurements caused by neurological changes linked to the symptoms of the diseases, although more often than not the direct relationship between the oscillatory changes and underlying pathology is yet to be determined (Uhlhaas and Singer, 2015; Whittington et al., 2018). In any case, there has been much work assessing the oscillatory changes in Schizophrenia and some work in age-related cognitive decline. Gamma oscillations are often the most associated with Schizophrenia (Moran and Hong 2011): there is evidence of abnormal gamma oscillations in schizophrenia, with reduced evoked gamma activity during cognitive task performance and a decrease in resting state, and all together a disruption of synchrony within the band (Moran and Hong 2011; Schnitzler and Gross 2005). A consistent finding in the EEG of patients with schizophrenia is an increase in overall delta/theta power both evoked and at rest,

which is often paired with a decrease in alpha power (Boutros, 2008; Moran and Hong 2011; Hong et al. 2010). Generally in mild cognitive impairment and early stages of Alzheimer's disease the overall picture of oscillatory changes during rest is an increase in lower frequency power (delta/theta) with a decrease in higher frequency power (alpha/beta/gamma), which correlates with decreases in cognitive task performances (Rossini et al. 2007, McBride et al. 2014, Benwell 2020, Schnitzler and Gross 2005). Analysis of oscillatory activity within the brain is a useful tool for translation to clinical states where understanding the underlying biological changes within the system that result in such oscillatory changes can inform on both biomarkers for diseases and potential drug targets.

Anaesthetic LFP States

Brain oscillations recorded in the presence of anaesthesia show distinct states to those in wake or natural sleep (Gwilt et al. 2020). For example, isoflurane anaesthesia has been shown to show two types of activity, suggested to be related to anaesthetic depth. Deeper anaesthesia is suggested to cause a burst-suppression activity, periods of 'bursts' with high amplitude deflections interspersed between quiet periods of low amplitude signal: 'suppression'. Whereas lighter anaesthesia results in a more continuous state that has a medium amplitude signal. Many have described similar activity under both isoflurane and other anaesthesia (refer to Table 1.1 for a review of such literature). Such states convolute power-frequency analysis due to over dominance of higher-amplitude states, and thus the separation of these prior to analysis is paramount.

Levetiracetam: A potential ameliorative agent for neural disinhibition?

A potential treatment strategy for such conditions affected by neural disinhibition is to rebalance this activity by restoring the excitation/inhibition balance; to curb the activity and return it to a normal level (Bast et al. 2017). The delicacy of this balance means simply increasing the inhibitory activity could result in functional inhibition, which is also detrimental to cognitive function (Pezze et al. 2014). Therefore, an idyllic drug

Table 1.1- **The continuous and the burst and suppression states of the hippocampal LFP in isoflurane-anaesthetised rats: comparison to previously described hippocampal and cortical LFP states under anaesthesia**

The direct quotations highlight state properties corresponding to the 'continuous' and the 'burst' and 'suppression' states shown in the present study. Additional comments regarding the authors' interpretation of these states, and any comments on the relation to the states described in the present study, are shown in the 'Additional Comments' column.

Paper	**'Continuous' State**	**'Burst' and 'Suppression' States**	**Additional Comments**
Clement et al. 2008	***State referred to as:*** Activated State ***LFP pattern:*** 'Activated EEG patterns consisted of low amplitude fast activity at neocortical sites concomitant with theta (rhythmic 3–5 Hz) activity at hippocampal sites' ***Unit activity:*** Not Reported	**No equivalent state reported**	***Species:*** Rats ***Anaesthesia:*** Urethane ***Recording area:*** Hippocampus A hippocampal slow oscillation state (see Wolansky et al. 2006, from the same research group) is mentioned.
Ferron et al. 2009	***State referred to as:*** Low-Isoflurane ***LFP pattern:*** [EEG] 'All recording sessions started under 1.5% isoflurane anesthesia, which produced activity patterns comparable to those recorded during slow-wave sleep (SWS) and under ketamine-xylazine anesthesia (Fig. 1A) ... Briefly, these patterns consist of a quasi regular slow oscillation with a frequency range just below 1 Hz.' ***Unit activity:*** Not Reported	***State referred to as:*** Burst-Suppression ***LFP pattern:*** [EEG] '[A] deep level of anesthesia, producing burst suppression (BS), generates a state of unstable cortical hyperexcitability... BS is an electroencephalographic (EEG) pattern consisting of an alternating pattern of (1) epochs with silenced cortical activity and associated EEG isoelectric line, and (2) periods displaying high-amplitude slow and sharp waves' ***MUA:*** [Intracellular Recordings] 'The EEG patterns during BS consisted of periods of bursting and isoelectric lines. During the latter, all recorded cortical neurons displayed a hyperpolarized membrane potential devoid of any synaptic activity, whereas	***Species:*** Cats ***Anaesthesia:*** Isoflurane ***Recording area:*** Neocortex It is unclear how this SWS mentioned here relates to our Activated state, as the isoflurane level (1.5%) is higher than we, and others, report for similar states. It may be a state which is part of the transition from

		bursts consisted of depolarizing triangular-shaped potentials, synchronous with corresponding field and EEG waves.'	our Activated to Deactivated State.
Kroeger and Amzica 2007	***State referred to as:*** Low-Isoflurane/SWS ***LFP pattern:*** [EEG] 'Lower doses (1–2% isoflurane), sufficient for painless surgical procedures, produced a pattern of continuous sleep-like slow waves' ***Unit activity:*** Not Reported (in absence of stimulation)	***State referred to as:*** Burst-Suppression ***LFP pattern:*** [EEG] '[A] state of deep anesthesia induced by various anesthetics (isoflurane, barbiturates, and propofol) associated with an electroencephalographic pattern of BS... BS was obtained with higher doses of anesthetic (in the case of isoflurane, 2%), and its patterns, in accordance with previous descriptions, were characterized at the EEG level by alternating periods of (1) bursts of high-amplitude and low-frequency (15 Hz) waves, and (2) isoelectric EEG.' ***MUA:*** [Intracellcular Recordings] 'This further supports the claim that the state of BS is a state of hyperexcitability. The onset of this state window is prefigured by a progressive increase in the extracellular Ca2+ concentrations that may, on the one hand, transiently enhance cortical synaptic processes, and, on the other hand, reduce spontaneous firing of neurons through enhanced screening of Na+ channels... thus contributing to the gradual onset of suppression episodes.'	***Species:*** Cats ***Anaesthesia:*** Isoflurane ***Recording area:*** Neocortex See comments above for Ferron et al. 2009 relating to the low-isoflurane state.
Land et al. 2012	***State referred to as:*** Light Anaesthesia/Low Suppression ***LFP pattern:*** 'After the decrease of isoflurane concentration to 0.7 vol … activity to finally return into the initial state of small amplitude LFP activity.' 'The light anesthesia state was characterized by theta oscillations in the subiculum with a mean peak frequency of 4.8 Hz (SD 0.3 Hz)' ***MUA:*** 'After the decrease of isoflurane concentration to 0.7 vol %, this sequence of events appeared in reversed order: suppression was followed by burst-suppression, then slow rhythmic activity to finally return	***State referred to as:*** Deep Anaesthesia/High Suppression/Burst-suppression ***LFP pattern:*** 'Increasing levels of anesthesia eventually produce burst suppression of cortical activity, a pattern of alternating high amplitude bursts and periods of suppressed activity (silent periods) signifying deep anesthesia' 'In anesthesia-induced burst-suppression, the duration of silent periods between bursts is dose-dependent' 'The deep anesthesia state was characterized by regular slow rhythmic burst-suppression in the subiculum, with a mean peak frequency of 0.17 Hz (SD 0.05 Hz)'	***Species:*** Mice ***Anaesthesia:*** Isoflurane ***Recording area:*** Hippocampus

	into the initial state of small amplitude LFP activity... Multiunit activity in V1 and the subiculum followed these changes in LFP activity [in this order or in reverse] with analogous changes in spiking patterns.'	***MUA:*** 'LFP bursts in V1 or the subiculum were always accompanied with bursts of strong multiunit activity at the respective electrode sites'	
Lustig et al. 2016	***State referred to as:*** Light isoflurane state ***LFP pattern:*** 'Recordings during the lighter level of isoflurane anesthesia (~1%) consistently displayed a slow oscillation with a peak frequency of 3.4 Hz +/– 0.57 Hz' 'The depth profile of the running associated theta oscillations was strikingly similar to the slow oscillation during the light isoflurane state (3.5 Hz).' '[D]uring the light isoflurane state, we observed a slow, theta-like oscillation in CA1 and a faster, gamma-like oscillation around DG.' ***Single unit activity:*** '[A]ctivity of neurons recorded in the CA1 and DG layers was modulated by theta-like and gamma-like oscillations, respectively'	***State referred to as:*** Deep isoflurane state ***LFP pattern:*** 'under a deeper level of isoflurane anesthesia (2%), hippocampal activity was dominated by an oscillation with a peak frequency of 11.18 Hz ± 0.1 Hz' '[T]he depth profile of SPWs [sharp wave ripples] during water reward and quiet … was strikingly similar to the individual cycles of the 11 Hz oscillation during the deep isoflurane state.' 'In addition to these fast oscillatory events, we frequently observed randomly interspersed sharp LFP spikes in the D3 region.' ***Single unit activity:*** 'Firing in both CA1 and CA3 neurons was strongly phase locked to the individual cycles (Fig. 4C, top). CA1 neurons tended to fire a burst of action potentials around the trough of each cycle'	***Species:*** Rats ***Anaesthesia:*** Isoflurane ***Recording area:*** Hippocampus 'We found that under different levels of isoflurane anesthesia activity in the hippocampus of rats displays two distinct states, which have several qualities that mirror the theta and LIA states.'
Pagliardini Gosgnach & Dickson 2013	***State referred to as:*** Activated or REM-like ***LFP pattern:*** 'The REM-like state was characterized by high power in the theta frequency bandwidth (range: 3.5-4.5 Hz) with a corresponding increase in power through the gamma band (25-40Hz), consistent with the expression of gamma activity during both natural sleep and during anesthesia in previous studies' ***Unit activity:*** Not Reported	**No equivalent state reported**	***Species:*** Mice ***Anaesthesia:*** Urethane ***Recording area:*** Hippocampus A hippocampal slow oscillation state (see Wolansky et al. 2006, from the same research group) is mentioned.
Steriade et al. 1994	**No equivalent state reported**	***State referred to as:*** Burst-Suppression	***Species:*** Cats ***Anaesthesia:*** Mixture of

		LFP pattern: 'The EEG pattern of burst-suppression that followed administration of various anesthetics generally consisted of sharp waves with high amplitudes, at frequencies usually ranging between 2 and 7 Hz, separated by progressively longer periods of complete flatness. The electrical silence lasted for 1-2 sec during the initial stage of this pattern (Fig. 1A3), but reached 5-15 sec in later stages (Figs. 1A 4 and 2C) and even 30 sec or more in some instances (see below, Figs. 7 and 9A).' ***Unit activity:*** [Extra- and Intra-cellular recordings] 'Only 60-70% of them (11 RE thalamic and 20 thalamocortical cells) ceased firing before the occurrence of burst-suppression; thereafter, those cells discharged during EEG wave bursts and were completely silent during flat periods of the EEG. '	various anaesthetics, including urethane (background anaesthesia), ketamine, or xylazine and ketamine, nitrous oxide (N20), sodium pentobarbital. ***Recording area:*** Neocortex and Thalamus
Wolansky et al. 2006	***State referred to as:*** Activated State or Theta State ***LFP pattern:*** 'The activated state [during sleep] consists of prominent 3–12 Hz rhythmical activity known as theta or rhythmic slow activity.' '[T]he same electrographic could be observed during spontaneous state changes under urethane anesthesia'. 'Under urethane, [Slow Oscillation state, see Additional comments] … appeared to be dependent on the level of anesthesia; increasing anesthetic dosage moderately increased the proportion of time spontaneously spent in the slow oscillatory state (correspondingly decreasing the amount of time spontaneously spent in theta).' ***Single unit activity:*** 'Most of the neurons that generated rhythmic action potentials during the SO also did so during theta '	**No equivalent state reported**	***Species:*** Rats ***Anaesthesia:*** Urethane ***Recording area:*** Hippocampus Wolansky et al. report a Hippocampal Slow Oscillation state at 1Hz with a strong gamma power. It is unclear how this relates to our states, but it is not directly comparable to our burst-suppression state.

would be able to decrease the excitation with limited effect on baseline activity. One drug that has shown potential for this is the second-generation anti-epileptic drug levetiracetam, which is widely used in the treatment of epilepsy due to its unique mechanism of action, high responder-rate and beneficial pharmacokinetics (De Smedt et al. 2007b; De Smedt et al. 2007a; Ji-qun et al. 2005). Studies in rodents have shown that in low doses, lower than the anti-epileptic dose, levetiracetam is able to ameliorate increased hippocampal electrophysiological activity and ameliorate cognitive impairments leaving baseline activity intact (Koh et al. 2010; Sanchez et al. 2012; Robitsek et al. 2015; Haberman et al. 2017). Additionally, studies in patients with mild cognitive impairment show the promise of levetiracetam ameliorating such impairments (Bakker et al. 2012).

Thesis Aims and Hypotheses

One aim of this thesis was to extend the evidence for the hippocampal neural disinhibition model to the oscillatory activity within the brain, with an aim to provide an element of translatability to clinic. To this end we started by creating and conducting an advanced oscillatory analysis of the LFP data previously recorded under anaesthesia (McGarrity et al. 2017) to assess the impact of hippocampal disinhibition on the local oscillatory activity (Chapter 2). Following this, we moved onto hippocampal LFP and frontal EEG recordings in freely moving rats along with the hippocampal disinhibition (Chapter 3). We hypothesised that, considering the alterations in oscillations in clinical conditions, and the altered neuronal burst firing seen in our model (McGarrity et al. 2017), we would see some effect in this area.

In conjunction with the above aim, another key aim of this thesis was to establish the potential of low doses of levetiracetam to ameliorate the effect of hippocampal disinhibition. To achieve this we combined levetiracetam treatment and picrotoxin infusions in a replication of elements previously shown to be affected by hippocampal disinhibition (McGarrity et al. 2017; Gwilt et al. 2020): increased electrophysiological

multi-unit activity (Chapter 4), altered LFP oscillations (Chapter 5), increased locomotor activity, and decreased performance in the delayed matching to place watermaze task (Chapter 6). We hypothesised that low doses of levetiracetam would be able to ameliorate the electrophysiological and behavioural effects of our hippocampal disinhibition model.

Chapter 2: Frequency- and state-dependent effects of hippocampal neural disinhibition on hippocampal local field potential oscillations in anesthetized rats

This chapter has already been published in a peer-reviewed journal, it is included here as a slightly adapted word-processed manuscript. The published article can be found:

Gwilt, M., Bauer, M., & Bast, T. (2020). Frequency- and state-dependent effects of hippocampal neural disinhibition on hippocampal local field potential oscillations in anesthetized rats. *Hippocampus, 30*(10), 1021-1043. doi:10.1002/hipo.23212

Abstract

Reduced inhibitory GABA function, so-called neural disinhibition, has been implicated in cognitive disorders, including schizophrenia and age-related cognitive decline. We previously showed in rats that hippocampal disinhibition by local microinfusion of the GABA-A receptor antagonist picrotoxin disrupted memory and attention and enhanced hippocampal multi-unit burst firing recorded around the infusion site under isoflurane anaesthesia. Here, we analysed the hippocampal LFP recorded alongside the multi-unit data. We predicted frequency-specific LFP changes, based on previous studies implicating GABA in hippocampal oscillations, with the weight of evidence suggesting that disinhibition would facilitate theta and disrupt gamma oscillations. Using a new semi-automated method based on the kurtosis of the LFP peak-amplitude distribution as well as on amplitude envelope thresholding, we separated three distinct hippocampal LFP states under isoflurane anaesthesia: 'burst' and 'suppression' states – high-amplitude LFP-spike bursts and the interspersed low-amplitude periods – and a medium-amplitude 'continuous' state. The burst state showed greater overall power than suppression and continuous states and higher relative delta/theta power, but lower relative beta/gamma power. The burst state also showed reduced functional connectivity across the hippocampal recording area, especially around theta and beta frequencies. Overall neuronal firing was higher in the burst than the other two states,

whereas the proportion of burst firing was higher in burst and continuous states than the suppression state. Disinhibition caused state- and frequency-dependent LFP changes, tending to increase power at lower frequencies (<20Hz), but to decrease power and connectivity at higher frequencies (>20Hz) in burst and suppression states. The disinhibition-induced enhancement of multi-unit bursting was also state-dependent, tending to be more pronounced in burst and suppression states than the continuous state. Overall, we characterized three distinct hippocampal LFP states in isoflurane-anaesthetised rats. Disinhibition changed hippocampal LFP oscillations in a state- and frequency-dependent way. Moreover, the disinhibition-induced enhancement of multi-unit bursting was also LFP-state dependent.

1. INTRODUCTION

Subconvulsive neural disinhibition, i.e. reduced inhibitory GABA function, within the hippocampus has been implicated in important neuropsychiatric disorders, including schizophrenia and age-related cognitive decline, and in the cognitive impairments characterizing these disorders (Bast, Pezze, & McGarrity, 2017; Benes & Berretta, 2001; Heckers & Konradi, 2015; McGarrity, Mason, Fone, Pezze, & Bast, 2017; Nava-Mesa, Jiménez-Díaz, Yajeya, & Navarro-Lopez, 2014; Palop & Mucke, 2016; Stanley, Fadel, & Mott, 2012; Thomé, Gray, Erickson, Lipa, & Barnes, 2016). In a recent study (McGarrity et al., 2017), we pharmacologically disinhibited the temporal (also known as ventral) to intermediate hippocampus in rats by acute local microinfusion of the GABA-A receptor antagonist picrotoxin. Such hippocampal disinhibition caused clinically-relevant cognitive impairments, including in hippocampal memory function and in attentional performance that relies on prefrontal-striatal mechanisms, consistent with the idea that hippocampal disinhibition disrupts both hippocampal processing and processing in hippocampal projection sites (Bast et al., 2017). In addition, electrophysiological recordings around the infusion site under isoflurane anaesthesia showed that disinhibition enhanced burst firing of hippocampal neurons, as reflected by multi-unit data. The purpose of the present paper is to report the

analysis of the impact of disinhibition on the hippocampal local field potential (LFP), which we recorded alongside the multi-unit data.

Brain rhythms or oscillations, i.e. synchronized changes in the activity of many neurons, as revealed by LFP recordings have been suggested to be important for cognitive processing, including memory, because they bind neurons into functional assemblies (Buzsáki & Draguhn, 2004; Colgin, 2016). Alterations in brain rhythms have been reported in many neuropsychiatric disorders and have been suggested to arise partly from GABA dysfunction (Uhlhaas & Singer, 2006, 2010). Two prominent, widely studied hippocampal LFP rhythms are the theta and gamma rhythms. In the rat hippocampus, theta ranges from 4-12 Hz, whereas gamma oscillations range from 25-100Hz, including 'slow' or 'low' gamma from 25-55 Hz (also known as beta rhythms) and 'fast' or 'high' gamma' from 60-100 Hz (Colgin, 2016; Colgin et al., 2009). Substantial evidence suggests that theta and gamma LFP rhythms depend on hippocampal GABAergic inhibition; this evidence leads to the hypotheses underlying our study of the LFP changes caused by hippocampal disinhibition, and will be considered in the following paragraphs. Another prominent hippocampal rhythm, sharp-wave ripples (110–250 Hz ripples superimposed on 0.01–3 Hz sharp waves) (Colgin, 2016), will not be considered further in this paper, because ripples are not expressed under volatile anaesthetics (Ylinen et al., 1995) and the frequency range of our LFP recordings (0.7-170Hz) did not encompass the full range of sharp waves and ripples.

Substantial evidence suggests that hippocampal disinhibition would facilitate hippocampal theta power. Septal projections to the hippocampus, including excitatory cholinergic projections and GABAergic projections, which disinhibit the hippocampus by innervating hippocampal inhibitory GABA interneurons (Borhegyi, Varga, Szilagyi, Fabo, & Freund, 2004; Freund & Antal, 1988; Hangya, Borhegyi, Szilágyi, Freund, & Varga, 2009; Tóth, Freund, & Miles, 1997), are thought to be a main theta driver (Colgin, 2016). In line with this, septal inactivation reliably abolishes hippocampal theta in freely moving rats (Brandon et al., 2011; Koenig, Linder, Leutgeb, & Leutgeb, 2011) and in urethane-anaesthetised rats with septal inactivation, hippocampal theta

could be reinstated by cholinergic stimulation or disinhibition (with the GABA-A receptor antagonist bicuculline) of the hippocampus (Smythe, Colom, & Bland, 1992). Moreover, cholinergic stimulation of rat hippocampal slices by carbachol reliably induces theta in vitro, and pharmacological disinhibition by GABA-A receptor antagonists has been reported to enhance the amplitude of such cholinergically induced theta oscillations (Golebiewski, Eckersdorf, & Konopacki, 1996; Konopacki, Gołebiewski, Eckersdorf, Błaszczyk, & Grabowski, 1997; Kowalczyk, Bocian, & Konopacki, 2013). In line with such theta-enhancing effects of hippocampal disinhibition, hippocampal inhibition with the GABA-A receptor agonist muscimol disrupted cholinergically induced theta in the rat hippocampus in vitro (Golebiewski et al., 1996) and in vivo (Smythe et al., 1992). These findings thus support an inverse relationship between hippocampal GABA function and theta amplitude (Kowalczyk et al., 2013).

However, there is also evidence that some types and properties of hippocampal theta are positively modulated by GABA function and disrupted by hippocampal disinhibition. Genetic ablation of synaptic inhibition of parvalbumin-positive GABAergic interneurons disrupted hippocampal theta in freely moving mice (Wulff et al., 2009). GABA-A receptor antagonists reduced the power of theta induced by septal activation in an in vitro septo-hippocampal preparation from rats (Goutagny, Manseau, Jackson, Danik, & Williams, 2008), and of nicotine-induced (Lu & Henderson, 2010) and electrically induced (Heynen, Sainsbury, & Bilkey, 1993) theta in rat hippocampal slices, and decreased frequency and coherence (connectivity) of carbachol-induced theta between the entorhinal cortex and subiculum in vitro (Levesque, Cataldi, Chen, Hamidi, & Avoli, 2017). Moreover, optogenetic activation of parvalbumin-positive GABAergic hippocampal interneurons strengthened, whereas silencing of these neurons disrupted, theta in an in vitro preparation of the mouse hippocampus with intact intrinsic but severed extrinsic connectivity, suggesting that GABAergic inhibition by parvalbumin neurons supports intrinsically generated theta (Amilhon et al., 2015). Finally, genetic knock-out of the GABA-A receptor subunit β_3 decreased power,

frequency and regularity of hippocampal theta and theta cross-correlation between different hippocampal subfields in freely moving mice (Hentschke et al., 2009).

There is also substantial evidence linking hippocampal gamma oscillations to inhibitory GABAergic hippocampal interneurons (Colgin, 2016). In rodents, firing of hippocampal interneurons is phase-locked to spontaneous hippocampal gamma oscillations (Belluscio, Mizuseki, Schmidt, Kempter, & Buzsaki, 2012; Mann, Suckling, Hajos, Greenfield, & Paulsen, 2005; Tiesinga, Fellous, José, & Sejnowski, 2001; Traub et al., 2000; Tukker, Fuentealba, Hartwich, Somogyi, & Klausberger, 2007), and intracellularly recorded inhibitory postsynaptic potentials of pyramidal cells, recorded in vivo, are reflected in gamma oscillations (Penttonen, Kamondi, Acsady, & Buzsaki, 1998; Soltesz & Deschenes, 1993). This indicates that hippocampal gamma is generated by hippocampal GABA interneurons (Colgin, 2016). Consistent with this, GABA-A receptor antagonists have been shown to disrupt different types of experimentally induced gamma oscillations in hippocampal slices, with the magnitude of this effect depending on the hippocampal subfield (Bartos, Vida, & Jonas, 2007; Fisahn et al., 2004; Traub, Bibbig, LeBeau, Buhl, & Whittington, 2004; Whittington, Traub, Kopell, Ermentrout, & Buhl, 2000).

Overall, the above review of GABAergic mechanisms of hippocampal theta and gamma oscillations leads to the hypothesis that pharmacological hippocampal disinhibition will cause frequency-dependent changes in LFP oscillations, with the weight of evidence suggesting that gamma amplitude may be reduced, whereas theta amplitude may be enhanced. However, there is also evidence suggesting that some features of the theta rhythm, including its coherence across the hippocampus, may be disrupted.

When analysing LFP recordings from anaesthetised rodents, it is important to consider that, under anaesthesia, many brain regions, including the hippocampus, show different LFP states characterized by distinct LFP patterns which can alternate (Clement et al., 2008; Kenny, Westover, Ching, Brown, & Solt, 2014; Land, Engler, Kral, & Engel, 2012; Lustig, Wang, & Pastalkova, 2016; Wolansky, Clement, Peters,

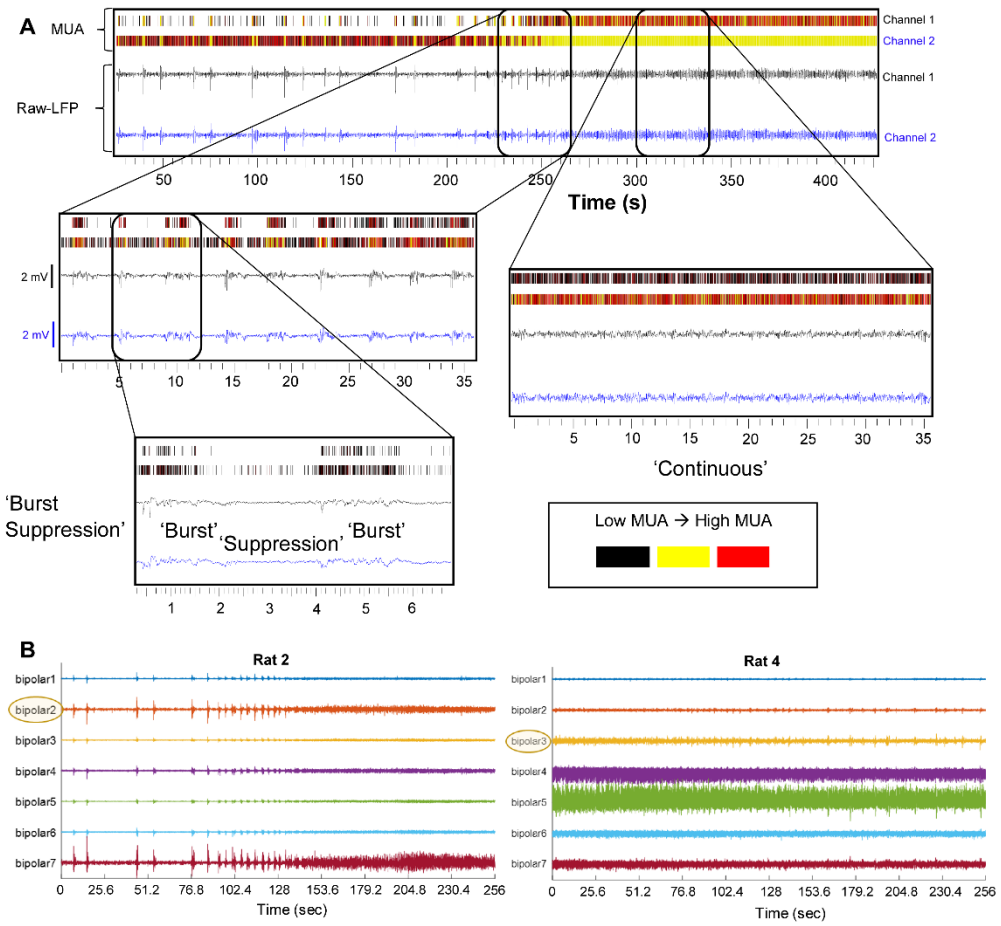


Figure 2.1: Three distinct LFP states in the rat hippocampus under isoflurane anaesthesia

For illustration purposes, example raw traces are shown, to familiarise the reader with the manifestation of the different LFP states.

A The top panel shows two 400-s long LFP traces, with corresponding multi-unit activity (MUA), recorded simultaneously from the temporal to intermediate hippocampus under isoflurane anaesthesia. They illustrate the transition from the burst-suppression state (left), comprising burst and suppression states, to the continuous state (right). The middle panel shows the 40-s sections indicated in the top panel with an expanded time line. The bottom panel depicts a 7-s period of the burst-suppression state with an expanded time line, showing the LFP signal during burst and suppression states in higher detail. The three distinct LFP states also differ with respect to multi-unit spiking, particularly MUA tends to be higher during the burst than in the suppression state (mind the colour-'scale', showing three distinct levels of MUA (besides zero which is transparent) – corresponding to different MUA frequencies; exported from Neuroexplorer v4).

B The two plots show the LFP traces recorded from the montage of 7 bipolar channels in two different rats to give a more representative impression of the distinctiveness of the states that differs greatly between different animals and, sometimes, electrodes. Bipolar channel 2 of Rat 2 was selected as the 'LFP state-defining' channel here because of very clear visual separation of the three states based on the amplitude differences (these are the data magnified in (**A**)). By contrast, in Rat 4, the three LFP states are visually less clearly separated. Channel number 3 was selected as the 'LFP state-defining' channel for this rat because, although it has smaller overall amplitudes than other channels, the three different states are visually more clearly separated, especially compared to channels 4-7.

Palczak, & Dickson, 2006) (for an example of our hippocampal recordings, see **Figure 2.1A**). One key LFP state observed with many anaesthetics, including isoflurane, is

the burst-suppression state, which can be further subdivided into a ‘burst’ state, characterized by LFP ‘bursts’ (i.e. high-amplitude LFP deflections), which alternates with a ‘suppression’ state, characterized by low amplitude LFP signal (Note: the burst-suppression state is often, or even typically, considered as one state, without further subdivision in two distinct states, although visual inspection of the LFP trace clearly suggests distinct properties of the ‘burst’ and ‘suppression’ components; our quantitative analysis reported in this paper also revealed distinct properties of these two states). A third LFP state is characterised by a more continuous LFP pattern with continuous LFP activity of lower amplitude than during LFP ‘bursts’. The balance between the burst-suppression and continuous states changes with anaesthetic depth, with burst-suppression tending to become more dominant the deeper the anaesthesia (Land et al., 2012; Lustig et al., 2016). To analyse the impact of neuropharmacological manipulations, including hippocampal disinhibition, on LFP oscillations under anaesthesia it is important to separate these different LFP states for two main reasons. First, the large-amplitude LFP signals characterizing the burst state reflect major non-stationarities in the otherwise low-amplitude signals and may thus dominate the power spectral analysis, occluding frequency components that may be more characteristic of the other LFP states. Second, given the distinct characteristics of LFP patterns in different LFP states, neuropharmacological mechanisms underlying oscillatory activity may be LFP-state dependent.

In the present study, we aimed to characterise the effect of hippocampal disinhibition, by picrotoxin infusions into the temporal to intermediate hippocampus, on hippocampal neural oscillations around the infusion site using the LFP data recorded by McGarrity et al. (2017). First, we developed an objective, semi-automated method to separate the three distinct LFP states described above (the continuous LFP state from the burst-suppression state, and, within the latter, the burst from the suppression state; **Figure 2.1A**) and compared several properties of these states (frequency-specific power and connectivity, and multi-unit parameters). Second, we examined the impact of picrotoxin on hippocampal LFP properties (frequency-specific power and connectivity) in the three distinct LFP states. Third, we examined if the disinhibition-

induced enhancement of multi-unit burst firing reported previously (McGarrity et al., 2017) is dependent on the LFP state.

2. METHODS

2.1 LFP and multi-unit data recording and pre-processing

Analysis was carried out on the hippocampal LFP and multi-unit data collected in our previous study (McGarrity et al., 2017). The recordings were carried out in accordance with the Animals (Scientific Procedures) Act 1986, and full details concerning the rats used for the recordings, housing conditions, surgical and recording procedures and equipment can be found in our previous study (McGarrity et al., 2017). In brief, LFP and multi-unit data were recorded simultaneously in isoflurane anesthetized male adult (2-3 months) Lister-hooded rats, using a custom-made assembly of a 33-gauge stainless steel infusion cannula and an 8-electrode (microwire) recording array that was implanted into the hippocampus (**Figure 2.2A**, top right). The cannula tip, through which saline or picrotoxin solution could be injected, touched the electrodes and was positioned about 0.5 mm above the tips of the central electrodes. The assembly was stereotactically implanted into the right hippocampus, such that the 8-electrode array was arranged perpendicular to the brain midline and anterior to the infusion cannula, with the cannula tip aimed at coordinates in the right temporal (also known as ventral) to intermediate hippocampus (5.2 mm posterior to bregma, 4.8 mm lateral from midline, and 6.5 mm ventral from dura). The 8-electrode array spread approximately 2 mm, in the medio-lateral direction (**Figure 2.2A**, top left). The extracellular signal recorded by the electrodes was band-pass filtered into LFP (0.7 and 170 Hz) and multi-unit (250 Hz to 8kHz) data, which were recorded for a 30-min baseline period and a 60-min period following infusion (over about 1 min) of either 0.5ul saline (n = 7 rats) or 150ng/0.5ul picrotoxin (n = 6 rats) in a between-subjects design. Isoflurane levels were kept at a relatively stable level (1-3% depending on the rat) over the entire recording period, such that the breathing rate was kept around 50 breaths per minute and the pedal reflex was absent. All data were

collected continuously and averaged in 5-min bins, i.e. six pre-infusion (baseline) and 12 post-infusion 5-min bins. Although the picrotoxin group in the original study included eight rats (McGarrity et al., 2017), only six of these rats could be included in the present analysis, because one of the datasets could not be read into MATLAB for analysis and another dataset was recorded using a bundle array and, therefore, could not be combined with the rest of the data for LFP analysis.

All data were processed in MATLAB (R2016a) (The MathWorks, Inc., USA) using the FieldTrip toolbox (Oostenveld, Fries, Maris, & Schoffelen, 2011). To reduce noise, far-field effects and shared signal from all the electrode recordings, a montage of seven bipolar channels was digitally created using a pairwise bipolar subtraction (Land et al.,

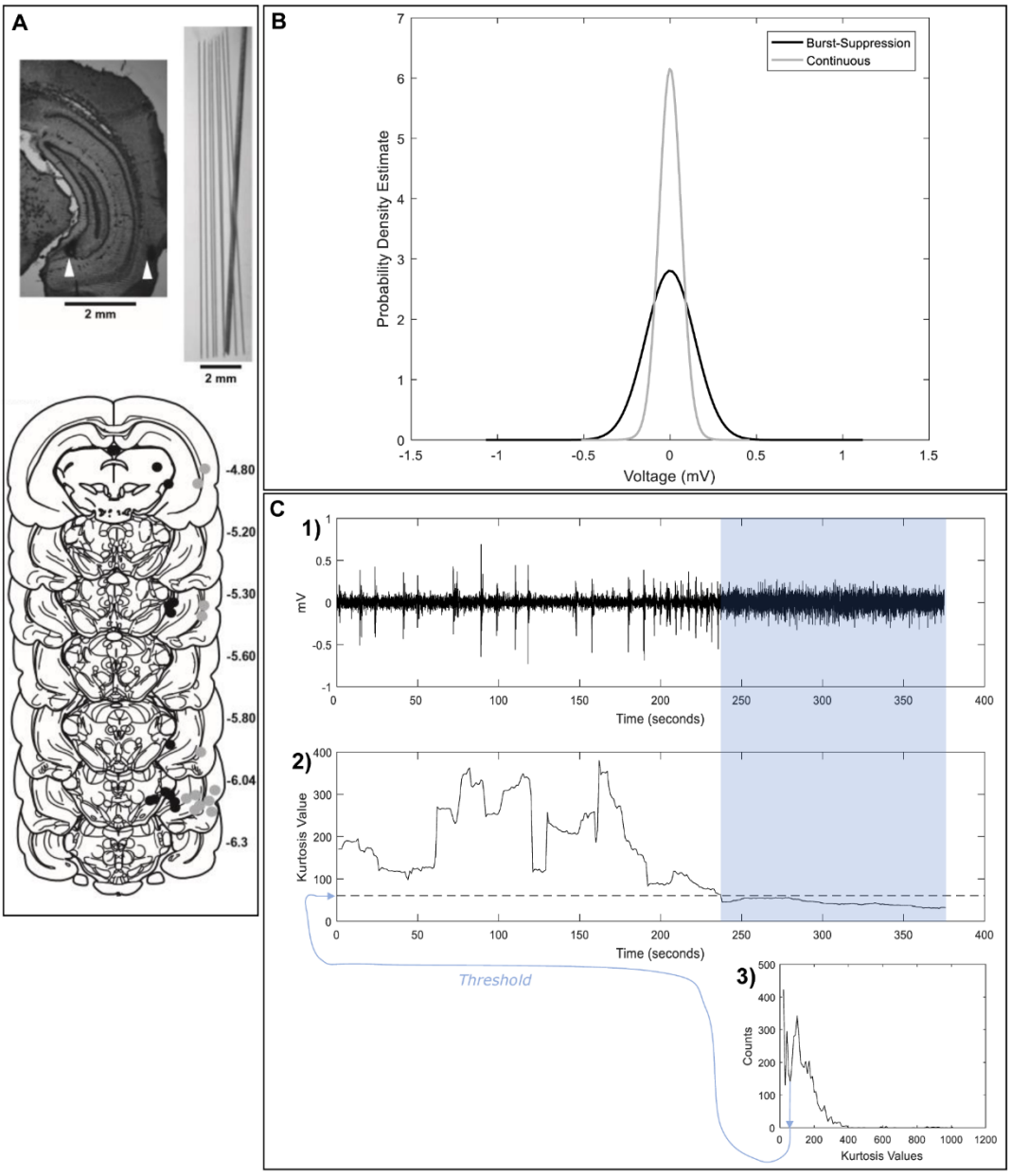


Figure 2.2: Methods: Hippocampal recordings and separation of hippocampal LFP states

A *Placement of the infusion-recording array within the temporal to intermediate hippocampus.* The top pictures show, left, the 8-electrode array with the attached infusion cannula and, right, an example coronal section through the hippocampus, with the placements of the most medial and most lateral electrodes indicated by the white arrow heads. The array was arranged perpendicular to the midline of the brain, with the infusion cannula located just posterior to the centre of the array. In the bottom, the most medial (black dots) and most lateral (grey dots) electrode placements are indicated for all rats included in the analysis on drawings of coronal brain sections taken from the atlas by (Paxinos & Watson, 1998). Note that the most medial and/or the most lateral electrodes of the 2-mm 8-electrode recording array were located outside of the hippocampus (typically 1–3 electrodes per rat) and data from these electrodes was excluded from the analysis. Figure is adapted from Fig. 5A in McGarrity et al. (2017).

B *The distribution of amplitude of peaks and troughs in the burst-suppression state and the continuous state differ in kurtosis, but not modality.* A histogram was calculated for the identified peaks- and troughs-amplitudes based on visually identified 100-s segments belonging to the combined burst-suppression or the continuous state, from the 400-s trace shown in Figure 1. Both states show a unimodal amplitude distribution, but the distribution of the burst-suppression state shows a higher kurtosis (tailedness).

C *Semiautomatic separation of burst-suppression and continuous LFP states, using the kurtosis values of the distribution of the peak and trough amplitudes of the LFP trace.* **1)** 400-s LFP trace, clearly showing separate burst-suppression (white background) and continuous states (shaded) (same 400-s trace as shown in **Figure 2.1A**). **2)** The time course of the kurtosis values of the 400-s LFP trace, calculated using a 10-s long, 1-s sliding window. **3)** Histogram of the distribution of kurtosis values over baseline and post-infusion data (i.e., the whole recording period, not only the 400-s period presented in **1)** and **2)**). The arrow from 3) to 2) represents, in this case, the second minimum in the histogram (3) which corresponds to the kurtosis threshold value (stippled line in 2) that separates burst-suppression from the continuous state.

2012) of the eight original electrodes. Data were then pre-processed in fieldtrip by re-referencing with a common reference over all bipolar channels (except for the functional connectivity analysis) to remove any remaining linear gradient affecting all bipolar pairs, DC offset removal for each episode, and a band-stop filter between 49.5 and 50.5 Hz to remove the electric line-noise. The most medial and/or the most lateral electrodes of the 2-mm 8-electrode recording array were located outside of the hippocampus (typically 1–3 electrodes per rat) (**Figure 2.2A**, bottom) and our previous multi-unit analysis revealed that hippocampal picrotoxin infusion did not affect any of the multi-unit parameters analysed from these electrodes (consistent with the densely packed fibre bundles surrounding the hippocampus) (McGarrity et al., 2017). If both of the electrodes used to calculate a synthetic bipolar electrode were outside of the hippocampus, that particular bipolar channel was removed, otherwise it was included in the analysis. As bipolar subtraction was not appropriate for multi-unit activity, in order to match the 7 bipolar channels used for the LFP analysis, electrodes 2 to 8 were selected and matched to their corresponding bipolar channel (i.e., electrode 2 to bipolar 1, electrode 3 to bipolar 2 etc.). Electrodes 2 to 8 were selected

in place of 1 to 7 because in most cases electrode 1 (the most medial) sat outside the hippocampus and had to be excluded anyway.

2.2 Semi-automated separation of LFP states

The hippocampal LFP recordings under isoflurane anaesthesia clearly showed the three distinct LFP states outlined in the Introduction, including a burst, suppression and continuous state (**Figure 2.1A**). The simultaneously recorded multi-unit activity also appeared to vary depending on the LFP state, with the burst state tending to show a higher multi-unit firing than the suppression state, and the continuous state characterized by continuous firing at a similar rate to that in the burst state. Our semi-automated separation strategy was to start by separating the combined burst-suppression state from the continuous state and then to separate the burst from the suppression state.

Simple thresholding based on continuous amplitude/power measures did, with our data, not result reliably in state separation that corresponded to the states that would be assigned by visual inspection (although thresholding worked for the example LFP traces in **Figure 2.1A**, it did not reliably separate the LFP states when these showed less pronounced differences; for examples, see **Figure 2.1B,** right). Therefore, we used a higher order moment (kurtosis) of the distribution of the peak amplitude values - rather than the mere amplitude of the continuous signal (see below). To separate the three states, for each rat the channel with the most marked difference between LFP states based on visual inspection of the raw LFP traces, the 'LFP state-defining' channel, was selected (see **Figure 2.1B** for example). For this LFP state-defining channel, the peaks and troughs of the LFP trace were identified (undifferentiated over baseline and post-infusion periods), by identifying the sign change of the first derivative. The distribution of these peaks and troughs identified from the sign-change turned out to be unimodal (**Figure 2.2B**), and thus not enabling a clear separation into discrete states. In contrast, a measure of the kurtosis ('tailedness') of the amplitude distribution of those peaks and troughs separated the burst-suppression and

continuous states. The kurtosis was calculated for a 10-s sliding window with a 1-s step size (the raw signal and the estimates of kurtosis are plotted in **Figure 2.2C panels 1 and 2, respectively**). A histogram of kurtosis values (a total of 4391) was plotted in 100 bins (**Figure 2.2C, panel 3**), and the most distinct local minimum (the first or second) separating peaks in the multimodal distribution, was selected as threshold to separate the combined burst-suppression states from the continuous state (**Figure 2.2C, arrow**). If kurtosis values exceeded this threshold, the corresponding time points were marked as being in the 'burst-suppression' state, whereas time points with subthreshold values were marked as in the 'continuous' state (**Figure 2.2C, shaded area**). These labels were then applied to the samples of every channel from the same rat.

In a final step, we further separated the 'burst-suppression' state into the burst and suppression components, using a semiautomatic LFP-amplitude thresholding routine in Fieldtrip. To this end, a distribution of the absolute amplitude-values of the signal was formed. Samples that exceeded a fixed z-value of 5 and those falling within a symmetrical 0.25s window around the threshold crossing were consecutively labelled as 'Burst' state. This thresholding was run on each individual channel to prevent summation of z-values, which could occur from synchrony across channels and convolute the routine. The output of this routine gave the boundaries between low amplitude activity, corresponding to the suppression state, and the burst state.

Not all rats were spending time in each of the LFP states for every 5-min bin of the recording period, and four rats were not spending any time in the continuous state during baseline (therefore not allowing baseline normalisation of the post-infusion data). Therefore, the number of rats contributing to the different analyses of state-separated data could differ from the overall number of rats from which recordings were made (**Figure 2.3**). The reduced sample size during the continuous state implies that the statistical power of any analysis in the continuous state is reduced compared to the analysis of the other two states.

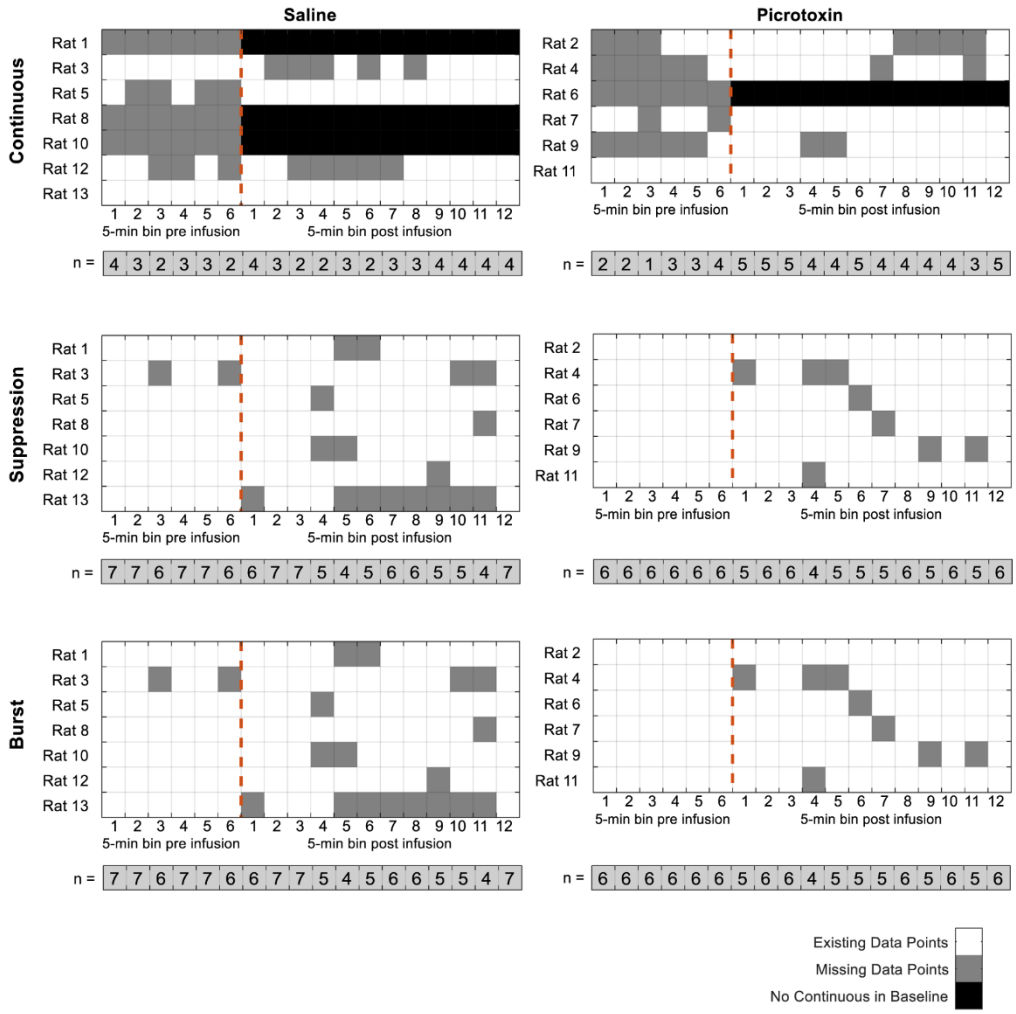


Figure 2.3*:* State-separated data available in saline and picrotoxin infusion groups for each of the 6 baseline and 12 post-infusion 5-min bins

For each of the drug (saline or picrotoxin)-state combinations a grid is shown to indicate missing data points, with the time bin on the x-axis and the rat ID on the y-axis. Underneath is the total number n of rats that contributed values for each 5-min bin in the different drug-state combination.

2.3 State-separated analyses of hippocampal LFP properties

2.3.1. Power-spectral density

Power at different frequencies was analysed separately for the different LFP states in FieldTrip, using Fast Fourier Transform (FFT) with a Hanning window from 0.5 to 40 Hz. These power-spectra were subsequently averaged across channels and compared across the different states. Given the substantial raw-power differences between the different states (already separated in this analysis) and in order to investigate potential differences in relative spectral density, for each individual

channel we additionally normalized the spectra to the total area under the curve of the power spectrum before comparison across states. The analysis presented here is of FFT over the entire recording session (pre-infusion and post-infusion); however, considering the time-dependent effects of picrotoxin in the MUA (McGarrity et al. 2017) we may anticipate a time-dependent LFP effect. For this analysis a time-frequency representation would be interesting, however the separation of anaesthetic states leads a large disparity between specific time-points in each state for each rat (refer to 2.2 Semi-automated separation of LFP states and figure 2.3) which would lead to confounds in such a time-based analysis. Therefore, we have not conducted such an analysis, nevertheless, previously we did restrict the FFT to the 15 to 40 minutes post-infusion (the time-window where peak picrotoxin effects are seen in the MUA) and found no difference in appearance or significance of picrotoxin-induced effects than from those of the entire hour (data not shown).

2.3.2. Connectivity

Phase-Locking Values (PLV) were calculated to indicate the phase-coherence (a measure of neuronal synchronization that is independent of amplitude correlations) of two signals originating from a pair of electrodes (measuring local activity due to their bipolar montage) (Aydore, Pantazis, & Leahy, 2013; Bastos & Schoffelen, 2015; Srinivasan, Winter, Ding, & Nunez, 2007). PLVs were calculated for every possible pair of hippocampal electrodes for every 0.5-Hz frequency bin. Because the individual electrodes between rats were not at consistent homological locations within the temporal to intermediate hippocampus, instead of averaging PLVs of electrode-pairs across subjects (as is common in EEG/MEG analysis where a standard mapping of electrodes does exist, e.g. Oostenveld & Praamstra, 2001), we used a different method to extract the communality of connectivity between all electrode pairs and to then calculate a statistic of this across rats (Cohen, 2015). To this end, we used singular value decomposition (SVD) over the imaginary part of the PLV matrix of all states and times. We used the imaginary part of the complex phase-locking-value

(complex cross-spectrum normalized on power in individual trials) as this is not corrupted by volume-conduction problems (Nolte et al., 2004). For each rat and frequency bin, we extracted the singular vectors U and V that satisfy the equation PLV = U * S * V', with S being the matrix of singular values and PLV the matrix of imaginary PLVs. The individual imaginary PLV matrices for each state and time combination were then projected into this space using the respective singular vectors and the first two 'singular values' were extracted. These two values represent the connectivity strength within the two dominant 'neural networks' of the rat in the area of the temporal to intermediate hippocampus sampled by the bipolar 7-electrode montage.

2.3.3. Multi-unit activity (MUA)

We compared the following key MUA parameters between LFP states: overall firing rate, bursts per minute, percentage of spikes in burst, and burst duration. The original MUA analysis in our previous study (McGarrity et al., 2017) had been completed using NeuroExplorer (version 4). However, in order to examine the state-dependency of MUA parameters (and, subsequently, also of the previously reported disinhibition-induced enhancement of MUA burst parameters, see below), we replicated the original analysis using MATLAB, where we could then separate the different snippets of MUA by their associated LFP state. In brief – all spikes (i.e. not sorted into different units) were combined for 'burst' analysis; all parameters included here were calculated as per their description. The MUA data were separated according to the different LFP states based on their time stamps in a way that preserved the original MUA bursts, with each burst assigned to the state occupied longest during the burst duration.

2.3.4. Statistical comparison of the three distinct hippocampal LFP states during baseline

To analyse the effect of the different states on the overall LFP and MUA we compared the baseline data, removing the factor of drug. For the baseline frequency specific effects (power-spectra and PLV eigenvalues) we compared each state to both other states in a separate analyses, after running a moving average over the frequency values, with a kernel of 1.5Hz sliding over 0.5Hz. The statistical analysis of these effects were carried out using pairwise comparisons at each frequency bin. In order to address the multiple comparisons problem arising from the simultaneous analysis of 80 different frequency bins, we conducted a cluster permutation analysis (Hayasaka, Phan, Liberzon, Worsley, & Nichols, 2004; Maris & Oostenveld, 2007). This method runs a mass-univariate independent samples t-test for each frequency bin, for both real data pairs (of the conditions to be compared) and randomly assigned pairs (combining data of both conditions to obtain a reference distribution). Adjacent frequency bins that pass the univariate significance threshold form a cluster and a summary statistic of these clusters (e.g. summed t-value) is calculated for real data and reference distribution data. Only those clusters from the comparisons of the real data pairs which cut-off less than 5% of the maximum cluster-statistic from the reference distribution (random pairs) were considered as statistically significantly different.

For the state-separated analysis of MUA, a problem of missing data points over time arose due to the limited time each rat spent in each state (see **Figure 2.3** for the missing data in different 5-min bins). Therefore, it was not possible to conduct a repeated-measures ANOVA and so we used a pooling strategy. More specifically, we used the 5-min bins in the different states as the units of observation, such that data from all rats and time bins were pooled according to state – after averaging across channels (for each rat). This was then subjected to a between-subjects one-way ANOVA, with LFP state as the between-subjects factor; this reflects a fixed-effect analysis.

2.4 Analyses of LFP state-dependent drug infusion effects

2.4.1 Power-spectral Density

For the comparison of frequency-specific effects of drug infusion, the difference between pre- and post-infusion power was expressed as log of the ratio between post-infusion (power-spectra over 60 min) and pre-infusion (baseline; power spectra over 30 min) values for each channel. These difference values were then averaged per rat for statistical analysis, then for each drug group for plotting. The statistical analysis of the frequency specific effects of picrotoxin compared to saline infusions on LFP power were carried out using cluster permutation where, separately for each LFP-state, the log-ratio of both drug groups was compared.

2.4.2 Connectivity

The first two PLV 'Eigenvalues' for each rat (see 2.3.2 State-separated analysis of hippocampal LFP properties, Connectivity) were averaged to give a single measure of aggregate connectivity. To normalise post-infusion values to pre-infusion (baseline) values, the pre-infusion values were subtracted from the post-infusion values. As was done for the spectral power analysis, the cluster permutation statistic was used to compare the effects of picrotoxin vs. saline for each of the LFP-states separately.

2.4.3 MUA

Our previous analysis, which did not separate MUA data according to LFP state, showed that hippocampal disinhibition by picrotoxin causes enhanced burst firing, as reflected by increased bursts per minute, percentage of spikes in burst, and burst duration (McGarrity et al., 2017). Therefore, our present analysis focused on these burst parameters.

To assess the effect of picrotoxin on the state-separated MUA analysis, we could not apply the mixed-model ANOVA of MUA parameters with drug as between-subjects and time (5-min bin – as done previously; McGarrity et al. 2017) as repeated-measures factors, which we used in our original MUA data analysis (which did not separate data by LFP state) (McGarrity et al., 2017). This is because of the many missing data points, following separation of data according to LFP state (see **Figure 2.3**). Therefore, we used the same pooled analysis as for the comparison of MUA parameters between LFP states during baseline, however, here with the additional factor of infusion group. Again, data were pooled over time and rats and separated according to LFP-state and infusion group. Prior to pooling, data for each rat, in each state, were normalised by subtracting the average of the pre-infusion values for each channel from the individual post-infusion values for the corresponding channel; subsequent to this, an average was taken across the channels, for each rat and time point separately. The normalised and pooled MUA data were subsequently analysed using a two-way ANOVA, with LFP state and infusion condition as between-subjects factors (and time-bins and rats as units of observation). A significant infusion condition X state interaction would statistically support state-dependent drug effects.

3. RESULTS

3.1. Three distinct hippocampal LFP states under isoflurane

3.1.1. Differences in frequency-dependent power and functional connectivity

To compare quantitatively the three distinct hippocampal LFP states (**Figure 2.1A**), we combined the baseline data (i.e., data recorded before any drug infusion) from all infusion groups. During the baseline period, all rats showed the burst and suppression states, but not all rats showed a continuous state, resulting in a sample size of n=13 rats for the burst and suppression state and of n=9 rats for the continuous state (**Figure 2.3**).

The three LFP states substantially differed with respect to overall raw power and with respect to relative power at different frequencies (**Figure 2.4**). The overall raw power in the burst state was significantly and substantially higher than in the suppression (cluster level p = 0.0010, corrected for multiple comparisons; cluster spanning across all frequencies, i.e. 1-39 Hz) and continuous states (p = 0.0050, cluster including 1-22.5Hz). Suppression and continuous states did not differ significantly (p>0.05) indicating similar overall power, although at lower frequencies power tended to be somewhat higher in the continuous compared to the suppression state (**Figure 2.4A**). With respect to relative power at different frequencies, the burst state showed a higher proportion of power within delta/low theta than the other two states and tended to show a lower proportion of power in high frequencies from about 20 to 40 Hz than both the suppression and continuous states, which were both characterized by conspicuous gamma 'bumps' in the normalised power spectra in this frequency range (**Figure 2.4B**). For the comparison between burst and continuous states, a significant cluster was found at 3.5-10 Hz (p = 0.024) and between burst and suppression states a significant cluster was found at 4-14 Hz (p = 0.009). The numerical differences at higher frequencies did not reach statistical significance: neither for the comparisons of continuous and burst states (p = 0.16) nor suppression and burst states (p = 0.10).

Regarding connectivity, we computed an aggregate measure of phase-locking between all electrode pairs spread across the temporal to intermediate hippocampus (see Methods). To exclude any contamination by volume conduction, only the imaginary part of the PLVs was used and submitted to a SVD, of which we report the first two diagonal (Eigen-)values. Across the frequency range examined (0.7 to 40 Hz), the burst state showed generally lower connectivity than both suppression and continuous states, which showed very similar connectivity (**Figure 2.4C**). One significant cluster was found for the comparison between burst and continuous states at 1.5-9 Hz (p=0.018), and two significant clusters for the comparison between burst and suppression states: one cluster at 2.5-13 Hz (p =0.019) and another cluster at 17-38 Hz (p = 0.005). In all these clusters connectivity was reduced in the burst state, in comparison to both the continuous and the suppression state.

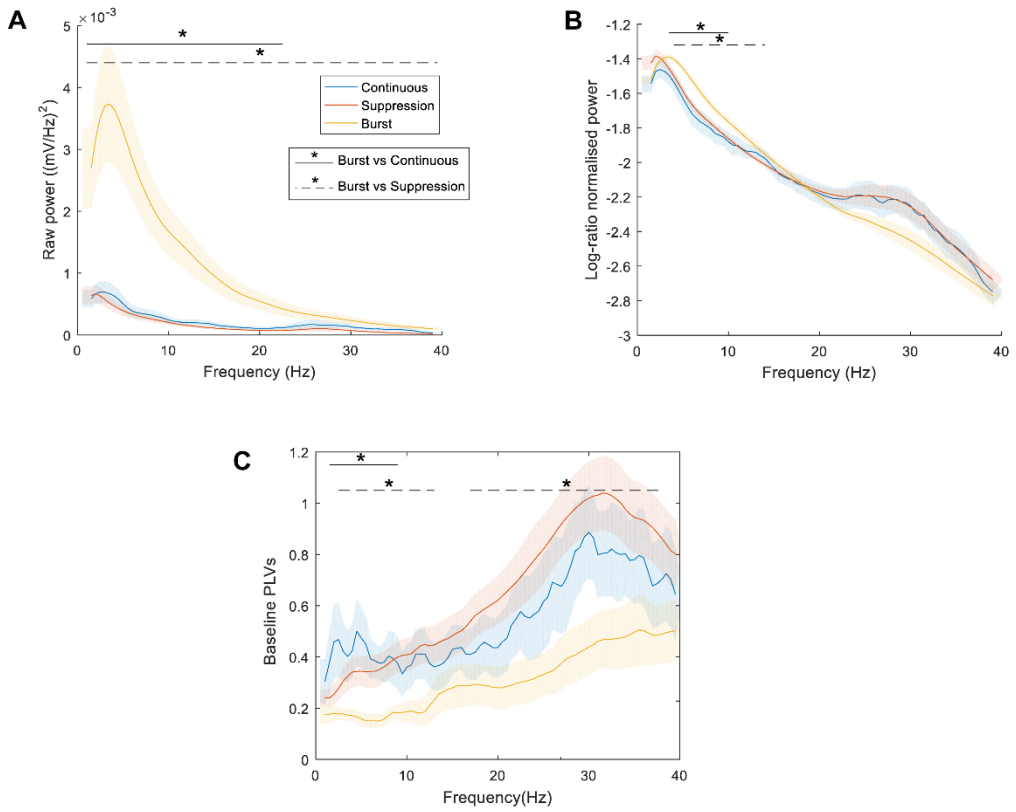


Figure 2.4: The three hippocampal LFP states – differences in frequency-dependent power and connectivity

(**A**) Raw power spectral density, (**B**) log-ratio of power divided by the total area under the curve (representing relative power at different frequencies), and (**C**) phase-locking eigenvalues are shown across frequencies for each of the three LFP states. All values shown as mean±SEM. The frequency ranges showing significant ($p<0.05$) differences based on cluster permutation statistics are indicated by an asterisk (*) and a solid line for comparisons between burst and continuous, and a dashed line for comparisons between burst and suppression states. Number

Overall, in terms of total power, relative power at different frequencies and functional connectivity, the burst state of the hippocampal LFP markedly differs from the suppression and continuous states, whereas the latter two states show similar characteristics in these parameters.

3.1.2. Differences in associated MUA

At baseline, some of the MUA parameters differed between states (**Table 2.1**), consistent with the impression based on visual inspection of hippocampal recordings (**Fig. 2.1A**). The pooled analysis explained in the methods revealed that states significantly differed with respect to overall firing rate (spikes per second) ($F(2,180) =$

3.37, p = 0.037), with the firing rate in the burst state being higher or tending to be higher, respectively, than in the suppression state (p = 0.02) and continuous state (p = 0.058), which did not differ (p = 0.90). States also differed significantly with respect to percentage spikes in burst ($F(2,177) = 9.44$, $p < 0.0001$), with both burst and continuous states, which did not differ significantly (p = 0.11), showing a higher percentage of spikes in bursts than the suppression state (p = 0.002 and p<0.0001, respectively). States did not differ significantly with respect to bursts per minute ($F(2,177) = 0.95$, p = 0.38) or burst duration ($F(2,172) = 1.19$, p = 0.31). Overall, this quantitative comparison of MUA parameters is consistent with the impression based on visual inspection of the MUA data in the three states (**Figure 2.1A**) that MUA activity is 'suppressed' in the suppression state compared to the burst and continuous state. It should be noted that, although these differences were suggested by visual inspection of most recordings, they were not always apparent even in recordings from different electrodes in the same rat. For example, in **Figure 2.1A** burst and suppression states clearly show higher MUA on channel 1 whereas on channel 2, which shows a higher overall firing rate, the states display similar MUA, possibly reflecting a ceiling effect.

Table 2.1: Baseline values for different MUA bursting parameters in the three LFP-states. Mean ± SEM. * indicates significant difference between states (p < 0.05), with the number indicating the pair of states that differ.

	Bursts per minute	% spikes in burst	Mean Burst duration (ms)	Spikes per second
Continuous	441.50 ± 65.95	35.10 ± 2.22*[2]	9.4 ± 0. 25	21.29 ± 5.12
Suppression	325.85 ± 47.75	20.26 ± 1.96 *[1] *[2]	8.8 ± 0. 39	24.06 ± 3.16*[1]
Burst	380.32 ± 44.03	29.26 ± 2.14*[1]	9.3 ± 0. 41	65.33 ± 18.86*[1]

3.2. Hippocampal neural disinhibition did not affect the expression of the three hippocampal LFP states

During the post-infusion period, the cumulative time spent in the different LFP states was similar in rats infused with picrotoxin and saline (**Figure 2.5**). Independent

sample t-tests revealed that there was no significant difference between the picrotoxin and saline groups in the total time spent in any of the three LFP states (continuous state, t(7)<1; suppression and burst state: t(11)<1).

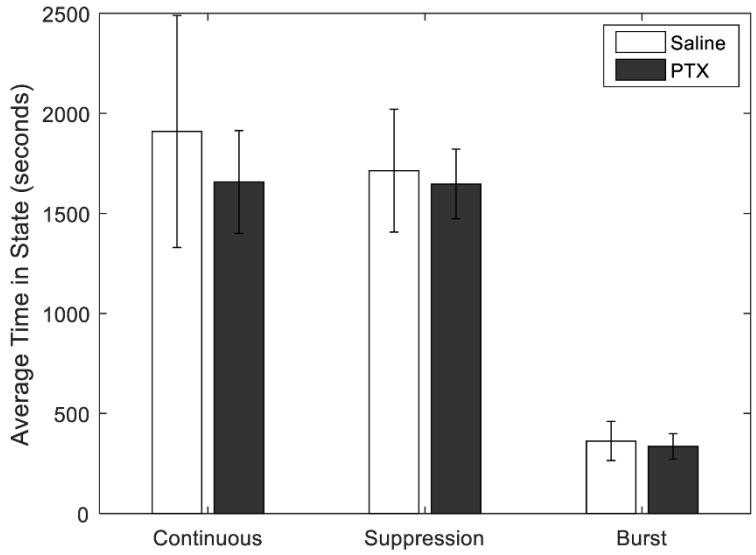


Figure 2.5: Hippocampal neural disinhibition does not affect the expression of the three hippocampal LFP states. Cumulative time (mean ± SEM) spent in each LFP state by the two drug groups during the post-infusion period.

3.3. Hippocampal neural disinhibition caused state- and frequency-dependent effects on hippocampal LFP power and functional connectivity

Hippocampal picrotoxin infusions, compared to saline, tended to increase power in the lower frequencies (<20 Hz) and to decrease power in the higher frequencies (>20 Hz), in both burst and suppression states, while having minimal effect in the continuous state (**Figure 2.6A,C,E**). However, only the picrotoxin-induced increase in power at 6-18Hz in the burst state attained statistical significance ($p = 0.017$). In the continuous state, power was numerically higher during the post-infusion period, as compared to the pre-infusion baseline; this was regardless of infusion, as indicated by a positive difference in log ratio power, especially at lower frequencies, which indicates 'baseline drift'. There was no difference between the drug groups in this state (no clusters) (**Figure 2.6A**).

Hippocampal picrotoxin tended to decrease functional connectivity (as reflected by phase-locking Eigenvalues) at higher frequencies in the burst and suppression states

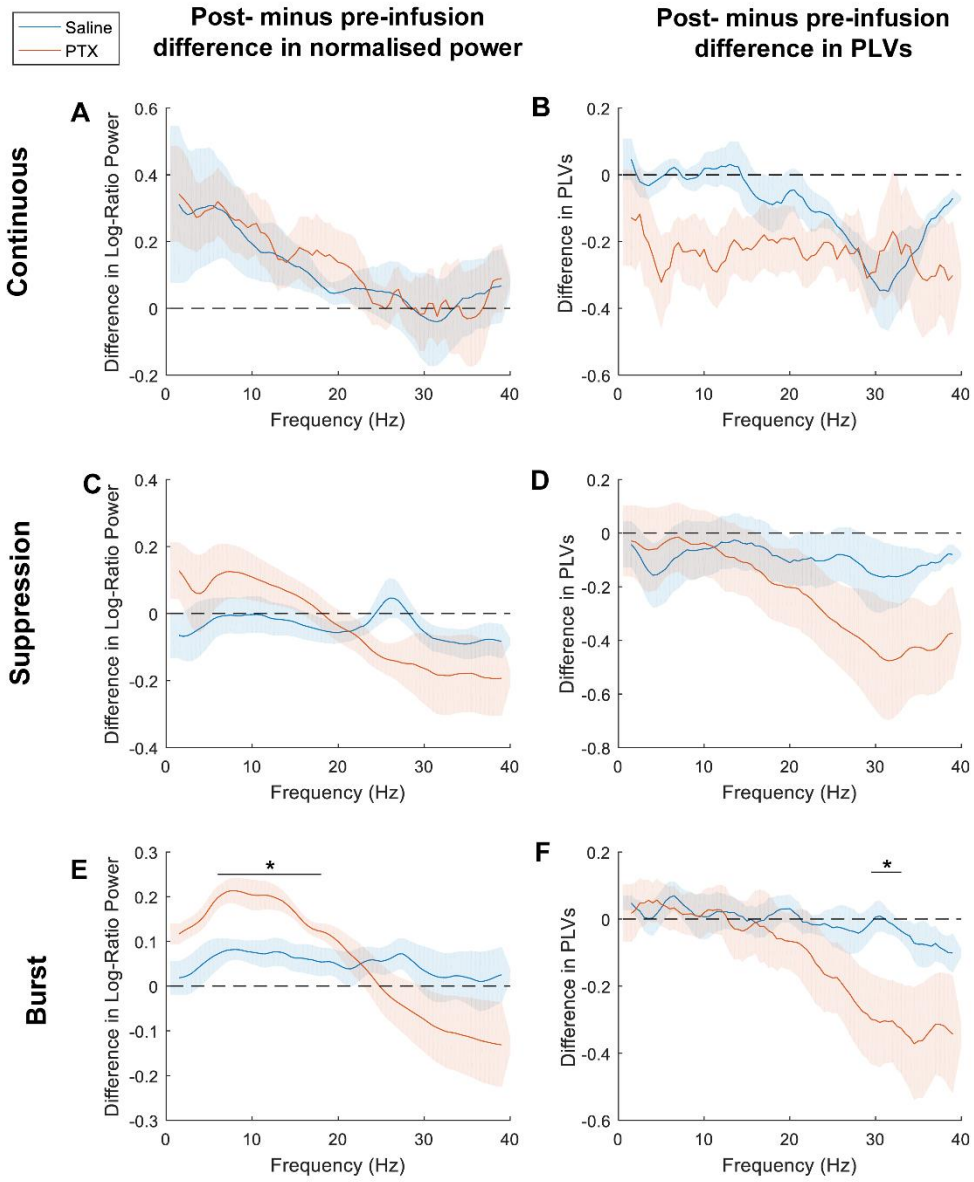


Figure 2.6: Hippocampal neural disinhibition causes state- and frequency-dependent effects on hippocampal LFP power and functional connectivity. Frequency-dependent impact of hippocampal picrotoxin or saline infusion on power (left) and on functional connectivity (right) in the continuous (top panel), suppression (middle panel) and burst (bottom) states. The logarithm of the ratio between post-infusion (saline or picrotoxin) and pre-infusion (baseline) power is shown as a measure of their respective 'difference' for both infusion groups across frequencies and separately for each state (**A, C, E**). The difference between post-infusion (saline or picrotoxin) and pre-infusion (baseline) phase-locking eigenvalues as a measure of aggregate functional connectivity is shown for both infusion groups across frequencies and separately for each state **(B, D, F).** All values shown as mean±SEM. The dotted line (value of 0) represents no change from the pre- to the post-infusion period, while positive numbers indicate an increase from baseline and negative numbers a decrease from baseline in the post-infusion period. The frequency ranges showing significant ($p<0.05$) differences between the picrotoxin and saline infusion groups based on cluster permutation statistics are indicated by an asterisk (*) and a solid line.

and at lower frequencies in the continuous state (**Figure 2.6B,D,F**). However, the picrotoxin-induced decreases in connectivity reached statistical significance only in

the burst state, in a high-frequency cluster ranging from 29.5-33 Hz ($p = 0.049$), but there was no significant picrotoxin-induced decrease in connectivity during the suppression state (no clusters). The visually apparent decrease in the continuous state (at lower frequencies) also failed to reach statistical significance, although there was a trend in a cluster from 6-7 Hz ($p = 0.065$).

3.4 State-dependence of enhanced multi-unit burst firing caused by hippocampal neural disinhibition

We first replicated the picrotoxin-induced increases in burst parameters, including burst per min, percentage of spikes in bursts and burst duration, as calculated by the Neuroexplorer software and originally reported by McGarrity et al. (2017), using a MATLAB code that could be run with the segmented LFP state-separated data (**Figure 2.7A,B,C**); the original neuroexplorer data for rats that were excluded from the LFP analysis (see Methods 2.1.) was inputted directly into MATLAB to complete the dataset for comparison of analyses (i.e., n=8 rats in the picrotoxin group and n=7 rats in the saline group). Next we plotted the time course of the multi-unit burst parameter following picrotoxin and saline infusions separately for the three different LFP states, using the state-separated multi-unit data (**Figure 2.7 D-L**) (with sample sizes for the different 5-min bins indicated in **Figure 2.3**). Visual inspection of these plots indicates that, numerically, the picrotoxin-induced increase of bursts per min appears to be weaker during the continuous LFP state (**Figure 2.7D-F**) compared to the burst state (**Figure 2.7G-I**) and suppression state (**Figure 2.7J-L**). In order to examine directly the LFP state-dependence of the picrotoxin effects, we pooled the time-deconstructed post-infusion values of the three multi-unit burst parameters, subtraction-normalised to baseline, and separated them by infusion group and LFP state (**Figure 2.7M-O**). ANOVA of these values, using LFP state and drug infusion as independent variable (see Methods 2.4.3.), revealed a significant main effect of drug infusion for all three burst parameters (outcomes of statistical analysis not shown), reflecting that, overall, picrotoxin infusion increased these values as compared saline

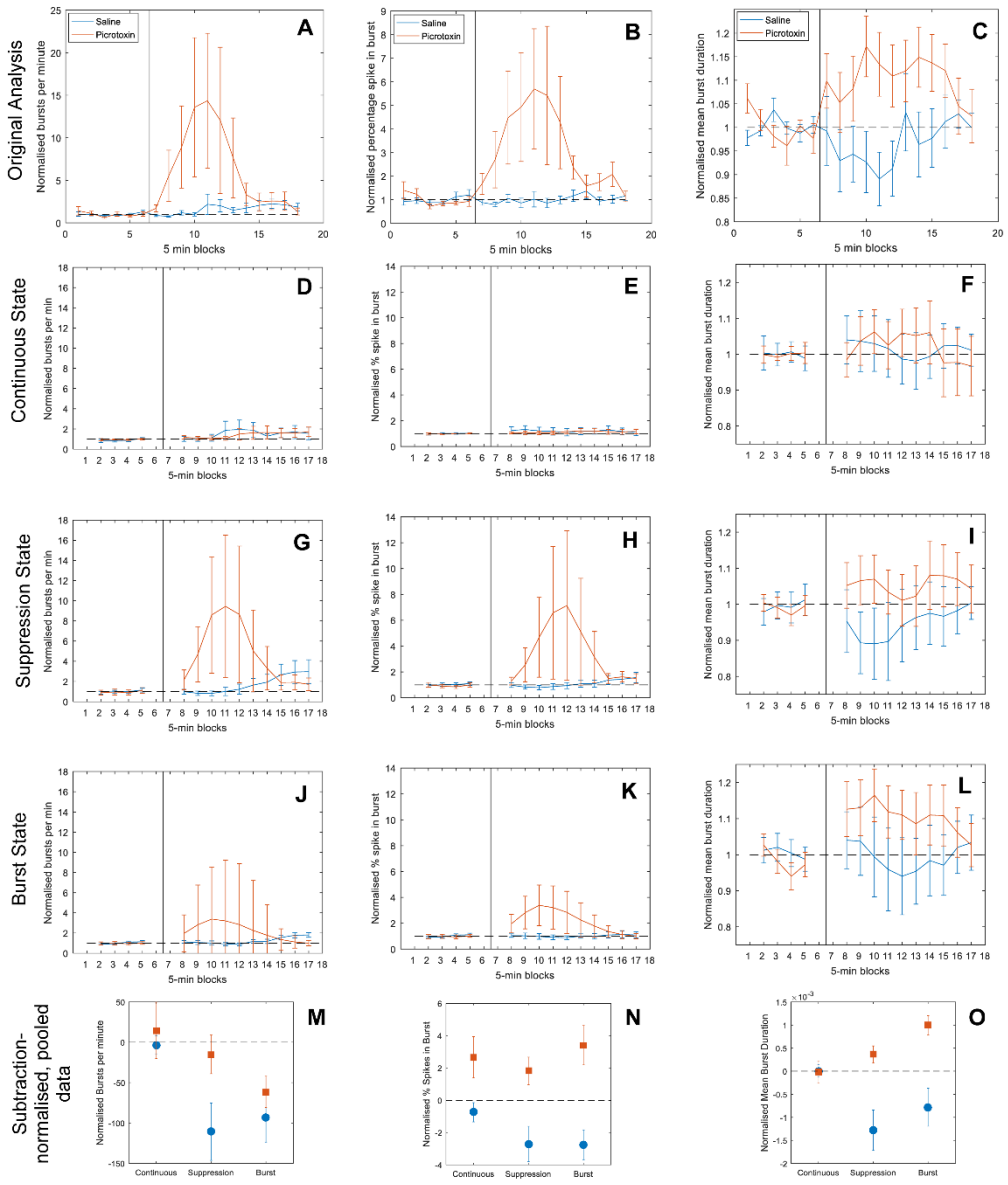


Figure 2.7: State-dependence of enhanced multi-unit burst firing caused by hippocampal neural disinhibition

The top row displays a replication of the time course of multi-unit burst parameters during baseline and following infusion of picrotoxin and saline, across all LFP states, i.e. without state separation, as originally reported by McGarrity et al. (2017), but carried out in MATLAB rather than Neuroexplorer v4. Hippocampal neural disinhibition by picrotoxin markedly enhanced hippocampal multi-unit burst firing as compared to saline infusions, as reflected by increases in (**A**) bursts per minute, (**B**) percentage spikes in burst, and (**C**) burst duration (and statistically supported by a significant infusion X time interaction, McGarrity et al., 2017). All values are division-normalised to the baseline value and mean±SEM. The three rows underneath display the same time course analysis, but separated by LFP state, using the MATLAB scripts developed in the present study: (**D,E,F**) continuous state; (**G,H,I**) suppression state; and (**J,K,L**) burst state. Visual inspection indicates that the picrotoxin-induced enhancement of burst parameters is less pronounced in the continuous, compared to the other two states. To visualise the potential interaction of hippocampal infusion and LFP state, the bottom row displays the time-deconstructed and pooled post-infusion values (subtraction-normalised to baseline, mean ±SEM) of (**M**) burst per min, (**N**) percentage spikes in bursts, and (**O**) burst duration, for the picrotoxin and saline infusion groups and separated by LFP state; these plots also indicate that the picrotoxin-induced increase in burst parameters is, at least numerically, less pronounced in the continuous than in the other two states.

infusion. Importantly, the ANOVA of burst duration (**Figure 2.7O**) revealed a significant interaction of drug infusion X LFP state ($F(2,316)=3.86$, $p=0.022$), reflecting that picrotoxin increased burst duration in the burst and suppression states, but not the continuous state. Although, numerically, the picrotoxin-induced increases in bursts per min and percentage of spikes in bursts also tended to be somewhat weaker in the continuous, compared to the other two states (**Figure 2.7M,N**), ANOVA did not support significant interactions of drug infusion X LFP state for these two parameters (burst per min: $F(2,343) = 1.118$, $p = 0.33$; percentage spikes in bursts: $F(2,343) <1$). Overall, the increased multi-unit burst duration following hippocampal neural disinhibition was markedly less pronounced in the continuous state of the hippocampal LFP, as compared to the other two states. The other two burst parameters showed numerical tendencies in the same direction, but these were not statistically significant.

4. Discussion

We, first, developed a semi-automated method based on the kurtosis of the LFP peak-amplitude distribution and amplitude envelope thresholding to separate three distinct hippocampal LFP states in the isoflurane anaesthetised rat: burst, suppression and continuous states (**Figure 2.1**), and we described some of the properties of these three LFP states. The burst state shows substantially larger overall raw power across the frequency range examined, compared to the suppression and continuous states (**Figure 2.4A**), as well as higher relative power in the delta/theta range (<15 Hz), but lower relative power in the high beta/low gamma range (>20 Hz) (**Figure 2.4B**). Moreover, compared to suppression and continuous states, the burst state showed lower frequency specific 'functional connectivity' across the recording area in the temporal to intermediate hippocampus, as reflected by reduced phase-locking eigenvalues of the LFP signals recorded from the different electrodes (**Figure 2.4C**). In terms of MUA, overall neuronal firing was higher in the burst state than in the two other states, whereas the percentage of spikes fired in bursts was higher in both the

burst and continuous states as compared to the suppression state (**Table 2.1**). Finally, the expression of the hippocampal LFP states, as reflected by the cumulative duration of these states across the recording period, was not affected by hippocampal neural disinhibition (**Figure 2.5**).

Second, and importantly, we then showed that hippocampal neural disinhibition by picrotoxin changed the hippocampal LFP in a state- and frequency-dependent way (**Figure 2.6**). In both burst and suppression states, but not the continuous state, hippocampal neural disinhibition tended to increase LFP power at lower frequencies (<20 Hz) and to decrease power and functional connectivity at higher frequencies (>20 or >15 Hz, respectively). There was also a trend towards picrotoxin decreasing functional connectivity in the theta range (6-7 Hz) during the continuous state.

Third, we also found that the increase in multi-unit burst parameters by hippocampal neural disinhibition, which we reported in a previous study (McGarrity et al., 2017), was partially dependent on the hippocampal LFP state: disinhibition-induced increases in burst duration were limited to the burst and suppression state and not apparent in the continuous state (**Figure 2.7**).

4.1 Three distinct hippocampal LFP states under isoflurane anaesthesia

Visual inspection of the LFP recorded from the temporal to intermediate hippocampus in isoflurane-anaesthetised rats indicates three distinct LFP states, including burst, suppression and continuous states (**Figure 2.1A**). We found that the kurtosis of the LFP peak and trough amplitude distribution was the best metric to separate the periods including burst and suppression states from the continuous state. Using this kurtosis measure, we thus separated the continuous state from the combined burst and suppression states, which could then be separated by amplitude envelope thresholding. Power analysis corroborated the impression based on visual inspection of the LFP traces, that raw power during the burst state is substantially higher than in the other two states, owing to large amplitude LFP bursts, and that the continuous state tends to show higher power than the suppression state (although the latter

difference failed to reach statistical significance). Interestingly, analysis of relative power revealed a marked beta/gamma shoulder (24 to 34 Hz) in the power spectra of continuous and suppression states which was absent in the burst state. Others have previously reported similar beta/gamma shoulders in the hippocampal LFP during continuous-like LFP states under anaesthesia (Land et al., 2012, *isoflurane*; Pagliardini, Gosgnach, & Dickson, 2013, *urethane*). However, if the burst state is not separated from the other LFP states, hippocampal LFP power spectra recorded under anaesthesia do typically not show a beta/gamma shoulder (Lustig et al., 2016, and our unpublished observations, *both isoflurane*). This likely reflects that the power spectra are dominated by the large-amplitude burst state (which lacks a beta/gamma shoulder). Overall, in the frequency range examined, continuous and suppression states tended to show higher connectivity, as indicated by phase-locking Eigenvalues, than the burst state across the recording area in the temporal to intermediate hippocampus. In the continuous state, a peak in connectivity was apparent at lower frequencies (<10 Hz, **Figure 2.4C**), which included the theta range, although statistically connectivity in this range did not significantly differ between continuous and suppression states. The numerically increased theta-range connectivity may correspond to findings of characteristic activity in the theta range in related hippocampal LFP states identified by others (**Table 1.1 – see Chapter 1**). More specifically, several studies have described hippocampal LFP states under anaesthesia, distinct from periods characterized by burst-suppression patterns and referred to as 'light anaesthesia' states (Land et al., 2012; Lustig et al., 2016, *both isoflurane)* or 'continuous'/ 'activated' states (Clement et al., 2008; Wolansky et al., 2006, *both urethane*), with distinct activity in the theta range (3-12Hz), although these studies did not examine connectivity within the hippocampal recording area at the frequencies we investigated. These previous studies, which all recorded from the septal (also known as dorsal) hippocampus, showed a more distinct theta peak compared to our recordings, which were from the temporal to intermediate hippocampus. This is consistent with the septo-temporal reduction in theta power that

has been reported by studies in freely moving and sleeping rats (Patel, Fujisawa, Berenyi, Royer, & Buzsaki, 2012; Royer, Sirota, Patel, & Buzsaki, 2010).

The three hippocampal LFP states differ with respect to the associated multi-unit activity. The burst state showed higher overall neuronal firing, as indicated by increased overall firing rate, than the suppression and continuous states. In addition, both burst and continuous state showed stronger burst firing than the suppression state, as reflected by a higher percentage of spikes in burst. Increased neuronal firing in the burst compared to the suppression state under isoflurane anaesthesia has been reported previously in neocortical regions (Ferron, Kroeger, Chever, & Amzica, 2009; Kroeger & Amzica, 2007; Steriade, Amzica, & Contreras, 1994) and in the subiculum (Land et al., 2012). To explain this difference, it was proposed that anaesthesia induces a hyperexcitable state with an increased extracellular Ca2+ concentration. During the burst state the high Ca2+ would facilitate synaptic transmission causing the Ca2+ to move into the neuron, which would then lead to the suppression state, a refractory period during which Ca2+ concentration is relatively high within (and relatively low outside) of the neurons, therefore decreasing the likelihood of neuronal activity until the Ca2+ is transported back into the extracellular space (Ferron et al., 2009; Kroeger & Amzica, 2007). In contrast, urethane anaesthesia does not cause such a hyperexcitable state, but instead reduces overall neural excitability by causing neural hyperpolarisation (Ferron et al., 2009; Hara & Harris, 2002; Pagliardini, Funk, & Dickson, 2013). This may explain why under urethane anaesthesia the hippocampal LFP does not show a burst-suppression pattern, but is instead characterized by a slow oscillation of about 1 Hz (Clement et al., 2008; Land et al., 2012; Pagliardini, Funk, et al., 2013; Pagliardini, Gosgnach, et al., 2013; Wolansky et al., 2006).

Taken together, our semi-automated separation method based on the kurtosis of the LFP amplitude distribution, revealed three distinct hippocampal LFP states under isoflurane anaesthesia – burst, suppression and continuous state – whose properties correspond to those of similar hippocampal LFP states under anaesthesia that had been identified previously based on visual inspection or other methods (**Table 1.1**). In unanaesthetised animals, i.e. awake or sleeping, the hippocampus (and other brain

areas) also show distinct LFP states that are characterized by the relative dominance of activity in different frequency bands and are associated with different neural firing patterns (Kay & Frank, 2019). Distinct unanaesthetised LFP states resemble distinct anaesthetised LFP states in terms of relative dominance of specific frequency bands and other properties (e.g., Lustig et al., 2016), although correspondence between specific anaesthetised and unanaesthetised LFP states is limited, not least because a defining feature of unanaesthetised LFP states is their close association with specific behavioural states (Kay & Frank, 2019). Our study of picrotoxin-induced changes in the hippocampal LFP under isoflurane allowed us to examine these changes separately from behavioural effects of hippocampal disinhibition, including locomotor changes (McGarrity et al., 2017) which are known to affect the hippocampal LFP (Kay & Frank, 2019). On the other hand, isoflurane may interact with picrotoxin, limiting the generalisability of our findings to unanaesthetised animals; at anaesthetic doses isoflurane primarily acts as a positive allosteric modulator of GABA-A receptors, enhancing the amplitude and duration of GABA's effects at this receptor (Garcia, Kolesky, & Jenkins, 2010). Isoflurane, thereby, may counteract some of the effects of disinhibition by picrotoxin, a non-competitive GABA-A receptor antagonist blocking the receptor's chloride channel (Olsen, 2006). In hippocampal neurons, picrotoxin has been shown to reduce both phasic and tonic GABA-A receptor currents (Bai et al., 2001), whereas isoflurane specifically enhances phasic GABA-A currents (Bieda, Su, & MacIver, 2009). Nevertheless, we have shown previously that hippocampal picrotoxin disinhibition enhanced hippocampal multi-unit bursting under isoflurane anaesthesia, consistent with similar effects of hippocampal disinhibition in vitro and in unanaesthetised rodents (see Discussion in McGarrity et al., 2017) and, as discussed below, LFP changes observed in the present study were consistent with previous in vitro findings. This supports that electrophysiological studies under isoflurane anaesthesia can reveal key neural effects of picrotoxin disinhibition in the hippocampus that are relevant to unanaesthetised animals. In the present study, the cumulative duration of each of the three hippocampal LFP states under isoflurane was not affected by local infusion of the GABA-A receptor antagonist picrotoxin, indicating

that the expression of the states does not depend on GABA-A receptor-mediated inhibition in the hippocampus. However, as discussed in the next two sections, hippocampal neural disinhibition by picrotoxin changed the LFP properties within the three hippocampal LFP states.

4.2 State- and frequency-dependent changes in the hippocampal LFP power by local picrotoxin disinhibition

In both burst and suppression states picrotoxin, as compared to saline infusions, tended to increase hippocampal LFP power at lower frequencies (<20 Hz) and to decrease power at higher frequencies (>20 Hz) although only the increase at 6-18 Hz in the burst state reached statistical significance. In contrast, there was no evidence of picrotoxin-induced power changes in the continuous LFP state. Our finding that hippocampal GABA antagonism by picrotoxin facilitates LFP oscillations at lower frequencies, including the theta range, is consistent with many previous in vitro and vivo findings indicating an inverse relationship between GABAergic inhibition and theta oscillations in the hippocampus (Colgin, 2016; Kowalczyk et al., 2013, also see Introduction). As reviewed in the Introduction, some previous studies have shown that GABAergic inhibition can facilitate theta oscillations under some conditions, including when more specific manipulations of GABA transmission are used (Wulff et al., 2009; Amilhon et al., 2015) and when specific mechanisms of theta generation, such as intrinsic mechanisms (Amilhon et al., 2015), are studied separately. In our study, broadly reducing hippocampal GABA-A receptor activation by picrotoxin and not separating distinct mechanisms of theta generation, we did not find evidence for such facilitating GABA mechanisms of hippocampal theta. Although we did not find any statistically significant effects of picrotoxin on hippocampal LFP power in the beta/gamma frequencies (specifically 20-30 Hz), picrotoxin tended to decrease power in this frequency band within the burst and suppression states. These numerical decreases are consistent with previous findings that pharmacological disinhibition disrupts hippocampal in vitro gamma oscillations and that GABAergic inhibition within

the hippocampus plays a key role in generating these oscillations (Bartos et al., 2007; Buzsaki & Wang, 2012; Traub et al., 2004; Whittington et al., 2000). Specifically, there is a wealth of in vitro studies showing that the GABA-A receptor antagonist bicuculline applied to hippocampal slices decreases the power of 20-30 Hz oscillations (Arai & Natsume, 2006; Boddeke, Best, & Boeijinga, 1997; Shimono, Brucher, Granger, Lynch, & Taketani, 2000; Trevino, Vivar, & Gutierrez, 2007).

4.3 Reduced functional connectivity within the temporal to intermediate hippocampus after picrotoxin disinhibition

In the suppression and burst states, functional connectivity within the temporal to intermediate hippocampus, as reflected by phase locking of the LFP signal across the different electrodes of our recording array, was decreased in the gamma range (> 20 Hz), this decrease was statistically significant in the burst state from 29.5 – 33Hz. This is consistent with previous in vitro findings that disinhibition by morphine disrupted synchrony of gamma oscillations across a hippocampal slice preparation (Faulkner, Traub, & Whittington, 1998; Whittington, Traub, Faulkner, Jefferys, & Chettiar, 1998). Synchrony was disrupted between areas that were 1.5-2.5 mm apart, whereas effects were not observed at shorter distances (Whittington et al., 1998). It is therefore possible that, in the present study, this effect was weakened, because we assessed the collective connectivity over our 2-mm electrode array, including short distances between neighbouring electrodes. Faulkner and colleagues (1998) also reported that a GABA-A receptor agonist applied to hippocampal slices causes a similar decrease in gamma-frequency synchrony, suggesting that such synchrony depends on a balanced level of hippocampal GABA inhibition. Furthermore, neuro-computational studies suggest that, through multiple mechanisms, GABAergic interneurons are important for the synchronisation of gamma oscillations (Bartos et al., 2007; Whittington et al., 2000). For example, in a neuro-computational model of hippocampal pyramidal cells and GABAergic interneurons, blocking GABA-A receptors on the pyramidal cells abolished coherence at gamma frequencies (Traub et

al., 2000). Our findings are the first in vivo findings to support these in vitro and modelling findings that the disruption of GABAergic inhibition, through blocking of hippocampal GABA-A receptors, disrupts synchronization of gamma oscillations across the hippocampus.

Finally, we found a numerical trend for picrotoxin to reduce functional connectivity in the theta frequency in the continuous hippocampal LFP state. This is consistent with previous findings that disruption of GABA-A receptor function disrupted theta coherence in vivo and in vitro (Hentschke et al., 2009; Levesque et al., 2017).

4.4 State-dependence of enhanced multi-unit burst firing caused by hippocampal neural disinhibition

Similar to the state-dependence of LFP changes, the picrotoxin-induced enhancement of hippocampal burst firing (McGarrity et al., 2017) tended to be more pronounced in the burst and suppression states than in the continuous state, although only the analysis of burst duration revealed a statistically significant interaction of the LFP state with the infusion effect. Previous findings suggest that in an isoflurane-induced burst-suppression state, the cortex is in a hyperexcitable state due to a decrease of excitation leading to a decrease in inhibition, which overall results in the excitation/inhibition balance being shifted towards excitation (Ferron et al., 2009). Neuronal hyperexcitability is also supported by the finding that, during the burst-suppression state, subliminal sensory stimuli activate cortical areas, including the subiculum, that are not activated by the same stimuli during other anaesthetised or the awake states (Kroeger & Amzica, 2007; Land et al., 2012). The more pronounced effects of picrotoxin during the burst and suppression states, compared to the continuous state, may reflect neuronal hyperexcitability during these states.

4.5 Conclusions and future directions

We have presented an objective, semi-automated method for separating three distinct hippocampal LFP states in isoflurane-anaesthetised rats, including the burst, suppression and continuous states. These states are characterized by different LFP properties and associated multi-unit activity, which are consistent with the properties of burst-suppression and 'activated' or 'light-anaesthesia' hippocampal LFP states that have previously been identified based on visual inspection and other methods (**Table 1.1**). Furthermore, our finding that the enhanced hippocampal multi-unit burst firing induced by hippocampal picrotoxin infusion is more pronounced in the burst and suppression state, compared to the continuous state, is consistent with previous studies suggesting that the burst and suppression states are characterized by neuronal hyperexcitability (Ferron et al., 2009; Kroeger & Amzica, 2007; Land et al., 2012). Our state-separated analysis of the impact of hippocampal picrotoxin infusion on LFP properties around the infusion site revealed that, in the burst and suppression states, neural disinhibition tended to increase low frequency oscillations (<20 Hz), including theta oscillations, and to decrease gamma frequency oscillations (>20 Hz), although only the picrotoxin-induced power increase between 6 and 18 Hz in the burst state was statistically significant. In addition, neural disinhibition reduced functional connectivity, as reflected by phase-locking Eigenvalues, across the recording area in the temporal to intermediate hippocampus at gamma frequencies in the burst state (with significant reductions compared to saline infusion between 29.5 and 33Hz). These findings support that GABA-A receptor-mediated mechanisms regulate hippocampal LFP oscillations in vivo (albeit under anaesthesia), confirming and extending previous findings mainly from in vitro studies that GABA-A receptor-mediated inhibition negatively modulates lower frequencies, including theta frequencies (Kowalczyk et al., 2013), and positively modulates power and connectivity at higher frequencies (Bartos et al., 2007; Buzsaki & Wang, 2012; Traub et al., 2004; Whittington et al., 2000). Similar findings albeit in neocortex have also been made in pharmacological human studies (Lozano-Soldevilla, ter Huurne, Cools, & Jensen, 2014). Cortical, including hippocampal, LFP oscillations have been suggested to be

important for memory and other cognitive functions, and alterations of such oscillations have been linked to memory and other cognitive impairments (Buzsáki & Draguhn, 2004; Colgin, 2016; Uhlhaas & Singer, 2006, 2010). Consistent with this prominent view, the frequency-specific alterations of hippocampal LFP properties caused by hippocampal neural disinhibition may contribute to the memory and attentional impairments caused by the same manipulation (McGarrity et al., 2017). However, direct evidence causally linking disinhibition-induced hippocampal LFP changes to the memory and attentional deficits is lacking and potential underlying mechanisms would also require clarification. Two important questions raised by the present findings include: i) whether similar changes in LFP oscillations would be observed without anaesthesia and ii) how such changes relate to alterations in surface EEG recordings that have been reported in relevant clinical conditions, including schizophrenia and age-related cognitive decline (Hunt, Kopell, Traub, & Whittington, 2017; Uhlhaas & Singer, 2006, 2010). To address these two questions, our ongoing studies examine the simultaneous impact of hippocampal neural disinhibition on the hippocampal LFP and on surface EEG recordings in freely moving rats.

Chapter 3: Frequency- and vigilance state-dependent effects of hippocampal neural disinhibition on hippocampal local field potential and frontal EEG oscillations, and heart-rate variability, in freely moving rats

The cognitive deficits seen within our hippocampal disinhibition model, including memory and attentional impairments, are similar to those seen in neuropsychiatric disorders, such as schizophrenia, as well as age-related cognitive decline (McGarrity et al. 2017; also refer to the introduction for a more detailed description). Importantly, the deficits seen in prefrontal cortex dependent attentional performance on the 5-choice serial reaction time test following hippocampal disinhibition suggest that hippocampal disinhibition may disrupt prefrontal function by way of hippocampo-prefrontal functional connectivity (McGarrity et al., 2017). Furthermore, in our previous experiments in anaesthetised rats we observed that ventral hippocampal disinhibition, caused by local microinfusion of the GABA-A antagonist picrotoxin, resulted in an increase in power in lower frequencies (< 20 Hz) and tended to decrease power at higher frequencies (20 – 40 Hz) in the vicinity of the infusion, indicating an effect of hippocampal disinhibition on oscillatory activity in the hippocampus (Gwilt et al. 2020; chapter 2). The purpose of the study presented in this chapter was to examine the impact of hippocampal disinhibition on hippocampal LFP activity in awake, freely moving rats and to include additional physiological measures that have greater translational utility than LFP recordings (EEG surface recordings and measures of heart rate variability, HRV).

While the recording of local-field potentials (LFPs) allows us great specificity in recording from brain areas in animal models (see introduction), opportunities to translate this measure to clinical conditions are limited due to the invasive nature of LFP recordings. The only LFP recordings available from humans are from patient populations already undergoing invasive procedures for therapeutic reasons (e.g. pre-surgical screening for medial temporal lobe resections, deep-brain-stimulation; Engel

et al. 2005; Thompson et al. 2014). Therefore, surface recordings, such as EEG, although providing limited spatial resolution, may serve as translational bridge from animal models to the clinic. While our model is focused on the hippocampus, clinical surface recordings, using EEG, are mainly limited to neocortical regions, close to the skull (Seeber et al. 2019).

There is strong anatomical and functional connectivity between the hippocampus and prefrontal cortex; the hippocampus has direct projections to the prefrontal cortex, specifically from the CA1 and subiculum to the medial prefrontal cortex (Jay and Witter 1991; Colgin 2011; Eichenbaum 2017). Hippocampal stimulation has also been shown to modulate prefrontal neural activity (Laroche et al. 1990; Degenetais et al. 2003; Tierney et al. 2004) as well as prefrontal dopamine transmission (Peleg-Raibstein et al., 2005). In addition to this, there is evidence for the interaction of the two in cognitive functions. Firstly, there is evidence that hippocampal disinhibition disrupts prefrontal cortex dependent tasks (McGarrity et al. 2017). Furthermore, recent SPECT studies from our group have shown that, following picrotoxin microinfusion into the ventral hippocampus, the activity within the prefrontal cortex is significantly increased (Williams et al., unpublished). There is also much data showing the correlation of electrophysiological activity between the two: particularly a strong correlation and connectivity between the theta-frequency and gamma-frequency activity (Colgin 2011; Eichenbaum 2017; Gordon 2011). The evidence of the high connectivity between the hippocampus and the prefrontal cortex combined with the ability to more easily record from prefrontal, as opposed to the hippocampus, in humans provides an avenue for us to investigate electrophysiological changes that may be translatable to clinic.

Another measure that can provide translatability between our rat model and clinical states is the heart rate variability (HRV), which is a measure of autonomic function within the cardiac system. HRV is normally high, thereby acting protectively against cardiac events such as myocardial infarction. In patients without any known cardiovascular disease, a decrease in HRV is the first indictor of an increased risk of a

cardiac event. Patients with psychiatric disorders have a decreased HRV, which is suggested to be linked to the increased risk they face of sudden cardiac arrest (Alvares et al. 2016). Furthermore, reduced HRV has been suggested as an endophenotype for psychotic symptom development (Clamor et al. 2016). When the HRV is assessed within the frequency domain two main bands, reflecting different functional systems, can be distinguished. The low-frequency (LF) component is mostly reflective of baroreceptor function, and is influenced by both the parasympathetic and the sympathetic nervous systems, whereas the high-frequency (HF) component reflects solely the parasympathetic nervous system activity, in particular the respiratory effects on heart-rate (Shaffer and Ginsburg, 2017). The ratio of these two frequency components (LF/HF) is sometimes considered as an indicator of dominance of either the parasympathetic or the sympathetic nervous system, however the validity of this is often questioned (Shaffer and Ginsburg 2017; Billman 2013).

Both the hippocampus and the medial prefrontal cortex have been shown to be connected with brain regions involved in cardiorespiratory control. Several anatomical retroviral tracing studies have shown bi-directional connections between the ventral hippocampus and the brainstem autonomic control regions (Westerhaus and Loewy 2001; Castle et al. 2005). Additionally, electrical and chemical studies targeting the ventral hippocampus have shown decreases in blood pressure and heart rate that is dependent on an intact medial prefrontal cortex (Ruit and Neafsey 1988), and similar manipulations of the medial prefrontal cortex results in the same (Verberne 1996). fMRI studies in humans have shown correlations between both the hippocampus and the medial prefrontal cortex, in the high frequency component of heart rate variability, with increased activity in the prefrontal cortex and anterior hippocampus correlating with increased HF/HRV (Napadow et al. 2008; Maier and Hare 2017).

Experimental plan and justification

We aimed to examine the effect of ventral hippocampus microinfusion of PTX on hippocampal LFP recording and surface EEG recordings above the frontal cortex in

unanesthetised and freely-moving rats to examine the impact on oscillations in these areas of our model. To this end, we combined our PTX microinfusion protocol with the telemetric-EEG protocol established by our industry partners at Boehringer Ingelheim (see Raith et al. 2020). Here, we implanted a depth electrode attached to a guide cannula into the right ventral hippocampus, along with a normal guide cannula in the left ventral hippocampus, an electrode over the surface of the right medial prefrontal cortex, electromyocardiogram (EMG) electrodes on the neck muscles, and electrocardiogram (ECG) electrodes to assess heart rate variability. The EMG electrodes are used to identify the existence of different vigilance states, in order to conduct analysis to mitigate changes in brain state. Additionally, as mentioned above, the heart rate variability in patients with psychotic symptoms is often decreased. Our disinhibition model already shows correlations to cognitive disorders such as schizophrenia, by assessing in these experiments the local oscillations within the hippocampus and the frontal region, as well as the heart rate variability, we will be able to add further support to our model.

Aims and Hypothesis

The aim of the study is to determine the effect of ventral hippocampal disinhibition on awake ventral hippocampal LFP and frontal surface EEG, as well as the HRV.

We hypothesise that picrotoxin infusions into the ventral hippocampus, causing disinhibition, will alter both local hippocampal oscillations recorded with a depth electrode, where we expect an increase in theta frequency power and a decrease in beta/gamma power based on previous findings (Gwilt et al. 2020), as well as oscillations within the medial prefrontal cortex, where a decrease in overall power may be anticipated based on the findings of Jodo and colleagues (2004), which may be picked up from the frontal surface electrode. This is based on the evidence in our model for the connectivity of the prefrontal cortex and hippocampus from both behavioural and imaging techniques, the impact of our model on local oscillations in the hippocampus under anaesthesia, and the well understood connectivity of oscillations between the prefrontal cortex and hippocampus. Additionally, due to the

connectivity of the ventral hippocampus to the cardiovascular system and considering evidence from human fMRI studies, we anticipate an alteration in HRV, particularly the HF component, following ventral hippocampal disinhibition.

Methods

Animals

A total of 16 young adult male Lister hooded rats (320-380g at time of surgery) (Charles River Laboratories, Germany) were used in the present study, but only 12 rats contributed data to the analysis presented (for further details and a sample size justification, please see Experimental Design). Rats were housed in single-story stainless steel cages (4 rats/cage) under a standard light cycle (6.00 a.m. – 18.00 p.m.) at a room temperature of 22 ± 2 °C and humidity of 55 ± 10 %. Water and food were available *ad libitum* throughout. All experiments were approved by the appropriate institutional governmental agency (Regierungspräsidium Tübingen, Germany) and performed in an AAALAC (Association for Assessment and Accreditation of Laboratory Animal Care International)-accredited facility in accordance with the European Convention for Animal Care and Use of Laboratory Animals. For a week prior to surgery the rats were handled daily to habituate them to the experimenters.

Surgery to combine telemetric EEG and LFP recordings with ventral hippocampal microinfusions

We adapted and combined our methods for tEEG surgery (Raith et al. 2020) and ventral hippocampal cannulae implantation surgery (McGarrity et al. 2017). The telemetric EEG system was a 4ET from Data Sciences International, (St. Paul,US), there were eight electrodes which were paired to form four channels with a positive (reference) and a negative (ground) lead, for the LFP and EEG channels the ground lead was placed over the left cerebellum. Input voltages were ±1.25mV and the recordings were filtered at 1-100Hz.

Rats were first induced into anaesthesia with isoflurane (3% in 500ml/min oxygen and 300ml/min medical air) and then further anaesthetised with a mixture of medetomidine (150ug/kg), midazolam (2mg/kg) and fentanyl (5ug/kg) injected intra-muscularly (i.m.). Following induction of anaesthesia 200ug/kg metacam was injected subcutaneously (s.c.) for analgesia. All incisions made during the procedure were cleaned with the skin disinfectant braunoderm® (BBraun, Germany). An incision was made over the abdomen where a telemetric transmitter sensing unit (4ET, DSI) was inserted in the intraperitoneal cavity and secured with a surgical stitch; the wires attached to this unit and the wire to attach the telemetric transmitter battery unit (4ET, DSI) were passed through the peritoneum. The positive electrode for the electrocardiogram (ECG) was placed above the sternum where it was secured with a surgical stitch. The peritoneum was then sutured together using a continuous suture with dissolvable suture material. Next, an incision was made above the trachea so that the negative electrode for the ECG could be tunnelled subcutaneously from the lower abdomen to be placed within the tracheal muscle and secured with a surgical stitch. This tracheal incision was then sutured close using a subcuticular suture. Next, a pocket within the subcutaneous cavity was created to house the telemetric transmitter battery unit, a stitch was made to secure placement. An incision was made to expose the skull and some neck muscle. A further tunnel within the subcutaneous cavity was created from the location of the telemetric transmitter battery unit up to the back of the skull, the remaining wires (i.e. those for EMG and EEG) were pulled through this cavity. The lower abdominal incision was then sutured up using a subcuticular suture.

The rat was then placed in the stereotactic frame where they were fixed within the ear bars with their teeth on the tooth-bar and the skull positioned flat horizontally. The EMG electrode and ground were then placed within the muscle of the neck and secured using surgical stitches. The skull was then fully exposed and Lidocaine (1%) was applied around the incision, the coordinates of bregma were taken. Holes were drilled for the EEG surface electrode above the right frontal area (+3.0mm AP, -

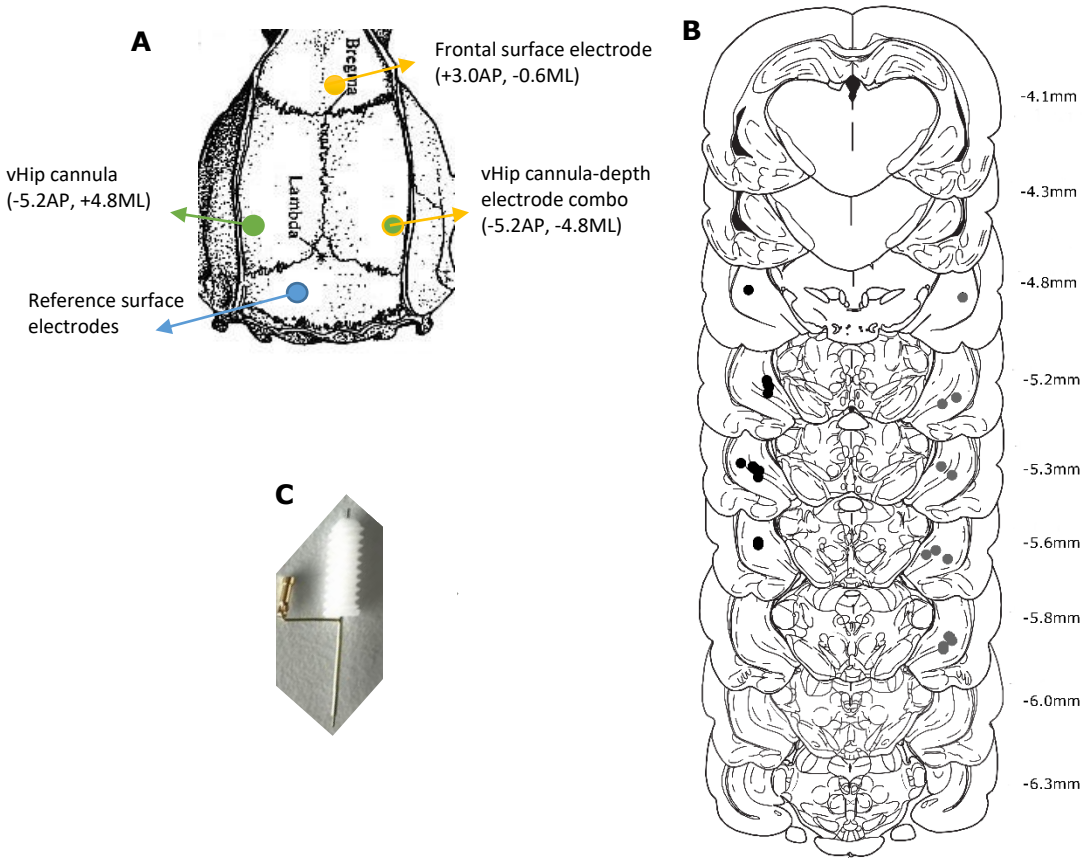


Figure 3.1

A shows the configuration of electrodes and cannulae on the skull of the rats; in the ventral hippocampus (vHip) and infusion guide cannula was implanted on the left (green dot) and a combined infusion guide cannula and depth electrode on the right (green dot with yellow outline). **B** is a representation of the ventral hippocampal cannula placements in the rats used for analysis, where the left-hand side cannula is shown in black and the right-hand side cannula-electrode combo in grey. **C** Photograph of the cannula-electrode combination, where the pin for the electrode connection can be seen on the right.

0.6mm ML) and over the left cerebellum for the ground (approximately -11.0mm AP, +1.5mm ML); drilled holes fully penetrated the skull, but dura was not punctured. Holes were then drilled bilaterally over the ventral hippocampus (-5.2mm AP, ±4.8mm ML), and dura was punctured for implantation of an infusion guide cannula (left hemisphere; stainless steel, 26-gauge, protruding 8.5mm from a plastic pedestal; Plastics One, Bilaney, US) and of an infusion guide cannula-depth electrode combination (right hemisphere; cannula specifications as above, with the addition of an insulated wire electrodes 0.23mm diameter, protruding 0.7mm from end of cannula, PlasticOnes, US); see figure 3.1A for representation of electrode montage on

the skull and depth placement in the hippocampus and figure 3.1B for a mapping of hippocampal depth placements determined through histology. Two additional holes for screws were placed bilaterally just posterior to bregma and a third hole for screws was placed on the opposite side of the cerebellum to the ground hole. The recording wire for the depth electrode was placed inside the pin of the LFP electrode (see figure 3.1C for the cannula-electrode photo) and clamped in place, then covered in silicon to minimise noise. The EEG electrode wasplaced within the drilled hole in a loop formation, the ground cerebellar electrodes (one for frontal and one for hippocampal) weretwisted together prior to insertion; these electrodes were secured in place using dental cement. The infusion guide cannula/depth electrode combination was then lowered into the ventral hippocampus, to a depth of -6.5mm from dura and again secured in place with dental cement. More dental cement was then used to cover all screws, cannulae and wires on the surface of the skull, so they were securely fixed to the skull. The head wound was then sutured up around the headcap, ensuring that wires were well covered by the skin. A mixture of atipamezole (750ug/kg), flumazenil (200ug/kg) and naloxone (120ug/kg) in saline was injected s.c. to antagonise the anaesthesia. Further metacam (200ug/kg s.c.) injections were subsequently given along with a dose of antibiotics (Marbocyl FD 1%, Vétoquinol GmbH, Ravensburg, Germany; 0.1 ml/rat, s.c.) and this was repeated for 3-5 days post-surgery.
After surgery rats were single housed for the recovery period (approximately 2 weeks) to prevent complications with the number of sutured wounds and cage-mate interaction. Upon re-entrance into mixed cages rats were observed to ensure minimal aggression towards one another.

Experimental design to measure the impact of hippocampal disinhibition on telemetric recording

Sixteen rats were used for this experiment. However, data were only collected from 12 of these because 3 rats had to be excluded due to complications with the surgery wounds and one rat had an unusable signal (i.e. non-physiological phenomenon appearing to relate to fluctuations in battery voltage). The sample size of n=12

provides power of >80% to detect differences between saline and picrotoxin conditions of Cohen's d=1, using paired comparisons and a significance threshold of 0.05. The experiment was run according to a within-subjects design, where each rat completed two recordings, one following hippocampal microinfusions of saline (0.5ul/side) and another one following hippocampal microinfusion of picrotoxin (150ng in 0.5ul saline/side) and with the order of the two drug conditions counterbalanced across rats. Prior to each infusion day, the rats were placed in the open-topped recording cages for 1 h of habituation. The infusion days consisted of the rats receiving 1 h baseline recording, before rats were removed from the recording cages, infused with saline or picrotoxin into the hippocampus, and immediately returned to the recording boxes for another 2 h of telemetric recordings. During these recording sessions data were collected using the DSI recording system for the LFP, EEG, EMG, ECG and locomotor activity.

Telemetric LFP, EEG, ECG, EMG and locomotor recordings

Recordings were made from rats within a home-cage acting as a recording chamber, grey-coloured bedding was used to cover the base of the cage to allow contrast for ethovision recording. To allow overhead video recordings, the roof of the cages were removed and a custom-made matted Perspex wall extension was placed on top to prevent rats escaping. The cages were placed on top of two RPC-2 receiver plates (DSI) to pick up and allow recording of the telemetry unit recordings, as well as measure the locomotor activity based on the movement of the rat over the plates via Dataquest ART software (DSI). There were four such recording-setups and two frequencies that were able to transmit signals, therefore to prevent interference, setups alternatively recorded from one frequency (i.e. setup 1 from frequency 1, setup 2 from frequency 2, setup 3 from frequency 1 and setup 4 from frequency 2). Prior to the beginning of recording for each rat the implanted telemetry system was switched on using a magnet passed over the implant, a PhysioTel Signal Detector (DSI) was then used to ensure the unit was switched on and transmitting.

Hippocampal drug microinfusions

For microinfusions rats were manually restrained. Drugs were administered through injection cannula's (protruding 0.5mm from tip of guide cannulae, stainless steel, 33 gauge; Plastics One, Bilaney) inserted within the guide cannula, connected to 5ul glass syringes (SGE) on an automated microinfusion pump (kdScientific, TSE systems) via flexible polyethylene tubing. The microinfusion pump was set up to dispense 0.5ul of liquid (sterile saline as a control, and 150ng/0.5ul picrotoxin) bilaterally over the course of one minute, the injection cannulas remained in place for a further minute post-infusion to ensure full infusion of the solution. Prior to infusion a bubble was marked within the tubing, success of the infusion was indicated through movement of this bubble. Post-infusion the rats were immediately returned to the recording arena.

Histology

Following completion of the experiments, rats were killed by an overdose of anaesthesia. The brains were extracted and stored in 4% paraformaldehyde for at least 3 days. The brains were then sliced on a vibratome at 80 um thickness. Cannula and electrode placements were then mapped on drawings of coronal brain sections taken from the atlas by Paxinos and Watson (1998), based on light microscopic examination of the unstained slices.

Data Analysis

Locomotor Activity

Arbitrary counts of locomotor activity were recorded from the DSI system, where the system recorded a value for each second. To compare to our previous locomotor studies with picrotoxin infusion (McGarrity et al. 2017, and chapter 6) we summed the activity measure into 10 min bins, which resulted in 6 baseline and 12 post-infusion bins. A two-way repeated measures ANOVA was run over the post-infusion period with 10-min bin and drug as the variables.

Vigilance states

To separate out different vigilance states based on locomotor and EMG data, the data were initially separated into 4-s segments as in a previous study (Raith et al. 2020). All 4-s segments where any locomotor activity was detected by the DSI system were extracted as ‘active wake’ data. For the remaining 4-s segments, a power analysis was performed on the EMG data, using a Hanning window encompassing 10-60Hz; this frequency range was selected based on Stephenson et al (2009) with 60Hz maximum instead of 100Hz due to our EMG cut-off. The sum of power over all frequencies in the EMG of each segment was then taken, and this was used to create a histogram with 500 bins. The threshold for separating ‘quiet wake’ from ‘sleep’ was determined in most cases as either the first or second minimum in the histogram (special cases meant a fourth and seventh minimum were used, based on visual separation comparable to other cases), reflecting the reduced muscle tone during sleep. 4 s segments that exceeded this threshold were marked as in the quiet wake state, and the sub-threshold segments were marked as sleep. To separate the sleep data further into REM and NREM the EMG power across all frequency sums were again combined into a histogram, this time with 50 bins, and the first, second or third minimum was selected, dependent on which separated the data most effectively, as the threshold. The segments that exceeded the threshold were assigned as NREM and those that were sub-threshold were assigned as REM, due to the REM state having extremely low muscle tone. It should be noted, that in contrast to the separation of states under anaesthesia (Gwilt et al. 2020), this method was designed to increase the efficiency of sleep scoring but is still largely reliant on subjective interpretation.

Heart-Rate Variability

Heart rate variability (HRV) analysis was conducted in Ponemah 6.41 (DSI), where the RR-interval was used to assess the heart rate variability (Based on methods in Meister et al. 2019; Fauchier et al. 2006). Data were parsed into four 1 min segments from 20-24 min in the baseline and 20-24 min post-infusion. The data were analysed

in the frequency domain where interpolation was at a rate of 50Hz using a quadratic method with 20ms tolerance, and the calculation of HRV used a Hanning window and analysed between 0 and 5Hz. The low frequency (LF) component was defined at 0.25-1Hz and the high-frequency (HF) was 1-3Hz. Data were averaged over the 4 min segments and then a mean and standard-error of the mean were calculated for plotting. Two-way repeated measures ANOVA was used to assess the difference between the baseline and post-infusion HRV measures in both drug conditions.

tEEG

All data were exported via EDF file and imported into MATLAB (R2016a, MathWorks) where analysis was run with the Fieldtrip software (Oostenveld et al. 2011). All data initially underwent an independent component analysis (ICA) rejection routine where any ECG and EMG contamination of the EEG/LFP channels was removed, and any contamination from ECG or EEG/LFP were removed from the EMG. Next, the EEG/LFP channels underwent preprocessing with a bandstop filter from 49.5-50.5Hz and baseline correction; the EMG channel also underwent pre-processing with a bandstop filter from 49.5-50.5Hz, a high-pass filter at 60Hz and a Hanning window filter. To remove movement artefacts from all channels, a z-value based artefact detection routine was run over the EMG channel where segments that exceeded the z-value of 14 with a minimum time of 0.5s and 0.05s padding were removed from all channels.

Prior to any further analysis, and following separation into vigilance states, all data underwent an artefact rejection routine to remove marked spike-wake discharges that were seen after infusion in the hippocampal LFP and frontal EEG recordings, especially during the first 10 min and in the picrotoxin condition (see Results, Visual inspection of frontal EEG and hippocampal LFP traces), so that the fast-fourier transformation was not convoluted. This was done using a z-score artefact detection in the fieldtrip toolbox, where a z-value cut-off was set at 5 and a 0.25 s padding was used.

Frequency Analysis

For the frequency analysis of EEG and LFP data, data were analysed separately for the 60-min baseline, first 60 min post infusion (0-60min) and the second 60 min post infusion (61-120min). The REM state was removed from any separated vigilance state analysis due to the low time spent in the state and therefore lack of sample size to analyse robustly. Similar to our previous analysis of anaesthetised LFP recordings (Gwilt et al., 2020; chapter 2), the frequency analysis was run using a fast Fourier transform with a Hanning window, from 0.5 to 45 Hz, over the raw data for each state. To compare the differences between the vigilance states during the baseline recording cluster permutation was run between each pair of groups in a similar manner to previously (Gwilt et al. 2020; chapter 2), however this time a dependent samples t-test was used in place of an independent samples due to the within-subjects design. All frequency-based graphs were plotted using a moving average of 5 bins (2.5Hz) over the mean values for each frequency with the standard error of the mean. To compare infusion effects in the picrotoxin and saline drug conditions, a difference score was calculated for each frequency bin by taking the log of raw power in the post-infusion frequency bin divided by the pre-infusion frequency bin, as in our previous analysis of anaesthetised LFP recordings. To assess statistically the difference between pre and post-infusion we used a cluster permutation test as previously described above for the baseline data.

Results

Cannulae and LFP electrode placements in the ventral hippocampus

All cannulae and LFP electrodes were consistently placed within the ventral hippocampus within -4.8 to -5.8 from bregma, as was to be expected (see figure 3.1B).

Locomotor Activity

Baseline locomotor activity was similar in picrotoxin and saline conditions and decreased similarly over the 1-h duration of the baseline session, reflecting locomotor

habituation (no main effect or interaction involving the prospective infusion condition, $F < 1.4$, $p > 0.26$, and a significant main effect of time $F_{5,55} = 55$, $p < 0.001$) (Fig. 3.2A, left). During the post-infusion period the picrotoxin condition showed increased locomotor activity compared to the saline condition for the first 40-50 min following infusion, after which activity levels were very low in both conditions due to habituation (interaction drug*time: $F_{11,121} = 13.6$, $p < 0.0001$) (Fig. 3.2A, right).

Time in vigilance states

Time spent in the different vigilance states showed similar time courses in the two prospective infusion conditions during baseline, but following infusion significant differences emerged between the two infusion conditions (Fig. 3.2B). During the baseline the time spend in the active wake gradually declined over time, while time in NREM sleep gradually increased. The time spent in the quiet wake state stayed relatively constant, with slightly more time spent in the middle of the baseline period, whereas the REM sleep was barely seen during the baseline, with a slight increase towards the end of the period. Time spent in the active wake state was increased following picrotoxin infusion compared to saline infusion, with both decreasing their time in this state over time (drug*time interaction $F_{11,121} = 11.28$, $p < 0.0001$), consistent with the locomotor data (Fig. 3.2A). Quiet wake was more prevalent in the saline condition for the first 20 min post-infusion and the last 20 min post-infusion compared to saline (drug*time interaction $F_{11,121} = 1.922$, $p = 0.043$). The time in the NREM state generally increased over time, but was reduced following picrotoxin infusions compared to saline infusions from about 10-40 min following infusions (drug*time interaction $F_{11,121} = 2.46$, $p = 0.0084$). Similarly to the NREM there is a general increase over time in the time spent in REM, however there was no difference between the drug conditions (drug*time interaction $F_{11,121} = 0.486$, $p = 0.91$, main effect of time $F_{11,121} = 6.43$, $p < 0.0001$). Overall, the differences seen between the drug conditions in the times spent in the different vigilance states were evident within

the first hour following infusions, when rats infused with picrotoxin spent more time in the active wake state, and, correspondingly, less time in quiet wake or sleep (NREM)

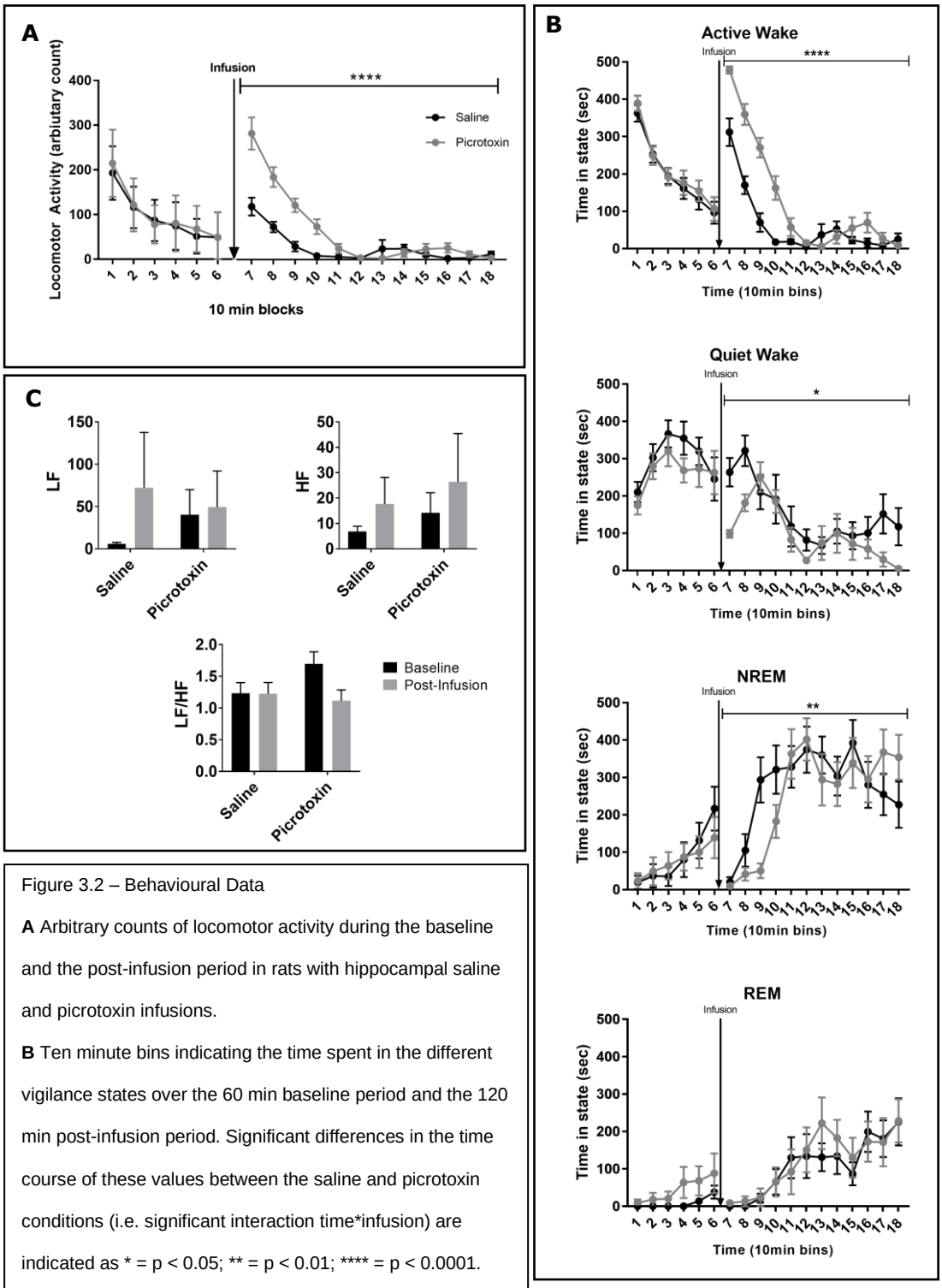


Figure 3.2 – Behavioural Data

A Arbitrary counts of locomotor activity during the baseline and the post-infusion period in rats with hippocampal saline and picrotoxin infusions.

B Ten minute bins indicating the time spent in the different vigilance states over the 60 min baseline period and the 120 min post-infusion period. Significant differences in the time course of these values between the saline and picrotoxin conditions (i.e. significant interaction time*infusion) are indicated as * = $p < 0.05$; ** = $p < 0.01$; **** = $p < 0.0001$.

C Heart Rate Variability: the Low-Frequency (LF) components, the high-frequency (HF) components and Ratio of LF and HR, all in a 4-min segment during the baseline and during the post-infusion for both drug infusion conditions.

states than rats infused with saline.

Heart-Rate Variability

LF and HF showed quite high variability and a statistical analysis did not reveal any significant changes related to the time point (pre- or post-infusion) or drug condition (saline or picrotoxin) (all $F<2.51$, $p>0.13$) (Fig. 3.2C, top row). The ratio between the LF and HF was very similar during both baseline and post-infusion in the saline condition, whereas this ratio was higher at baseline than post-infusion in the picrotoxin condition, suggesting that picrotoxin decreased the LF/HF ration (Fig. 3.2C, bottom). However, although infusion induced changes were mainly apparent in the picrotoxin condition, the ANOVA of the LF/HF ratio revealed only a significant main effect of time ($F_{1,11} = 5.46$, $p = 0.039$), but no effect of drug ($F_{1,11} = 0.99$, $p = 0.34$) or a significant drug*time interaction ($F_{1,11} = 1.83$, $p = 0.20$), which would have statistically supported any differential time course in the two drug conditions.

Comparison of frequency-dependent power in the different vigilant states

There were marked and statistically significant differences in raw power between vigilance states in the frontal EEG recordings (Fig. 3.3A), but not in the hippocampal LFP recordings (Fig. 3.3B). More specifically, in the frontal EEG recordings, raw power was significantly higher at lower frequencies in the NREM state compared to the active wake (9.5-23Hz cluster $p = 0.0027$) and quiet wake (1-18.5Hz cluster $p = 0.0013$) states, whereas raw power at higher frequencies was significantly lower in the NREM state than the quiet wake state (27-44.5Hz cluster $p = 0.0020$). Moreover, in frontal EEG recordings, the quiet wake state had higher power at the lower frequencies than the active wake (1-7Hz cluster $p = 0.006$, 10.5-15.5Hz cluster $p = 0.0073$, 18 – 23.5Hz cluster $p = 0.0033$) and lower power at the higher frequencies (32-44.5Hz cluster $p = 0.0006$).

There were marked and significant differences in relative power at different frequencies, as revealed by the analysis of the normalised power, between vigilance states both in the frontal EEG recordings (Fig. 3.3C) and the hippocampal LFP

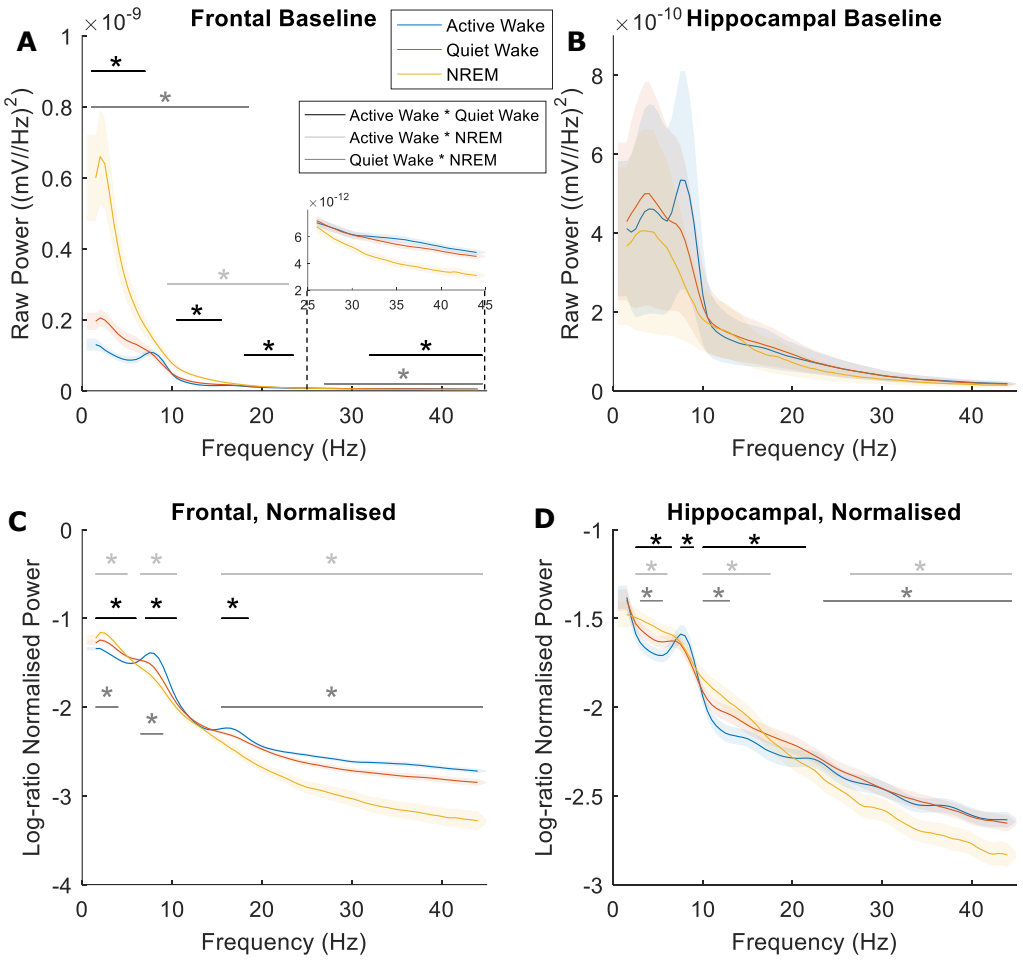


Figure 3.3 – Baseline (i.e., pre-infusion) power spectra of hippocampal LFP and frontal EEG recordings during different vigilance states.

A and **B** show the raw power spectra for of the frontal EEG and hippocampal LFP, respectively. Significant differences between vigilance states are indicated as * = $p < 0.01$, with the legend indicating between which groups the significance lies. **C** and **D** show the log-ratio normalised power spectra for the frontal EEG and hippocampal LFP, respectively. Significant differences are indicated as in **A** and **B**.

recordings (Fig. 3.3D). In both frontal EEG and hippocampal LFP recordings, there was a marked theta (6-15 Hz) peak in the active wake state, which was substantially diminished in the quiet wake state and absent during NREM sleep. Moreover, in both recordings the quiet and active wake states were characterized by higher relative beta/gamma activity (16-45Hz) (a gamma 'shoulder' in the power spectrum) compared to NREM sleep. More specifically, statistical analysis revealed an increased relative theta power in the active wake compared to the quiet wake (Frontal: 7-15.5Hz cluster $p = 0.019$; HPC: 7.5-9Hz, cluster $p = 0.045$) and the NREM (Frontal: 6.5-10.5 cluster p

= 0.019) states, whereas the quiet wake had greater power in this range than the NREM (Frontal: 6.5-9Hz cluster p = 0.044). At the higher frequencies less relative power was seen in the NREM than the active wake (Frontal: 15.5-44.5Hz cluster p = 0.0006; HPC: 26.5-44.5Hz cluster p = 0.0033) and quiet wake (Frontal: 15-44.5Hz cluster p = 0.0013; HPC: 23.5-44.5 cluster p = 0.004), with mostly little difference between active and quiet wake apart from in the frontal region from 15.5-18.5Hz (cluster p = 0.029) where the active wake had greater power than the quiet wake. Additionally, at delta frequencies there was greater relative power in the NREM state than the active wake (Frontal: 1.5-5Hz, cluster p = 0.019; HPC: 2.5-6Hz, cluster p =

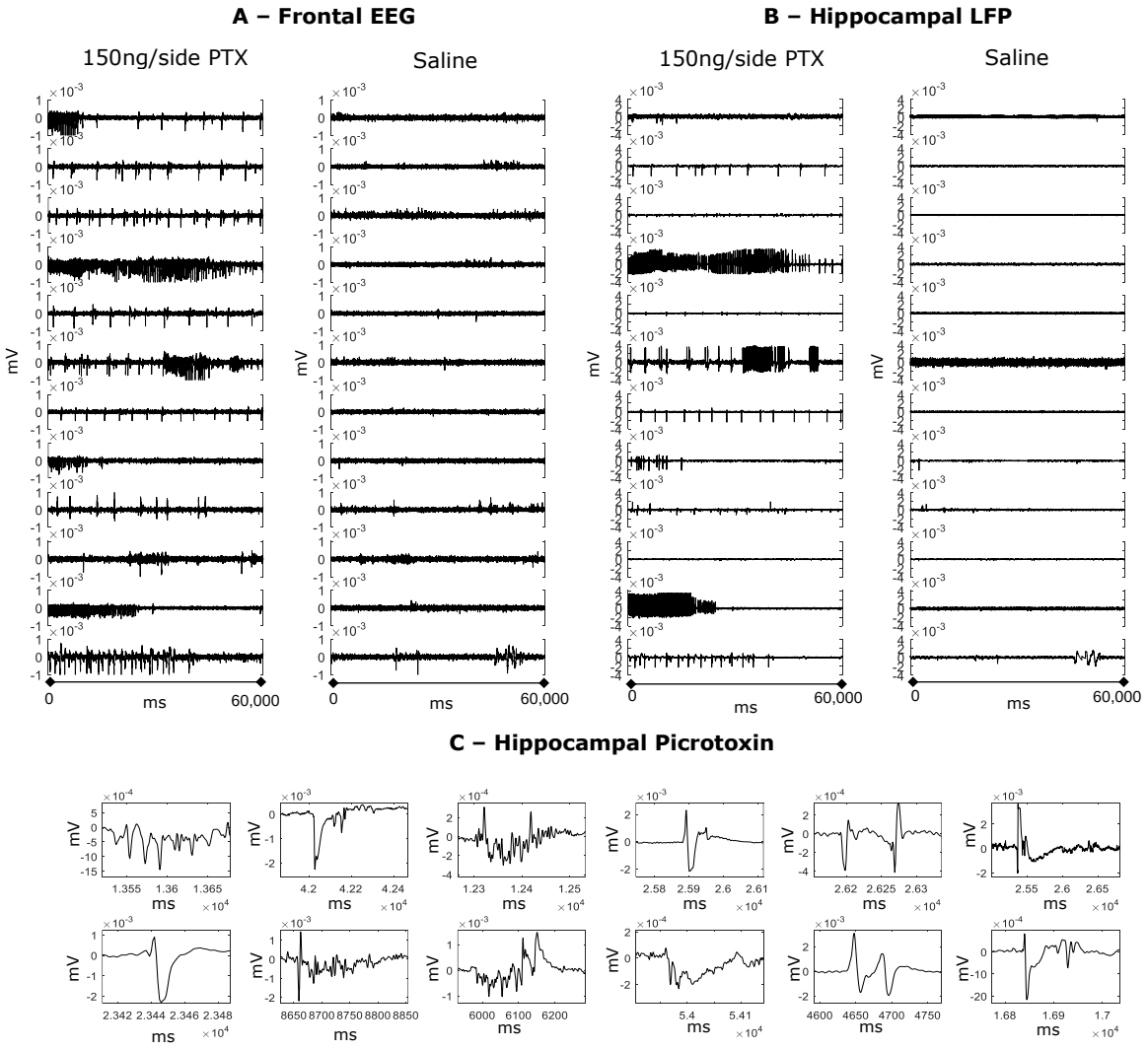


Figure 3.4 – Raw traces of one minute segments from 1.5 minutes post-infusion

A shows the frontal traces and **B** shows the hippocampal traces in all 12 rats used in analysis after both their picrotoxin and saline infusions. **C** shows randomly selected examples of an individual spike-wave pattern from each rat's hippocampal LFP trace in the picrotoxin condition (shown in **B**) with an expanded time line to show the shape of the spike-wave pattern.

0.019) and quiet wake (Frontal: 1.5-4Hz cluster p = 0.0453; HPC: 3-5.5Hz, cluster p = 0.049), while the active wake had higher relative power than the quiet wake (Frontal: 1.5-6Hz cluster p = 0.016). In the hippocampal, but not the frontal, recording the active wake state had relatively lower mid-frequency power than either the NREM (10-17.5Hz cluster p = 0.012) or the quiet wake (10-21.5Hz cluster p=0.002), while the quiet wake had lower relative power than the NREM (10-13Hz cluster p = 0.045).

Visual inspection of frontal EEG and hippocampal LFP traces following hippocampal infusions

As can be seen in figure 3.4 there was a distinct spike-wave like activity after infusion, particularly in the picrotoxin condition in both the frontal and hippocampal recordings. This activity was not analysed in detail, however anecdotally it was most prevalent for the first 10 minutes post-infusion. Closer visual inspection of the spike-wave pattern revealed substantial heterogeneity across different rats (figure 3.4C).

Frequency analysis: All States Combined

When data across all vigilance states were combined (Fig. 3.5), power increased over time, i.e. between pre- and post-infusion periods at lower frequencies (<20 Hz), especially in frontal EEG recordings, but to a lesser extent also in the hippocampal LFP recordings, regardless of the infusion condition; this was reflected by positive difference scores between post-infusion and pre-infusion measures. In contrast, in both frontal EEG and hippocampal LFP recordings, power decreased at higher frequencies (>20 Hz), reflected by negative difference scores. Hippocampal picrotoxin infusions tended to decrease overall power in both frontal EEG and hippocampal LFP recordings at frequencies > 10 Hz, compared to saline infusions, especially during the first 60 min after infusions, as reflected by lower difference scores in the picrotoxin compared to the saline condition. This decrease in power was statistically significant in the frontal EEG recordings from 15.5 to 22.5Hz (cluster p = 0.043).

Frequency analysis: State-specific

Significant picrotoxin-induced changes were mainly limited to a decrease of power at higher frequencies (>15 Hz) in the hippocampal LFP during the first 60 min after infusions, whereas consistent picrotoxin-induced changes were not evident from the frontal EEG and during the second 60 min post-infusions. During the active wake state the significant decreases in the hippocampal electrode in the first hour (figure 3.6A) lay between 16.5 and 44.5Hz (cluster p = 0.0053). While in the quiet wake (figure 3.6B) significance was seen from 30-34Hz (cluster p = 0.037) and from 36.5-39.5Hz (cluster p = 0.043), and during the NREM state (figure 3.6C) the difference was seen from 25-29.5Hz (cluster p = 0.032), 32-36.5Hz (cluster p = 0.023) and 38-

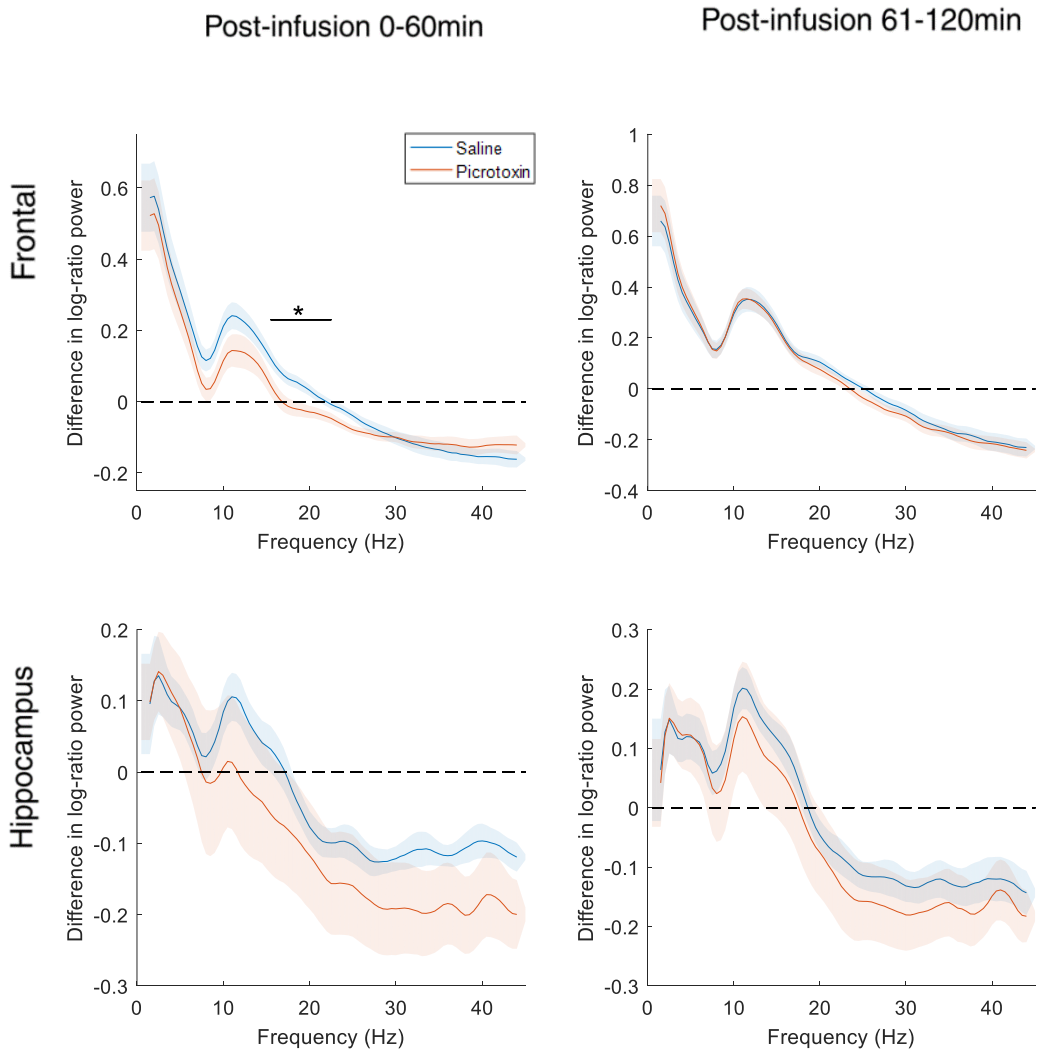


Figure 3.5 – Difference in the log-ratio power between both the post-infusion 0-60min and post-infusion 61-120min and the baseline power over all data

Significant differences between drug groups where * = p < 0.05

44.5Hz (cluster p = 0.019). While changes in the second hour post-infusion were only detected as a picrotoxin-induced decrease from 24.5-28Hz in the hippocampus during active wake (cluster p = 0.027), and a picrotoxin-induced decrease in the frontal electrode during NREM from 24-26Hz (cluster p = 0.049). Although no significant

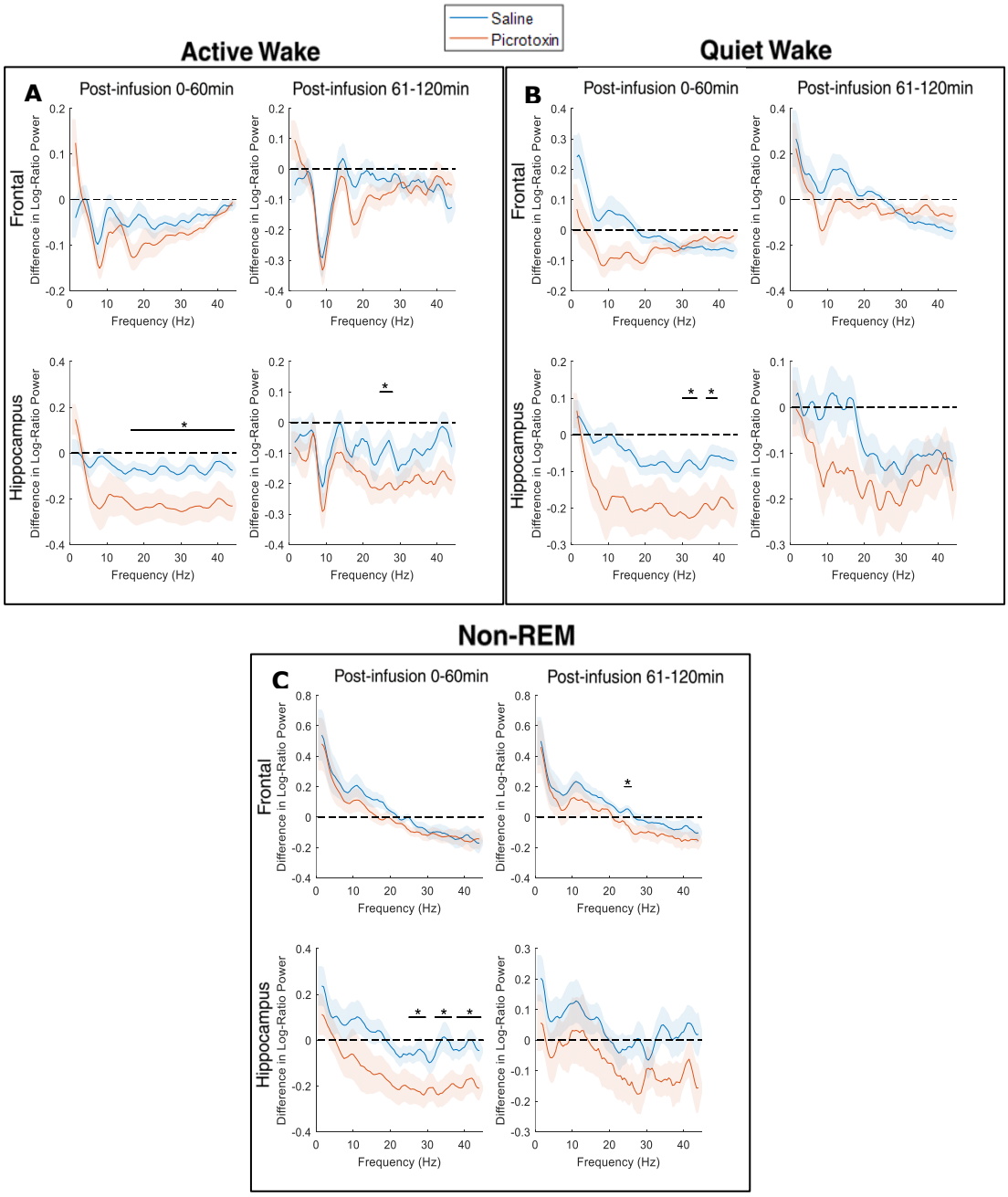


Figure 3.6 - Difference in the log-ratio power between both the post-infusion 0-60min and post-infusion 61-120min and the baseline power over **A** the active wake **B** the quiet wake and **C** the NREM states, in the frontal EEG (top) and hippocampal LFP (bottom)

Significance is indicated as * = p < 0.05

differences were seen at the lower frequencies, there was a general decrease induced by picrotoxin in all except the active wake state.

Discussion

We confirmed that hippocampal disinhibition increases locomotor activity and extended these findings by showing that this corresponds to picrotoxin-induced changes in the time the rats spend in different vigilance states, with hippocampal picrotoxin increasing the time in the active wake state and decreasing time in the quiet wake state and NREM sleep. Moreover, we showed that hippocampal disinhibition decreased power at the mid-to-high frequencies in the hippocampal LFP recorded in unanaesthetised rats, whereas there was limited evidence that hippocampal disinhibition would markedly affect frontal EEG recordings (apart from the spike-wave discharges apparent mainly within the first 10 min after infusion, see discussion below).

Encouragingly, the normalised frequency spectra of the baseline vigilance states shows the aspects by which each is defined. The active wake state shows a distinct theta-peak that is higher than in either the quiet wake and the NREM and is characteristic of the locomotor activity within this period (Colgin 2011; Brown et al. 2012). Whereas the NREM state shows greater relative power at lower frequencies, within the delta range, which is commonly shown as characteristic of this stage of sleep (Brown et al. 2012; Adamantidis et al. 2019). While quiet wake does not have such strong peaks associated with it like the active wake and the NREM do, the quiet wake state is shown to have greater gamma-frequency power (Brown et al. 2012); our data shows such a relatively greater power at gamma in the quiet wake compared to the NREM, but not to the active wake.

Hippocampal disinhibition initially causes globalised neurological activity

The raw traces from the frontal EEG and hippocampal LFP regions shows a noticeable pattern in the picrotoxin condition, where distinct spikes can be seen,

occurring rarely in the saline condition. The presence of this frontal activity, as well as the hippocampal activity, is indicative of picrotoxin in the hippocampus causing a globalised effect. Under anaesthesia we did not see such an effect of spiking within the hippocampus (McGarrity et al. 2017), while somewhat comparable activity was noted in the prefrontal cortex under anaesthesia when picrotoxin was infused locally (Pezze et al. 2014). Furthermore, in contrast to seizure-like spike-wake discharges (Bragin et al. 2009), the individual waveforms of the spikes in our data was not consistent over all of the rats (figure 3.3C). Most importantly, the activity we see within this data set is not what is seen in seizure activity, i.e. spike and wake discharges, which is corroborated by the absence of any behavioural signs of seizure in the rats.

Hippocampal disinhibition reduces time spent in quiet wakefulness and NREM sleep

When frequency analysis was run over the whole data set, irrespective of vigilance state, the only significant difference between drug conditions was a decrease in the power of the picrotoxin condition at 15-22.5Hz during the first hour in the frontal electrode. However, nothing alluding to this change was detected in any of the vigilance states analysed, and therefore this is likely a result of differences in the vigilance states of each condition during this time-window. Most notably, during the picrotoxin condition rats spent more time in the active wake state and less time in the quiet wake and NREM sleep states. This emphasises the importance of separating out the different vigilance states from one another in order to reveal specific drug-induced effects in the power spectra, much the same as the anaesthetic states previously (Gwilt et al. 2020). Consistently in all states there was a decrease in the power during the first hour post-infusion in the hippocampal recording, spanning approximately 17 to 44.5Hz when comparing picrotoxin to saline infusion. Some changes within this range appeared to linger, or appear, in the second hour post-infusion in the active-wake of the hippocampal LFP and during the NREM of the frontal EEG, although being more restrained to 24-28Hz.

Hippocampal disinhibition reduces low gamma power in hippocampal LFP, but does not markedly affect theta in unanaesthetised rats, with limited effects on frontal EEG recordings

Somewhat contrasting with our previous findings that picrotoxin infusion into the ventral hippocampus increased power in the theta frequencies and tended to decrease power in the high beta/low gamma frequencies in the hippocampal LFP of anaesthetised rats (Gwilt et al. 2020), the present study of picrotoxin-induced changes in the hippocampal LFP in unanaesthetised rats revealed only a decrease of power in the high beta/low gamma frequencies with no significant effect (and, if at all, a decrease) in the theta frequencies. The significant decrease in high beta/low gamma power within the hippocampus adds support to the trend seen in our previous study in anaesthetised rats, and is in line with the literature (predominantly in vitro) that consistently shows a decrease in low gamma frequencies from GABA-A antagonism in the hippocampus (see section 4.2 of Gwilt et al. 2020 for a more detailed discussion). The differences that we see in the effect of picrotoxin on theta amplitude under anaesthesia and wake/sleep states is likely a consequence of the anaesthetic action. As discussed in the introduction of Gwilt et al. 2020, there is varying evidence for whether hippocampal theta is increased or decreased following GABA-A antagonism. Generally, decreased theta power is seen in the hippocampus under isoflurane anaesthesia (Gwilt et al. 2020; MacIver and Bland 2014); therefore, it is possible a ceiling effect during natural wake and sleep prevents the theta-power increase we see under anaesthesia.

One of the interesting additional findings from this study is a lingering effect on high beta/low gamma power from picrotoxin in the second hour post-infusion; previously we have only assessed the LFP in the first hour post-infusion (Gwilt et al. 2020), due to both the behavioural and multi-unit peak effects falling at around 15-45mins post-infusion, and appearing to taper off after 1 hour post-infusion (McGarrity et al. 2016). Therefore, the lingering effects around 24-28Hz may indicate this as the strongest affected frequency range. Furthermore, the only effect seen within the frontal electrode is in the second hour post-infusion at this frequency range. The lack of

significant effect in the frontal electrode in general is likely due to the lack of specificity in recording compared to the hippocampal depth electrode; where the mPFC that we expect to be altered lies below the motor cortex, which does not have similar connections to the hippocampus and therefore is not likely to be altered as much by our hippocampal disinhibition. Therefore, the significant change we see in this recording is likely reflective of either: a substantial effect within the mPFC or an event within another region around the recording site, or a sampling error. Considering the occurrence of this change at the same frequency as effects are seen within the hippocampus (24-28Hz) as well as these changes being seen only within the NREM sleep suggests this change is less likely a sampling error and may arise from the mPFC. Synchrony between the hippocampus and mPFC is shown to be greater in NREM and cognitive tasks, than in resting wake (Sigurdsson and Duvarci 2016; Headley and Paré, 2017; Colgin 2011). Our evidence for downstream effects of hippocampal disinhibition on the frontal regions is tentative at best. Considering the differences in anatomy of rat brains and human brains, a more sensitive measure may be to record medial prefrontal cortex activity with a depth electrode instead of a surface electrode to establish if there are downstream effects that may be picked up in human surface recordings. In any case, the inter-species differences in medial prefrontal cortex results in limits to the translation from rats to humans in this case.

Hippocampal disinhibition had, if at all, only moderate effects on parameters of HRV

The most consistent HRV change in unmedicated patients with schizophrenia is a decrease in the high-frequency component (Clamor et al. 2016; Hempel et al. 2009; Bar et al. 2005; Mujica-Parodi et al. 2005; Chang et al. 2010; Liu et al. 2016), with often no change in the low-frequency component (Hempel et al. 2009; Bar et al. 2005; Chang et al. 2010; Chang et al. 2009). A few studies show a decrease in the low-frequency component (Mujica-Parodi et al. 2005; Liu et al. 2016). In our data we do not see any difference in either the low-frequency or the high-frequency component after picrotoxin infusion. We did see a reduction in the LF/HF ratio from baseline to post-infusion in the picrotoxin condition, however this is in contrast to the high-

frequency component reducing and the low-frequency component staying constant in schizophrenia patients, which is confirmed in the findings of an increased LF/HF in Chang et al. 2010. There is one study that appears to support the reduction in LF/HF ratio that we see, where despite not reporting the LF/HF, they saw a reduction in both the LF and the HF but the LF decreased more, which would result in a decreased LF/HF (Mujica-Parodi et al. 2005). Although this measure has been used in varying degree's within patient literature, there is very little work assessing the heart rate variability in rodent models of schizophrenia; a pubmed search of 'heart rate variability rat schizophrenia' throws up one paper (Klarer et al. 2017). However, instead of assessing the impact of a rodent schizophrenia model on the heart rate variability, they instead model the reduced vagal activity that results in the changes in HRV, and assess the impact on behavioural and chemical phenotypes of schizophrenia.

In addition to this, the heart rate variability is shown to be different between different stages of wake and sleep (Vanoli et al. 1995; Kontos et al. 2020). Given the significant differences we see in the time spent in each wake/sleep state post-infusion, this will be acting as a confounding factor when assessing the effect of picrotoxin on the HRV. Thereby, although we see a difference in the LF/HF ratio, we cannot attribute this to a direct impact of picrotoxin (independent of picrotoxin's effect on sleep) and therefore cannot draw conclusions in light of the significant effects seen within schizophrenia patients.

Clinical implications and conclusions

These findings alongside our previous findings under anaesthesia (Gwilt et al. 2020) confirm that hippocampal disinhibition decreases high beta/low gamma power in the hippocampal LFP. The stark difference we saw within the theta ranges after picrotoxin, that is a significant increase in power under anaesthesia and a lack of effect in wake/sleep, suggest that the increase we see in this range under anaesthesia may be caused by some kind of ceiling effect (see above). It indicates, therefore, that the more relevant frequency change to the behavioural impact of hippocampal disinhibition is the decrease in beta/gamma power.

Our data shows that, due to fundamental differences in inter-species anatomy, more exploration would be needed to ascertain a neural oscillatory effect of hippocampal disinhibition on the medial prefrontal cortex detectable in patients. Additionally, the HRV provides some interest as a translational measure, however due to the uncontrolled wake/sleep in this experiment it is not a suitable method for this study.

Chapter 4: Low doses of systemic Levetiracetam alleviate increased hippocampal burst-duration induced by local neural disinhibition

Introduction

Previous work within our lab used acute hippocampal microinfusion of the GABA-A antagonist picrotoxin to model hippocampal neural disinhibition in rats and to examine the neuro-cognitive effects (McGarrity et al. 2017). Using in-vivo electrophysiology under isoflurane anaesthesia, it was established that the microinfusion of 150ng/0.5ul of picrotoxin into the ventral hippocampus increased neuronal activity in the hippocampus, especially neural burst firing (more than 2 spikes that occur at an inter-spike interval of 6ms or less), as reflected by an increase in the percentage of spikes fired in bursts, and increase in the number of bursts per minute and burst duration. In low doses levetiracetam, a second generation anti-epileptic, has shown promise in reducing memory deficits and electrophysiological activity related to this model.

Levetiracetam's amelioration of hippocampal hyperactivity and associated cognitive impairments

Previous in vitro electrophysiological studies suggest that levetiracetam may antagonize aberrant enhancements in hippocampal neural activity that are caused by GABA dysfunction, while having limited impact on normal hippocampal neural activity, as would be required for normal hippocampal memory function (Birnstiel et al. 1997). In rodents, levetiracetam has been shown to improve cognitive deficits in models of age related cognitive decline, as well as to ameliorate aberrant increases in cortico-hippocampal neural activity (Koh et al. 2010; Sanchez et al. 2012; Devi and Ohno 2013). Comparable findings were made in human studies, where levetiracetam ameliorated hippocampal hyperactivity and associated memory impairments in patients with Amnestic Mild Cognitive Impairment (Bakker et al. 2012). Both in animal models and in patients, the dose used for beneficial cognitive effects was well below the dose used to treat epilepsy. In the patient study, doses of 125mg a day were

administered, in comparison to the 1000-2000mg a day used for epilepsy patients (Bakker et al. 2012). Similarly, in rats, doses of 5mg/kg and 10mg/kg were seen to have beneficial effects on memory, but not doses of 20mg/kg (Koh et al. 2010), whereas higher doses (>50mg/kg) are typically used to reveal the full anticonvulsant effects of levetiracetam in rat models (Gower et al. 1995; Klitgaard 2001). Additionally, Haberman and colleagues (Haberman et al. 2017) showed, in rats, that increased c-fos expression correlated with age-related memory impairments. They also showed that 10mg/kg a day of Levetiracetam for 28 days decreased such age-related increases in c-fos expression without affecting younger or memory unimpaired rats and only in affected areas (i.e. not affecting baseline activity).

Levetiracetam – Mechanism of Action

Although the mechanism of action of levetiracetam is yet to be fully understood, many studies have allowed some insight as to its action (Wright et al. 2013). Patch-clamp studies in rat neurons have shown that levetiracetam has no effect on voltage-gated Na+ currents, the low voltage (Ttype) Ca2+ current, nor the rapidly activated (A-type) K+ current (Zona et al. 2001; Madeja et al. 2003). However, there is a marked reduction in high voltage Ca2+ currents and delayed rectifier K+ currents after levetiracetam application (Niespodziany et al. 2001; Lukyanetz et al. 2002; Madeja et al. 2003).

Radio-ligand studies have shown that although levetiracetam binds in the CNS it does not bind to any common drug binding sites (eg. NMDA, GABA-A, Glycine) (Noyer et al. 1995). However, more recently a binding site for levetiracetam has been identified on synaptic vesicle glycoprotein 2A (SV2A) in both rat and human brains (Gillard et al. 2006; Vogl et al. 2012; Meehan et al. 2011). SV2A is known to be mainly expressed on presynaptic terminals, and there is evidence that it plays a role in neurotransmission, specifically vesicle exocytosis (Daniels et al. 2013; Vogl et al. 2012; Janz et al. 1999). Evidence from SV2A knockout mice shows increased presynaptic Ca2+ leading to increased neurotransmitter release, and henceforth an

increase in seizure frequency (Janz et al. 1999). It is suggested that levetiracetam binds to an intravesicular portion of SV2A, causing an inhibition of the synaptic vesicle priming and release (Mendoza-Torreblanca et al. 2013). Furthermore, in vitro studies in rat superior cervical ganglion neurons showed that levetiracetam both inhibited synaptic activity and reduced Ca2+ currents, whereas a levetiracetam enantiomer, which does not bind SV2A, did not cause any changes in the Ca2+ current (Vogl et al. 2012). There is also evidence that levetiracetam may inhibit Ca2+ release from intracellular Ca2+ stores (Angehagen et al. 2003; Surges et al. 2008; Cataldi et al. 2005), which would prevent the signalling cascades that result in synaptic vesicle release. This would curb the amount of neurotransmitter release, where if it were in relation to glutamate it would decrease excitation. In fact, in vitro studies showed that levetiracetam decreased glutamate release, through effect on the high voltage Ca2+ channel (Lee et al. 2009).

Importantly considering that our model involves blockade of the GABA-A receptor, this receptor has been shown not to have a levetiracetam binding site (Noyer et al. 1995; Poulain and Margineanu 2002). Additionally, radio-ligand binding studies for levetiracetam showed no displacement of levetiracetam binding after picrotoxin addition, indicating picrotoxin and levetiracetam do not bind in the same place (Noyer et al. 1995). Therefore, although levetiracetam may affect GABAergic signalling (De Smedt et al. 2007a), it does not directly interact with GABA-A receptors, suggesting that our disinhibition model is suitable to examine the in vivo neuro-behavioural effects of levetiracetam.

Aims and Hypothesis

We aimed to examine the effects of systemic administration of levetiracetam on the enhanced neuronal firing, especially enhanced burst firing, caused by hippocampal neural disinhibition (induced by local picrotoxin microinfusion McGarrity et al. 2017). We hypothesized that levetiracetam can re-balance the aberrant neural activity, while causing minimal effects on baseline neural activity. If our experiments confirm this

hypothesis, we aim to test whether levetiracetam can also antagonize the behavioural and cognitive consequences of hippocampal neural disinhibition, including impairments in hippocampus-dependent memory performance caused by hippocampal neural disinhibition (McGarrity et al. 2017).

Methods

Rats

59 adult male Lister Hooded Rats (Charles River, Kent, UK) weighing between 306g and 375g (9-12 weeks old) were used for the in vivo electrophysiological experiments, with only 34 used for analysis (for sample size justification and exclusion criteria, refer to the *Experimental Design* section). Rats were housed four per cage in double-decker individually vented cages (462mm x 403mm x 404mm; Techniplast, UK). Temperature and humidity were controlled (21 ± 1.5 °C; 50 ± 8%) and the rats were kept on an alternating light-dark cycle with lights on at 0700h and off at 1900h. Rats were provided with ad libitum water and food. Before the start of the experiment, rats had at least 4 days of acclimatization to their holding conditions, during which they received regular handling by the experimenter. All experiments were carried out during the light phase and in accordance with the Animals (Scientific Procedures) Act of 1986. All methods were based on our previous study involving electrophysiological recordings in the vicinity of the infusion during hippocampal neural disinhibition in isoflurane anaesthetised rats (McGarrity et al. 2017).

Electrophysiological Recordings

An electrode-injector array was custom-made, similar to our previous studies (McGarrity et al. 2017; Pezze et al. 2014). The infusion cannula was comprised of approximately 4cm of 33-gauge stainless steel injector, attached to 50cm of Teflon tubing (Bioanalytical systems INC, USA; type FEP MF-5167) with Portex fine bore Polythene tubing for connections (Scientific Laboratory Supplies, Nottingham, UK. Smiths medical international Ltd). The electrode array had 4 wires, made of 50um diameter stainless steel and Teflon coated, in a single line. The overall width of the

array was approximately 1mm. The array was wired to an Omnetics connector with a ground lead and coated with either Polyethylene glycol (NB labs, US) or epoxy (Plexon, US) from which the wires protruded 1-2cm. The infusion cannula was attached to the array using blu-tac and an epoxy adhesive (RS Components Northants UK; Quick Set Epoxy Adhesive; RS 850-940), so that the tip of the injector was at the centre of the electrodes and approximately 0.4mm above the tip of the electrodes (figure 4.1A).

Systemic Drug Administration

Levetiracetam (Sigma, Germany) was dissolved in saline at a concentration of 10mg/ml and 50mg/ml, and injected intraperitoneally at a volume of 1ml/kg (compare Stratton et al. 2003 for saline preparation of levetiracetam). For control injections, 1ml/kg of saline was injected in the same manner. The lower dose was chosen, because it has been shown by others to ameliorate memory impairments associated with hippocampal hyperactivity in rats (Koh et al. 2010), and the higher dose was chosen because it was shown to have anti-convulsant effects in Lister hooded rats (Stratton et al. 2003). Therefore, these doses were suitable to test the hypothesis that lower doses of levetiracetam can ameliorate mild, subconvulsive hippocampal hyperactivity while leaving baseline intact, whereas higher doses (i.e. antiepileptic) which do not have such ameliorative effects may impact on baseline hippocampal activity. Furthermore, a dose of 20mg/kg, which lies between our two doses, was shown to neither ameliorate these memory impairments nor act as a reliable anti-epileptic (Koh et al. 2010; Stratton et al 2003). Levetiracetam appears to cross the blood-brain barrier quite readily, which provides explanation for its neurological effects. In rats, levetiracetam effects can be seen, at and from, 60 minutes following systemic injection (Koh et al. 2010; Klitgaard et al. 2003; Gower et al. 2003; Ji-qun et al. 2005; Stratton et al. 2003). Additionally, CSF sampling and microdialysis studies in rat show that levetiracetam concentration in the CSF and hippocampus peak approximately 90 minutes after i.p. injection (Doheny et al. 1999; Tong & Patsalos

2001), Therefore, in this study we inject levetiracetam 60mins prior to picrotoxin infusion.

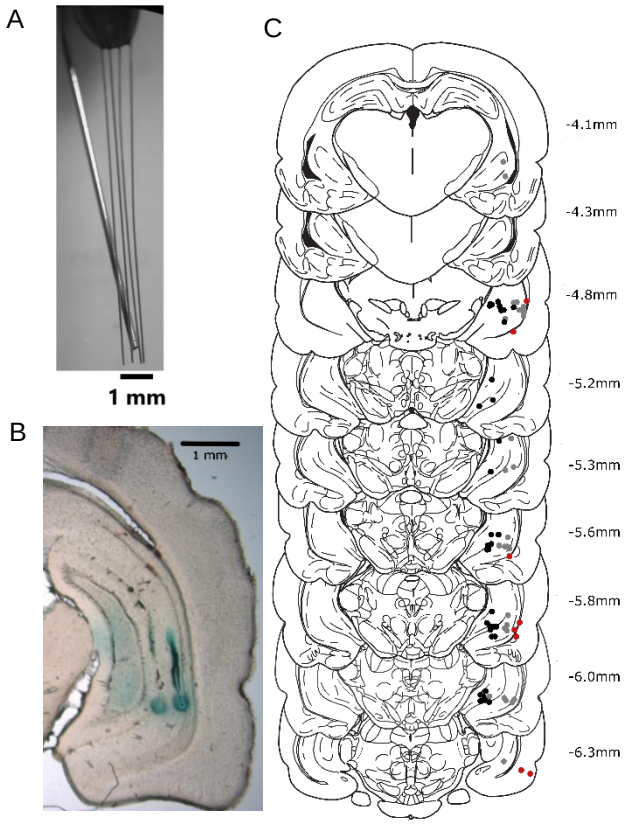


Figure 4.1 *Electrode placements in the ventral hippocampus.*

A A photograph of an example electrode-injector array where the electrodes were supplied by Plexon

B Photograph of one example hippocampus slice showing the location of the two electrodes marked with the prussion blue reaction as well as electrolytic lesions.

C Representation of electrode placements within the ventral hippocampus. The black dots represent the most medial electrodes and the grey dots the most lateral electrodes. Only rats that were included in analysis (saline/saline = 9; saline/PTX = 9; LEV10/PTX = 8; LEV50/PTX = 8) are represented, but even electrodes outside of the hippocampus are shown and marked in red. These electrodes, which were outside of the hippocampus, were removed from the analysis. Markings are shown on coronal slices adapted from (Paxinos and Watson 1998), numbers representing distance from bregma.

Drug Microinfusion

Picrotoxin doses and procedures for drug microinfusions were based on our previous study (McGarrity et al. 2017). Picrotoxin (150ng/0.5ul; Sigma, UK) was either diluted from 300ng/0.5ul frozen aliquots or used straight from a 150ng/0.5ul frozen aliquot each experimental day. Prior to insertion into the brain, the Teflon tubing and the injector were filled with picrotoxin solution or saline and the Teflon tubing was

connected to a 1ul glass syringe already pulled up to 1ul (Hamilton, SYR7226 from SLS, UK). The piston of the syringe was pushed to verify viability of the injector and then a 0.25ul airplug was pulled up from the tip of the injector to minimize drug leakage from the injector while it sat in the brain, prior to infusion. An air bubble was included at the end of the Teflon tubing, just in front of the tip of the glass syringe, to monitor if moving the syringe piston resulted in the bolus moving into the brain.

Multi-unit and LFP Recording

The electrode array was connected to a multichannel preamplifier (Plexon, Inc., USA), via a unity gain multichannel headstage, which amplified the analog signal x1000 and band-pass filtered it into multi-unit spikes (250Hz to 8kHz) and LFP signals (0.7Hz to 170Hz). Anaesthesia was induced using 5% isoflurane and 600ml/min medical oxygen before having the scalp shaved and transferring the rat onto a stereotactic frame with anaesthesia 3% isoflurane and 600ml/min medical oxygen. EMLA cream was applied to the ear bars of the stereotaxic frame prior to inserting the animal, to minimise the possibility of pain. Isoflurane concentration was lowered gradually throughout the experiment and kept at a level dependent on the individual rat to ensure an anaesthetic state where there was no pedal reflex and the breathing rate was at least above 40 (stable breathing while the rats were areflectic varied between 44-68 breaths per minute dependent on the rat). The electrode-injector array was attached to an arm of the stereotactic frame so that the linear 4-wire array was perpendicular to the midline of the brain and anterior to the injector. Stereotactic co-ordinates were taken from the tip of the cannula. Dura and bone plate were removed above the ventral hippocampus (-5.2mm AP; +4.8mm ML), and the electrode-injector array was slowly lowered to the target region (-6.5mm DV). The ground wire was clamped to the ear-bars with a crocodile clip.

At the end of the experiment, the rat was killed with an overdose of isoflurane, or pentobarbital if necessary. Electrode placement locations (most medial and most lateral) were marked by passing 0.2mA of current for 10s (see figure 4.1B for an

example). The brain was then extracted from the animal and stored in potassium ferrocyanide for histological validation of recording sites.

Experimental Design

The target sample size was 8 rats per group, based on the fact that an n of 7-8 per group were sufficient to reveal picrotoxin effects in our previous study as reflected by highly significant interaction between drug group and time (McGarrity et al. 2017). A total of 59 rats were used for this experiment, however only 34 were used in the analysis, this was due to some rats having either: the electrodes placed outside of the hippocampus as determined by histology (n=11); failed intracerebral microinfusion due to a blocked injector (n=10) (the high incidence of this may be related to the long time the injector sat within the brain because of the 30-min baseline before the systemic injection and the 60-min period between systemic injection and hippocampal infusion); unexplained and uncontrollable noise during the experiment (n=2), such that was clearly non-physiological; or complications under anaesthesia where breathing ceased unexplainably, for several minutes, soon after induction of anaesthesia resulting in abnormal neural activity (n=2). Rats were randomly assigned to groups until the numbers (8 per group) for the group were made up. Rats were always ordered in cages of 4, therefore two groups exceeded the target sample size of 8.
A baseline recording was made for 30 minutes, followed by the administration of either LEV 10mg/kg, LEV 50mg/kg or saline i.p. and a further 60 minute recording to obtain a post-systemic drug-baseline. Either picrotoxin (150ng/0.5ul) or saline (0.5ul) was then infused to result in the following four groups (systemic injection-hippocampal infusion): saline/saline (n=9); saline/PTX (n=9); LEV10/PTX (n=8); LEV50/PTX (n=8). Following the hippocampal microinfusion, recording continued for another 90 min (figure 4.2A).

Spike and Burst Analysis

All multi-unit spike data were processed offline using Neuroexplorer (Version 4.135; Nex Technologies, USA) and analysed using the same parameters as in our previous

study (McGarrity et al. 2017). Firing rates were obtained in 5 min bins using the 'Rate Histogram' function in Neuroexplorer, the 5-min bins were to be comparable to previous data (McGarrity et al. 2017). Burst parameters were calculated from the 'Burst Analysis' function in Neuroexplorer, using interval parameters, which classed a burst as greater than 2 spikes with a 6ms (0.006s) maximum interspike interval. All data were normalised to baseline to reduce variability. This was achieved by taking an average of the six baseline bins for each electrode and then dividing the value for every 5 min bin (including the baseline ones) by this average. Other methods of normalisation, such as z-score or subtraction normalisation, are beneficial in that when firing rates are low, such as this data set, they prevent inflation of small changes or of noise. While these are perhaps more appropriate for the current data set, to compare to the previous study (McGarrity et al. 2017) the same normalisation method is conducted here i.e. division normalisation. Data for each rat were averaged over the four electrodes, and then these averages were used to calculate the averages for the different treatment groups (i.e., the units of observation were the individual rats, not the electrodes). If the histology revealed that any of the electrodes were outside of the hippocampus, but the injector and other electrodes remained within, the misplaced electrodes were removed from analysis. Furthermore, in line with our previous study (McGarrity et al., 2017) we restricted the post-infusion analysis to the first 60min of the whole 90min recording.

Statistical Analysis

Following McGarrity et al (2017), we used mixed ANOVA with a within-subjects factor of time and a between-subjects factor of drug group to examine if the time course of the various parameters differed between groups. First, this analysis was applied to the raw baseline data (before normalisation) to examine if there were any baseline difference between the four groups. Then, we examined group differences following systemic and intra-hippocampal drug application. Firstly, we applied the mixed ANOVA to the normalised data during the post-i.p. period only, to examine the effect of LEV before any hippocampal drug infusion. Second, we conducted an ANOVA of

the normalised data from the post-infusion period alone, similarly to our previous study (McGarrity et al. 2017). In contrast to our previous study, we had four drug groups instead of two. Therefore, we started by carrying out one overall ANOVA of the data from all four drug groups. Then, if the drug*time interaction or the main effect of drug were significant or at trend level ($p < 0.1$), we examined which differences between drug groups gave rise to this main effect or interaction. To this end, we completed six additional 'pair-wise' mixed ANOVAs to compare the time course for each pair of drug groups. While a better method of analysis would be a three-way ANOVA examining systemic drug*infusion drug*time, inclusion of additional drug groups to complete such a comparison (i.e. LEV10 with Saline infusion, and LEV50 with Saline infusion) would have increased the rats used considerably. Therefore, the above planned analysis method (only completing pair-wise comparisons if $p \leq 0.1$), and treating subsequent pair-wise comparisons with caution was a compromise to reduce the number of rats used.

Additionally, to compare the baseline values in our study to the baseline parameters in McGarrity et al. (2017) we combined data across drug groups and performed an independent samples t-test comparing the means from both studies during baseline.

Our analysis using ANOVA revealed that drug treatments had distinct effects on distinct burst parameters. Based on these findings, we conducted additional analysis to examine the relationship between distinct burst parameters at baseline and following the drug treatments. To further understand both the effect of picrotoxin on the MUA and the action of levetiracetam on this effect, we conducted a correlation analysis between pairs of parameters including the parameters significantly changed by picrotoxin previously and the peak frequency in burst (due to LEV 50mg/kg effect here, see Results). This was conducted as a post-hoc analysis to disentangle the effects we saw levetiracetam produce; changes in some of the parameters but not in others opened up the question of how these correlated to one another without and with the presence of levetiracetam and picrotoxin. To this end, we started by running a linear regression analysis in SPSS over data for all of the drug groups combined during the baseline period, for each pair of parameters, with an ANOVA to assess the

probability of the regression model fitting the data. Secondly, we ran linear regression analysis over the post-i.p. period to assess the effect of pre-treatment with levetiracetam. We did this for three drug groups (saline pre-treatment, levetiracetam 10mg/kg pre-treatment, and levetiracetam 50mg/kg pre-treatment) for each pair of parameters, again assessing the probability of a fit using ANOVA, and further testing for the null-hypothesis that there was no difference between the regression values of each drug group by using them as predictors in the model. Finally, similarly to for the post-i.p. period, we ran linear regression analysis over the four drug groups and each pair of parameters in the post-infusion period, assessing the probability of fit and any difference between drug groups.

Results

Histology

Figure 4.1C shows the histological validation from the rats included in the analysis, where the most medial (black) and the most lateral (grey) electrodes are shown. Misplaced electrodes from rats included in the analysis are indicated in red, however these specific electrodes were not included in the analysis. Although the exact position of electrodes differed across animals, all the included electrodes were verified as lying within the ventral hippocampus. There was no consistent sub-layer within the ventral hippocampus that the electrodes sat in, therefore we assess the overall activity in the ventral hippocampus independent of cell-layer.

Baseline multiunit firing parameters

Although baseline firing parameters varied numerically across groups, tending to be higher in the saline/saline and LEV50/PTX groups compared to the other groups (Table 4.1), ANOVA did not reveal any significant main effect of group or group*time interaction during the six 5-min baseline bins (all $F < 1.5$, $p > 0.2$). Furthermore, baseline firing parameters generally tended to be lower in all groups in the present study compared to the two groups in our previous study (McGarrity et al., 2017). A

Table 4.1: Baseline values (mean ± SEM) for the core parameters and firing rate for each of the drug groups from our current study, and the original values reported in McGarrity et al. (2017).

	Drug Group	Burst Duration (ms)	% spike in burst	Bursts per minute	Firing Rate (spikes per second)
Current Study	Sal i.p., Sal inf.	10.3 ± 0.3	24.0 ± 2.0	117 ± 26.9	17.7 ± 3.5
	Sal i.p., PTX inf.	8.9 ± 0.2	18.5 ± 1.5	65.3 ± 12.3	13.8 ± 1.7
	LEV10mg/kg i.p., PTX inf.	8.7 ± 0.2	17.4 ± 1.4	69.3 ± 16.9	11.2 ± 1.6
	LEV50mg/kg i.p., PTX inf.	9.2 ± 0.3	22.6 ± 1.9	131 ± 24.3	20.8 ± 3.0
McGarrity et al. (2017)	Saline infusion	10.1 ± 0.5	28.8 ± 3.9	266 ± 75.5	42.1 ± 11.8
	PTX infusion	9.2 ± 0.2	25.6 ± 1.6	251 ± 27.7	35.4 ± 3.4
Statistical Comparison between current study and McGarrity et al. (2017)		*t(285) = 2.59, p = 0.010 **	*t(291) = 2.89, p = 0.0042 ***	*t(291) = 5.07, p < 0.0001 ****	t(291) = 5.34, p < 0.0001 ***

comparison of baseline firing parameters between all rats in the present study (n=34) and all rats in the previous study (n=15), using independent t-tests revealed that all baseline parameters were lower in the present than in our previous study (all $t > 2.59$, all $p < 0.0101$).

Effect of pre-treatment with levetiracetam on multi-unit firing parameters

Levetiracetam did not affect multi-unit firing parameters during the post-i.p. period, with the exception of the peak frequency in burst, which was reduced by the higher dose (50mg/kg) (Fig. 4.2). An overall ANOVA of peak frequency in burst including the post i.p. data from all four groups revealed a significant drug group*time interaction ($F_{33,319} = 1.54$, $p = 0.033$; figure 4.2H). Subsequent pairwise ANOVAs revealed a significant drug group*time interaction when the groups receiving levetiracetam (50mg/kg or 10mg/kg) were compared to the saline/PTX group ($F_{11,143} = 2.39$, $p = 0.0096$; $F_{11,165} = 2.01$, $p = 0.030$) and a trend towards a drug group*time interaction when the groups receiving 50mg/kg levetiracetam and saline/saline were included ($F_{11,165} = 1.66$, $p = 0.09$), with no evidence for a main effect or interaction involving drug group for any other pair of drug groups (all $F < 1.46$, all $p > 0.153$). There were no significant, or near significant, interactions during this period in any other parameters (all $F < 1.23$, all $p > 0.188$). There was a significant effect of time during

this period in the spikes per second ($F_{11,330}$ = 2.16; p = 0.016) indicating a possible baseline drift in this parameter. No such effect of time was seen during any other point of the experiment (baseline, post i.p. and post-infusion) where there was no drug*time interaction (all F < 1.64, all p > 0.086).

Effect of pre-treatment with levetiracetam on picrotoxin induced changes in burst-parameter

Hippocampal PTX, compared to saline, increased the bursts per minute, and this increase was not ameliorated by pre-treatment with 10 or 50mg/kg levetiracetam; numerically, the picrotoxin-induced increase in burst per minute was slightly delayed and enhanced by the lower levetiracetam dose (figure 4.2B). This was supported by a significant drug*time interaction ($F_{33,330}$ = 1.94, p = 0.0020) in the overall ANOVA of the data recorded during the 12 5-min bins following hippocampal infusions. Additional pairwise ANOVAs revealed that hippocampal picrotoxin increased bursts per minute compared to hippocampal saline, independent of pretreatment; there was a significant drug*time interaction between the saline/saline group and: LEV50/PTX ($F_{11,165}$ = 2.27, p = 0.014) , LEV10/PTX ($F_{11,165}$ = 2.57, p = 0.0050), and a trend towards an interaction when the saline/PTX group was included ($F_{11, 176}$ = 1.62, p = 0.10). Additional pairwise ANOVAs revealed significant drug*time interactions when data from the LEV10/PTX group were compared with the other groups (saline/PTX: $F_{11,165}$ = 1.94, p = 0.037; LEV50/PTX: $F_{11, 154}$ = 2.17, p = 0.019). A pairwise ANOVA did not indicate any difference in the time course of the burst per min parameter between the saline/PTX and the LEV50/PTX groups (Main effect of drug group and drug group* time interaction, F <1).

The pattern observed in the percentage of spikes in burst was similar to that seen in the bursts per minute (figure 4.2C), where there is an increase post-infusion from picrotoxin with no apparent amelioration by either doses of levetiracetam. Again, there was a significant drug*time interaction ($F_{33,330}$ = 1.51, p = 0.040), however further tests only revealed a significant drug*time interaction between the saline/saline and

LEV10/PTX groups ($F_{11,165}$ = 1.95, p = 0.037), with a trend towards significance in the saline/saline and saline/PTX groups ($F_{11,176}$ = 1.76, p = 0.06). There were no other significant or near significant interactions (all F < 1.11, p > 0.109).

Hippocampal ptx, compared to saline, increased burst duration, with the magnitude of this increase being smaller than ptx-induced increase in burst per minute or in the percentage of spikes in bursts; importantly, levetiracetam tended to ameliorate this increase in burst duration, especially at the lower dose (Fig. 4.2D). More specifically, burst duration in the LEV10/PTX was more similar to the saline/saline group than to the saline/PTX group, with the LEV50/PTX group lying between the two. The overall ANOVA of burst duration during the post-infusion period, including data from all four drug groups, revealed a trend towards a significant drug*time interaction ($F_{33,308}$ = 1.39, p = 0.08). Further 'pair-wise' ANOVAs revealed a strong trend towards a drug*time interaction between the saline/PTX and LEV10/PTX groups ($F_{11,154}$ = 1.82, p = 0.055), with no further significant main effects of drug group or drug group*time interactions for any other pair of drug groups (all F < 1.47, all p > 0.182).
There was no evidence that the time course of any of the other multi-unit firing parameters (firing rate, peak frequency in burst, frequency in burst, inter-burst interval, and inter-spike interval) differed between drug groups (all main effects of drug group or drug*time interactions; F < 1.28, all p > 0.145) (figures 4.2E-I).

Correlation between different multi-unit firing parameters and the impact of levetiracetam pretreatment and hippocampal disinhibition

The correlations were used in order to further understand the drug effects observed from the analysis of each parameter, specifically the interplay between levetiracetam and picrotoxin. The correlation between all parameters significantly affected by picrotoxin in the previous study (bursts per minute, percentage of spikes in burst, burst duration and firing rate; McGarrity et al. 2017), as well as the peak frequency in burst (due to the significant effect of 50mg/kg levetiracetam in this parameter) were

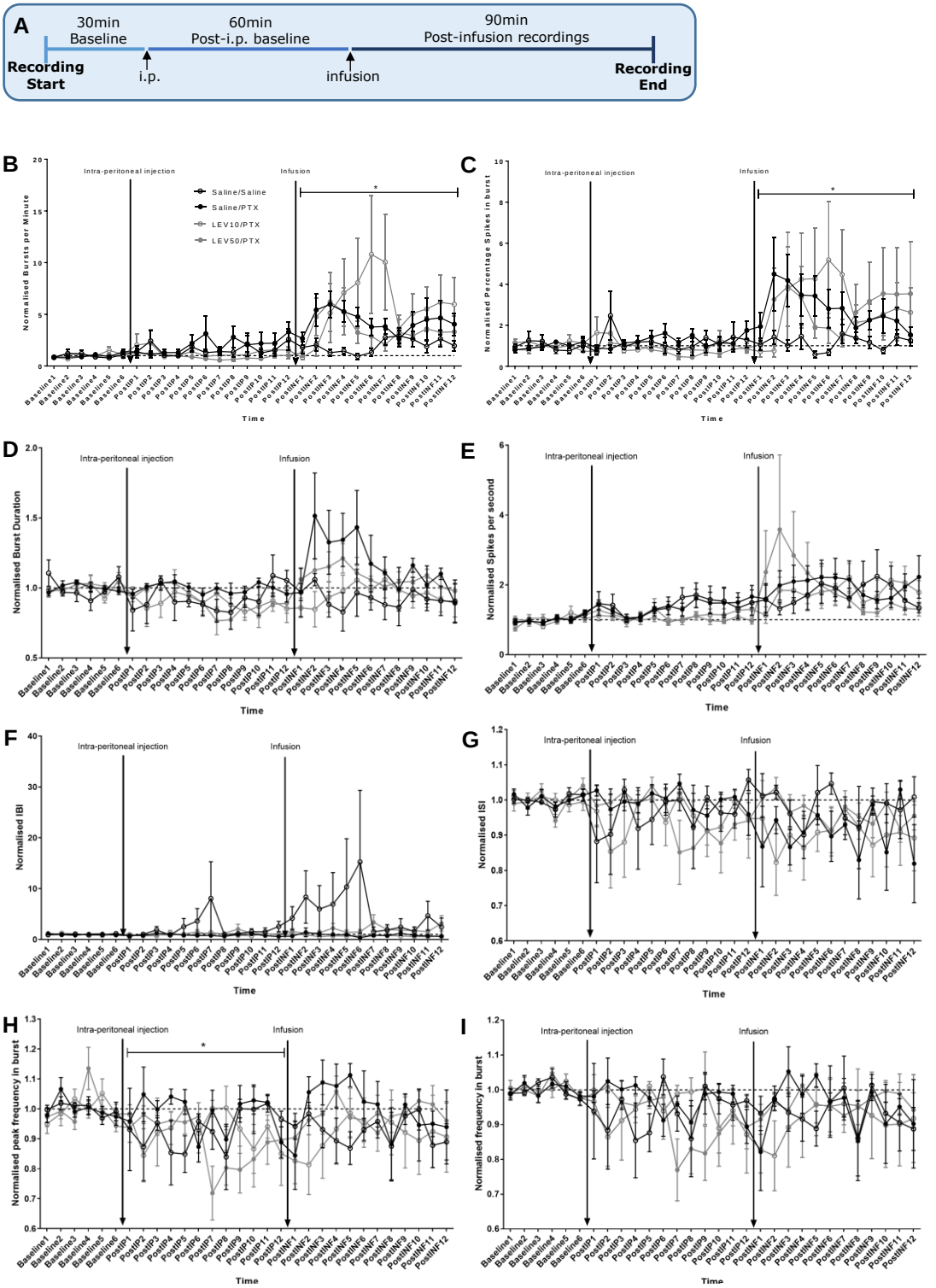


Figure 4.2 *Levetiracetam's effect on the core bursting parameters and the spikes per second*

A shows the timeline of the experiment **B-I** shows the baseline, post-IP and post-infusion periods which were normalised to baseline, for each parameters, showing the four drug groups (saline/saline; saline/PTX; LEV10/PTX; LEV50/PTX). * = $p < 0.05$ for a drug*time interaction over the period indicated.

compared to one another to assess their correlation, in each drug group (figure 4.3).

Baseline

At baseline, there was a significant correlation between all pairs of MUA parameters (see figure 4.3A; with the significant correlations showing: $0.36 < r < 0.98$). A particularly strong correlation were shown between the bursts per minute and firing rate (spikes; $r = 0.98$).

Effect of levetiracetam pre-treatment

Pre-treatment with levetiracetam compared to saline caused a shift in many of the correlations (figure 4.3B). Specifically, both doses of levetiracetam (10mg/kg and 50mg/kg) removed any significant correlation between the bursts per minute and the peak frequency in burst. Additionally, after levetiracetam 10mg/kg there remained no significant correlation between either the burst duration and bursts per min, or the burst duration and spikes. While 50mg/kg levetiracetam removed the correlation between peak frequency in burst and the spikes. In other parameters, where a significant correlation still occurs after levetiracetam pre-treatment, there is a significant effect of drug (except for the percentage of spikes in burst and spikes correlation; figure 4.3D). In several cases (burst duration and bursts per minute, and percentage of spikes in burst and peak frequency in burst) the levetiracetam appears to reduce the correlation in a dose dependant manner. Whereas other parameters show a reduction in correlation in the levetiracetam 10mg/kg but no reduction by the levetiracetam 50mg/kg (bursts per minute and percentage of spikes in burst, and bursts per minute and spikes). The burst duration and peak frequency in burst correlation appears to be strengthened by levetiracetam 10mg/kg but reduced by 50mg/kg.

Effect of levetiracetam pre-treatment on picrotoxin-induced effects

Picrotoxin infusion, compared to saline infusion, removes the significant correlation between burst duration and bursts per minute, as well as between the burst duration and spikes; reducing the correlation between bursts per minute and peak frequency in burst, and burst duration and percentage of spikes in burst (figure 4.3C). There was a significant effect of drug (figure 4.3D) for all of the pairs of parameters, except for the burst duration and peak frequency in burst, and the percentage of spikes in burst and spikes. There remained no change in the correlations showing significance after LEV50mg/kg during the post-i.p. and post-infusion period. However, while the parameters that showed no significant correlation during the post-i.p. period with levetiracetam 10mg/kg remained as such, the significant correlation between percentage of spikes in burst and spikes as well as between the bursts per minute and the percentage of spikes in burst, was lost upon picrotoxin infusion.

Discussion

Our results reveal that levetiracetam, especially at the lower dose (10mg/kg), can antagonise the increased burst duration caused by hippocampal disinhibition. The disinhibition-induced increases in other hippocampal burst parameters, including bursts per minute and percentage spike in burst, were not affected by levetiracetam treatment. In addition, the high doses of levetiracetam (50 mg/kg) decreased the peak frequency in bursts before hippocampal picrotoxin or saline infusions, but levetiracetam did otherwise not affect basal hippocampal multi-unit firing.

Baseline

The baseline hippocampal multi-unit parameters recorded in the present study were comparable in their scale to those reported in our previous study. However, firing parameters in the present study were generally somewhat lower than in the previous (with differences ranging from ~17% reduction for percentage of spikes in burst, to ~58% reduction for firing rate). The finding that all multi-unit parameters at baseline were similarly decreased in the present compared to the previous study is consistent with the strong correlation between parameters at baseline revealed in the present study. This may be, in part, due to slight differences in cell layers where the bulk of

electrodes sat. Nevertheless, our baseline values do not differ significantly between the drug groups, indicating that, despite differing from previously, there is consistency

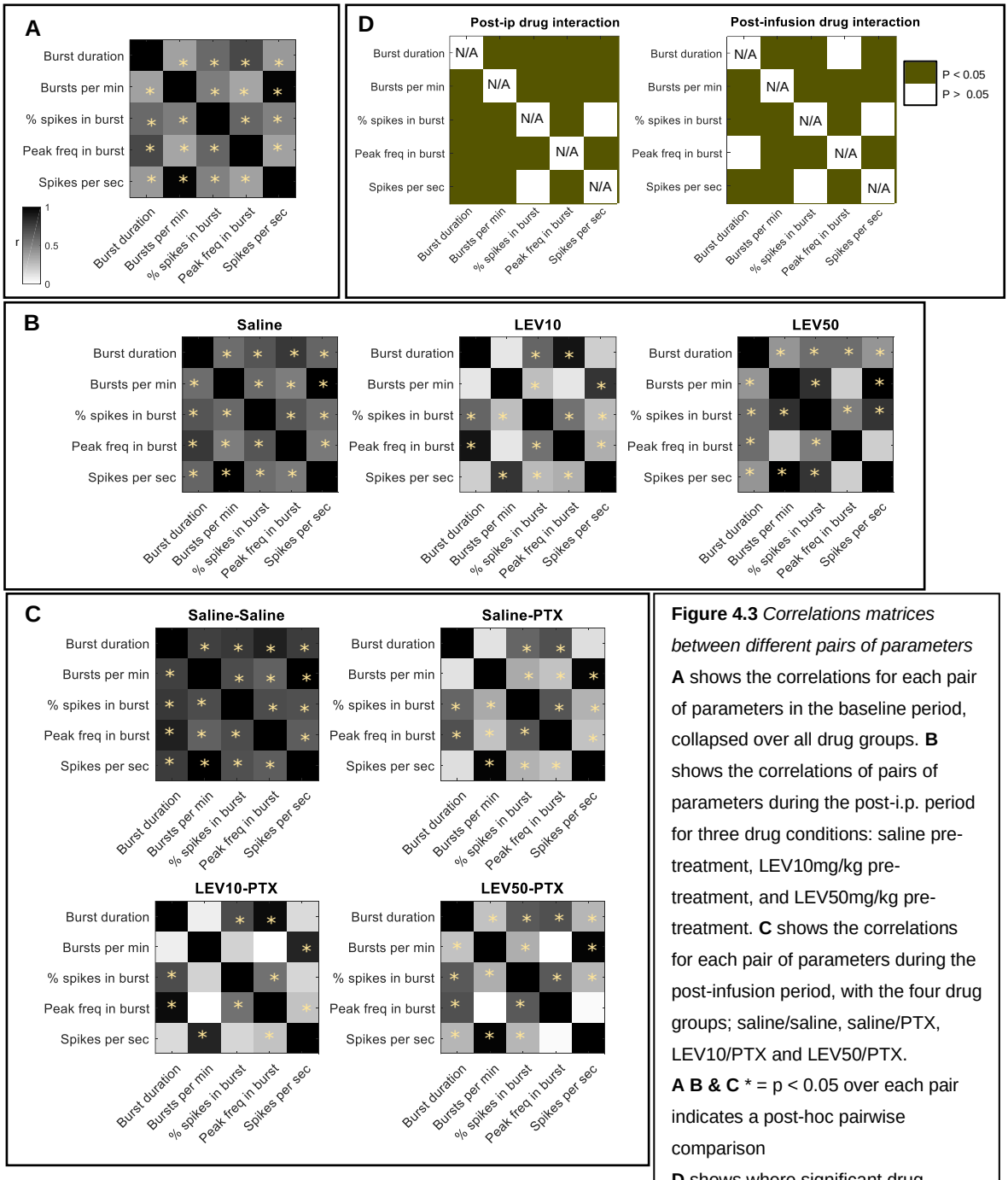


Figure 4.3 *Correlations matrices between different pairs of parameters*
A shows the correlations for each pair of parameters in the baseline period, collapsed over all drug groups. **B** shows the correlations of pairs of parameters during the post-i.p. period for three drug conditions: saline pre-treatment, LEV10mg/kg pre-treatment, and LEV50mg/kg pre-treatment. **C** shows the correlations for each pair of parameters during the post-infusion period, with the four drug groups; saline/saline, saline/PTX, LEV10/PTX and LEV50/PTX.
A B & C * = $p < 0.05$ over each pair indicates a post-hoc pairwise comparison
D shows where significant drug interactions lay in the post-i.p. period and post-infusion period.

within our recordings. Furthermore, as may be anticipated, all burst parameters analysed were significantly correlated to one another during the baseline period.

Levetiracetam's effect on baseline hippocampal firing

On baseline, the low dose of levetiracetam had no substantial effect. The higher dose of levetiracetam decreased numerically the spikes per second in comparison to the saline pre-treatment groups. In addition, there was also a significant decrease by this dose on the baseline peak frequency in burst in comparison to the saline and picrotoxin pre-treatment groups. The limited effect during the baseline from both doses of levetiracetam is consistent with findings of others showing limited effects in normal conditions (Birnstiel et al. 1997). Although the effect of the levetiracetam 50mg/kg on the peak frequency in burst during the baseline was somewhat unexpected, we had not ruled out the possibility of a less therapeutic dose (for our model) having baseline effects. This finding is consistent with the proposed mechanism of action of levetiracetam and the baseline effect may account for the higher doses of levetiracetam not ameliorating memory impairment associated with hippocampal hyperactivity. It is also possible that this parameter would not result in any behavioural phenotypes, thereby limiting its impact on normal activity.

Further insight into the effect of levetiracetam on baseline, through the correlation analysis, revealed that all correlations with the peak frequency in burst are significantly affected by levetiracetam pre-treatment. Its correlation with bursts per minute was abolished with both doses of levetiracetam, while the correlation with spikes was abolished with 50mg/kg and reduced with 10mg/kg. Interestingly, its correlation with burst duration appeared to increase with 10mg/kg and decrease with 50mg/kg. Furthermore, the levetiracetam 10mg/kg, that had no significant baseline effects on the parameters, removed any significant correlation between the burst duration and both bursts per minute and spikes.

Impact of levetiracetam on the picrotoxin-induced changes

Picrotoxin had similar effects on bursting parameters as it did in the previous study (McGarrity et al. 2017), specifically increasing the percentage of spikes in burst, bursts per minute and burst duration. However, in the present study picrotoxin did not affect overall firing rate, whereas our previous study found a slight increase in overall firing rate following hippocampal picrotoxin compared to saline infusion. The lack of change in spikes per minute could be reflective of interaction with baseline-drift, which was observed previously and seen during our post-i.p. period.

Our current data show that levetiracetam did not ameliorate the picrotoxin-induced increase in burst parameters, except for the increase in burst duration. Levetiracetam 10mg/kg caused a near significant amelioration of the increased burst duration induced by picrotoxin infusion, while visual inspection indicated that 50mg/kg caused a slight amelioration in burst duration while leaving both bursts per minute and percentage of spikes in burst unchanged. In contrast, the data indicates that 10mg/kg levetiracetam may attenuate the picrotoxin-induced increase in bursts per minute, delaying its onset; indicated by a significant drug*time interaction between saline/saline and LEV10/PTX, and saline/PTX and LEV10/PTX, but only a trend towards an interaction between saline/saline and saline/PTX. While levetiracetam 10mg/kg combined with picrotoxin did not appear to differ from the effect of picrotoxin alone in the percentage of spikes in burst.

Further to this, picrotoxin abolished the correlation between burst duration and both bursts per minute and spikes, while reducing the correlation between percentage of spikes in burst and both burst duration and spikes, and between the peak frequency in burst and spikes. While, overall, there were limited alterations in the effects of pre-treatment with either dose of levetiracetam upon the addition of picrotoxin. The picrotoxin further attenuated the decreased correlation between burst duration and bursts per minute after 50mg/kg, and completely abolished the significant correlation between percentage of spikes in burst and both bursts per minute and spikes, after

10mg/kg. Contrastingly, the addition of picrotoxin caused the correlation between percentage of spikes in burst and peak frequency in burst to be somewhat restored from the decrease observed with levetiracetam 50mg/kg pre-treatment.

The correlation analysis reveals more of the nuances of how picrotoxin affects the bursting parameters, and levetiracetam's effect on this. It appears that the effects seen in the burst duration, bursts per minute, and percentage of spikes in burst after picrotoxin infusion are correlated with each other. Similarly, the firing rate only appears to increase at the same degree as the bursts per minute (indicated by a similar correlation when compared to the saline infusion). Interestingly, we see an effect in the drug baseline of 10mg/kg on the correlations between burst duration and all other analysed parameters, with some abolished significant correlations (bursts per minute and spikes), some reduced (percentage spikes in burst) and some increased (peak frequency in burst), but limited alterations in these correlations after picrotoxin. This indicates that the alterations in burst duration from levetiracetam 10mg/kg appear, relatively undetected, at baseline and upon the picrotoxin addition either remain unchanged thus preventing any effect of picrotoxin (correlation with percentage of spikes in burst), or acting as a buffer for picrotoxin induced effects (correlation with peak frequency in burst).

Furthermore, in support of the indication of levetiracetam 10mg/kg attenuating the effect of picrotoxin in the bursts per minute, and to some degree in the percentage of spikes in burst, it can be seen that the addition of picrotoxin attenuates levetiracetam 10mg/kg's effect on correlations between percentage spikes in burst and both the bursts per minute and spikes. Adding further emphasis to the idea that levetiracetam cannot ameliorate the effects of these parameters. In contrast, the addition of picrotoxin appears to restore the correlations between the percentage of spikes in burst and bursts per minute (increased), and peak frequency in burst (decreased) caused by 50mg/kg levetiracetam.

As was hypothesised, there was no effect of low dose of levetiracetam during the drug-baseline period, with a minimal effect of the high dose levetiracetam. In accordance with literature that suggests that lower doses of levetiracetam are effective in models of aging or other cognitive disorders compared to the higher doses used for epilepsy, we see a significant effect of the 10mg/kg and not the 50mg/kg dose, hypothesised to be the case. Contrary to what we expected, the levetiracetam 10mg/kg did not have any effect on the increased percentage of spikes in burst or bursts per minute, which we suspected to be the parameters underlying the cognitive deficits observed after picrotoxin-infusion in awake rats (McGarrity et al. 2017). However, an amelioration of picrotoxin-induced increase in burst duration, but not the other parameters, indicates that this may be the most relevant parameter for these behavioural impairments.

A common in vivo electrophysiological finding following levetiracetam administration is a decrease in firing rate; this is often in disease models where there is an increase in firing rate that levetiracetam (at a higher dose) alleviates, while leaving basal firing unchanged (Sanchez et al. 2012; Margineanu and Wulfert 1997). We do not see evidence of levetiracetam reducing the firing rate in our model, however we also did not find a significant picrotoxin-induced increase in overall firing rate, and therefore an amelioration is not possible. There is some evidence of levetiracetam decreasing the firing rate in ‘healthy’ brains, however this is with a much higher dose (170mg/kg) than we use (Loscher et al. 1996).

We observed levetiracetam 10mg/kg ameliorating the increased burst duration induced by picrotoxin disinhibition. Although there are, to our knowledge, no studies which examined the effect of levetiracetam on the burst duration parameter, there is evidence that levetiracetam can alter the duration of other parameters indicating intense neural activity (although at different time scales). Doses of LEV 40mg/kg i.p. (Husum et al. 2004) 80mg/kg and 160mg/kg i.p. (Ji-qun et al. 2005) have been shown to significantly decrease the duration of seizure in kindled and spontaneously epileptic

rats, respectively. Furthermore, after-discharge duration (the length of time where LFP spikes are greater than prior to electrical stimulation) which is a common electrophysiological measure in kindling epilepsy studies is found to be reduced after levetiracetam treatment in rats. Levetiracetam doses similar to our highest dose have consistently been shown to reduce the after-discharge duration in kindling rat models of epilepsy: 50mg/kg (Stratton et al. 2003), 54mg/kg (Loscher and Honack 2000; Loscher et al. 1998; De Smedt et al. 2005). In contrast, the evidence for doses more similar to our lower dose (10mg/kg) is limited, with some studies showing mild anticonvulsant effects (13mg/kg; Loscher et al. 1998) and others no anticonvulsant effect (12.5mg/kg; Stratton et al. 2003). In other models of seizures, such as genetic models and ischemic brain damage models, the spike-and-wave discharge, which are one EEG feature accompanying seizures, is measured. Levetiracetam has been shown consistently to decrease the duration of these spike-and-wave discharges at both doses similar to those used in the present study (5.4mg/kg, 17mg/kg and 54mg/kg: Gower et al. 1995; 20mg/kg and 40mg/kg: Tokuda et al. 2010; 50mg/kg: Bouwman and van Rijn 2004) and those a lot higher, commonly used for epilepsy in rodent models(100mg/kg: Bouwman et al. 2004 and Cuomo et al. 2013; 96mg/kg and 170mg/kg: Gower et al. 1995; 80mg/kg and 160mg/kg: Tokuda et al. 2010). What is particularly interesting from the data on spike-and-wave discharge duration is that the lower doses (e.g. 5.4mg/kg) had the same degree of attenuation as the higher doses did.

Interestingly, the specific impact of levetiracetam on burst duration is in line with a recently proposed mechanism of action for levetiracetam. Meehan and colleagues (2011) demonstrate that levetiracetam exerts its effect through decreasing the readily releasable pool of synaptic vesicles via SV2A. Using rat hippocampal slices *in vitro* they saw that levetiracetam decreased EPSC (excitatory post-synaptic current) amplitudes after high-frequency firing trains induced either through stimulation or through spontaneous activity. They noted that the EPSC amplitude in the presence of levetiracetam was kept consistent in lower-frequency trains and at the beginning of

firing trains, indicating a limited effect on normal activity. They also showed that the readily releasable pool of vesicles was decreased in the presence of levetiracetam, and that levetiracetam did not change the time-course of vesicle recycling. Although the underlying mechanisms remain to be determined, this study showed that levetiracetam: 1) has no effect on the beginning of trains and low-frequency firing, 2) is decreasing the number of vesicles which release neurotransmitter during each burst/firing train, 3) is exerting a short-term effect within each train/burst and therefore is not limiting the number of trains/bursts. These suggestions are further supported by other findings (Garcia-Perez et al. 2015), although there is controversy over the mechanism underlying levetiracetam's effect on the vesicle pool (Mendoza-Torreblanca et al. 2013). Our findings of a significant decrease in burst duration after levetiracetam, while leaving baseline burst-duration unaffected, is in line with this evidence of levetiracetam's action, furthermore, the lack of effect of levetiracetam on number of bursts is also anticipated considering levetiracetam's proposed mechanism of action presented here.

Furthermore, the decrease we found in the peak frequency in burst from LEV50mg/kg prior to infusion may also be consistent with this mechanism of action. The peak frequency in burst represents the most extreme frequency within the burst, in other words the shortest inter-spike-interval for each bin. Therefore, if levetiracetam exerts even a minimal baseline effect through depletion of the readily releasable pool, while this would leave other parameters unaffected, it would reveal a change in the peak frequency in burst.

The increase in correlation between the burst duration and the peak frequency in burst in the levetiracetam 10mg/kg and picrotoxin infusion group further corroborates the proposed mechanism of action. As the readily releasable pool is depleted, the peak frequency cannot be reached and the burst duration is reduced because the burst cannot continue, thereby meaning both are impacted in a way they are not without levetiracetam.

While the levetiracetam 50mg/kg does not show the same degree of ameliorative effects as the 10mg/kg there is a significant baseline effect of this dose on the peak frequency in burst. The LEV50/PTX group's correlations do not appear to follow a similar pattern as the LEV10/PTX groups. It is possible that the limited effects of our higher dose on the amelioration of picrotoxin-induced increases is due to the interplay of our two manipulations.

Conclusions

Levetiracetam decreased the increased hippocampal burst duration caused by hippocampal neural disinhibition, while having no effect on baseline parameters. This is consistent with levetiracetam decreasing the number of synaptic vesicles available during the short time of a burst (Meehan et al., 2011). Considering the behavioural impairments we observe with picrotoxin in awake rats (McGarrity et al. 2017), our findings open the question of whether the burst duration is a correlative parameter for these impairments and if levetiracetam would therefore be able to ameliorate these effects.

Chapter 5: Can levetiracetam ameliorate the LFP-changes induced by hippocampal disinhibition?

There are limited studies assessing the impact of levetiracetam on neural oscillations, the majority of these are in animal models of epilepsy or in human cases of epilepsy. Overall, in epilepsy patients whole-brain EEG reveals a general decrease in delta and theta (1-7Hz) oscillations and an increase in alpha and beta oscillations (10-13 and 19-24Hz) in the background EEG after levetiracetam treatment (Cho et al. 2012). In various animal models of epilepsy where recordings were made from the hippocampus, there is a consistent decrease in delta-range oscillations (0.5-4Hz) and increase in theta-range oscillations (4-8Hz) after treatment with anti-convulsive doses of levetiracetam (Santana-Gomez et al. 2018; Svetlana et al. 2019; Boido et al. 2010). However, the evidence for the effect of levetiracetam on higher frequencies than these are contentious; while some see a decrease in 8-13Hz (Santana-Gomez et al. 2018), others see an increase (Boido et al. 2010). Similarly, at frequencies greater than 15Hz some see an increase in power after levetiracetam (Santana-Gomez et al. 2018), others see a decrease (Boido et al. 2010). In all cases, however, the change induced by levetiracetam tends to counter those changes induced by the epilepsy model, demonstrating the ameliorative effect of levetiracetam on electric seizures is apparent in oscillatory activity.

Please also refer to chapters 2 and 4 for further introductions relevant to this chapter.

Aims and Hypothesis

We aimed to assess the impact of picrotoxin and systemic levetiracetam administration on the LFP in the different LFP states present under isoflurane anaesthesia.

Firstly, we anticipate that the LFP states separated out show similar frequency-specific power properties to previously (see chapter 2) while we expect, due to a

smaller electrode-array size and thereby area recorded from, to see some differences within the frequency-specific connectivity.

Secondly, we expect to see a replication of state-specific frequency-dependent power changes induced by picrotoxin microinfusion, and hypothesise the levetiracetam can ameliorate any such changes, returning them towards baseline.

Thirdly, considering the limited effect of both doses of levetiracetam on baseline MUA we expect to see a similar lack of effect in the LFP baseline.

Methods

Animals and Recordings

Data were collected alongside the multi-unit data analysed in chapter 4. Therefore, refer to the methods outlined in that chapter (Methods: *Rats, Electrophysiological Recordings, Systemic Drug Administration, Drug Microinfusion Mulit-unit and LFP recording, and Experimental Design*). Overall, only 33, not 34, rats were used for this LFP analysis as although portions of visible noise were removed from MUA (as noted during experiments and outlined in chapter 4), there was evidently more at these points which was not visible but still affected the LFP, this prevented the separation of continuous and burst-suppression states using our newly established method (see chapter 2). Furthermore, similar noise, which did not prevent the first instance of state separation, did prevent the threshold-based separation of burst and suppression states, therefore two rats were excluded from the burst and suppression analysis due to this. Additionally, similar to our previous study (chapter 2), for some rats, LFP did not show all three LFP states during all recording periods (baseline, post-IP period and post-infusion period). Therefore, the overall number of rats contributing to the analyses was as follows: continuous state: overall 26, saline/saline = 7, saline/picrotoxin = 6, LEV10/picrotoxin = 8, LEV50/picrotoxin = 5; burst and suppression states, overall 26, saline/saline = 7, saline/picrotoxin = 5, LEV10/picrotoxin = 6, LEV50/picrotoxin = 8.

Data Analysis

The LFP data were analysed as outlined in chapter 2 (*2.2 Semi-automated separation of LFP states 2.3 State-separated analyses of hippocampal LFP properties 2.4 Analyses of LFP state-dependent drug infusion effects*), except for changes due to the inclusion of the systemic drug injection and the 60 min post-IP period, which are highlighted below.

Comparisons across time-periods

Previously, to assess the impact of hippocampal microinfusions we used a log-ratio normalisation of the 60 min post-infusion to the 30 min pre-infusion. Here, we did the same for the 60 min post-infusion period, where we normalised to the 30 min baseline, similarly, with the 60 min post-IP period we normalised to the 30 min baseline. However, we also normalised the 60 min post-infusion period to the 60 min post-IP period in order to disentangle any possible baseline effects of systemic injections (e.g. baseline drift during the post-IP period).

Statistics

Cluster permutation statistics, as explained in chapter 2, were used to assess the impact of our various drug manipulations on the frequency specific (i.e. power differences and PLV differences) LFP effects at the different time points. Similar to the ANOVA's run for the MUA in chapter 4, a cluster permutation test was initially run over all four drug groups combined. If any significant effects were detected a cluster permutation test was run for each pairing of drug groups (i.e. six pair-wise comparisons) to ascertain between which drug groups the initial significance arose.

Results

State-dependent LFP properties at baseline

The three distinct hippocampal LFP states under anaesthesia differed with respect to power and functional connectivity (Fig. 5.1). With respect to raw power and relative power at different frequencies, we largely replicated the findings of our previous analysis (Gwilt et al., 2020). The burst state showed substantially higher overall power

than the suppression (1-39.5Hz cluster p = 0.0010) or continuous states (1-28Hz cluster p = 0.003 and 31-39.5Hz cluster p = 0.023; figure 5.1A). Although, numerically, the continuous state showed higher power than the suppression state, especially within the lower frequencies, there were no significant clusters found during the analysis. The normalised power spectra showed that the burst state was characterized by a higher proportion of power at lower frequencies, and a lower proportion at higher frequencies than both the continuous (4-14Hz cluster p = 0.003

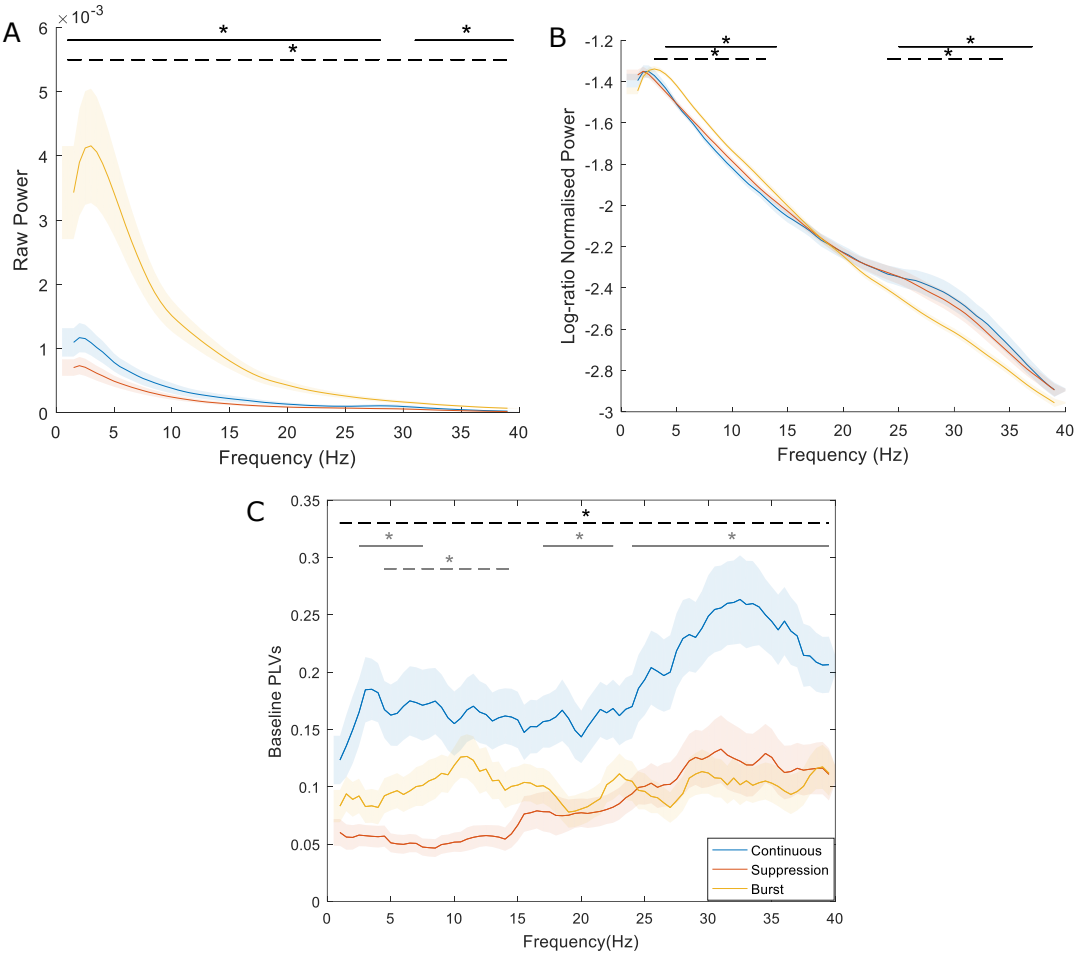


Figure 5.1: The three hippocampal local field potential (LFP) states—differences in frequency-dependent power and connectivity. (a) Raw power spectral density, (b) log-ratio of power divided by the total area under the curve (representing relative power at different frequencies), and (c) phase-locking values (PLVs) are shown across frequencies for each of the three LFP states. All values are shown as mean ± SEM. The frequency ranges showing significant ($p < .05$) differences based on cluster permutation statistics are indicated by an asterisk (*) and a solid line for comparisons between burst and suppression, a dashed black line for comparisons between burst and continuous states, and a dashed grey line between suppression and continuous. The number of rats contributing to each state was 26, however these were not always the same 26 rats.

and 25-37Hz cluster p = 0.008) and suppression states (3-13Hz cluster p = 0.007 and 24-35Hz cluster p = 0.016), which did not differ from one another (no significant clusters) (figure 5.1B). With respect to connectivity, as reflected by PLVs (figure 5.1C), we replicated our previous finding that connectivity was higher in the continuous compared to the burst state, but overall PLVs were lower than in our previous study and the suppression state showed similarly low connectivity to the burst state. More specifically, the continuous state showed higher connectivity, as reflected by PLVs (figure 5.1C), across most frequencies compared to the burst (2.5-7.5Hz cluster p = 0.029, 17-22.5Hz cluster p = 0.024 and 24-39.5Hz cluster p = 0.0010) and the suppression (1-39.5Hz cluster p = 0.0010) states. The burst state showed higher connectivity than the suppression state at lower frequencies (4.5-14.5Hz cluster p = 0.006), whereas connectivity did not differ between these two states at higher frequencies.

Power

From figure 5.2A-C it can be seen that there is a general increase in power in all frequencies during the post-IP period compared to the baseline period. This change is most pronounced in the lower frequencies of the continuous and the suppression states, and is quite similar across all drug groups. There is a non-significant decrease in power in the mid-frequencies in the saline/PTX group during the continuous state, but overall there were no significant effects of drug group in this post-IP period. When the power was compared between the post-infusion period and the baseline period (figure 5.2D-F) we can again see an overall increase in power across all drug groups and states, particularly in the lower frequencies. In both the continuous and the suppression states the saline/PTX group appears to sit below both the other drug groups and the zero change from baseline line in the mid-frequencies. Although, this was only significant in the continuous state with a significant cluster from 17-24Hz (cluster p = 0.019) over all drug groups, with further pairwise comparisons revealing clusters from 17-24Hz (cluster p = 0.008) and 34.5-35.5Hz (cluster p = 0.049) between the saline/saline and saline/picrotoxin groups and from 17.5-28Hz (cluster p

= 0.011) and 33.5-36Hz (cluster p = 0.049) between saline/picrotoxin and LEV10/picrotoxin groups.

Figures 5.2G-I show the difference between the post-infusion period and the post-IP period, contrary to the other two time-period comparisons in the continuous state

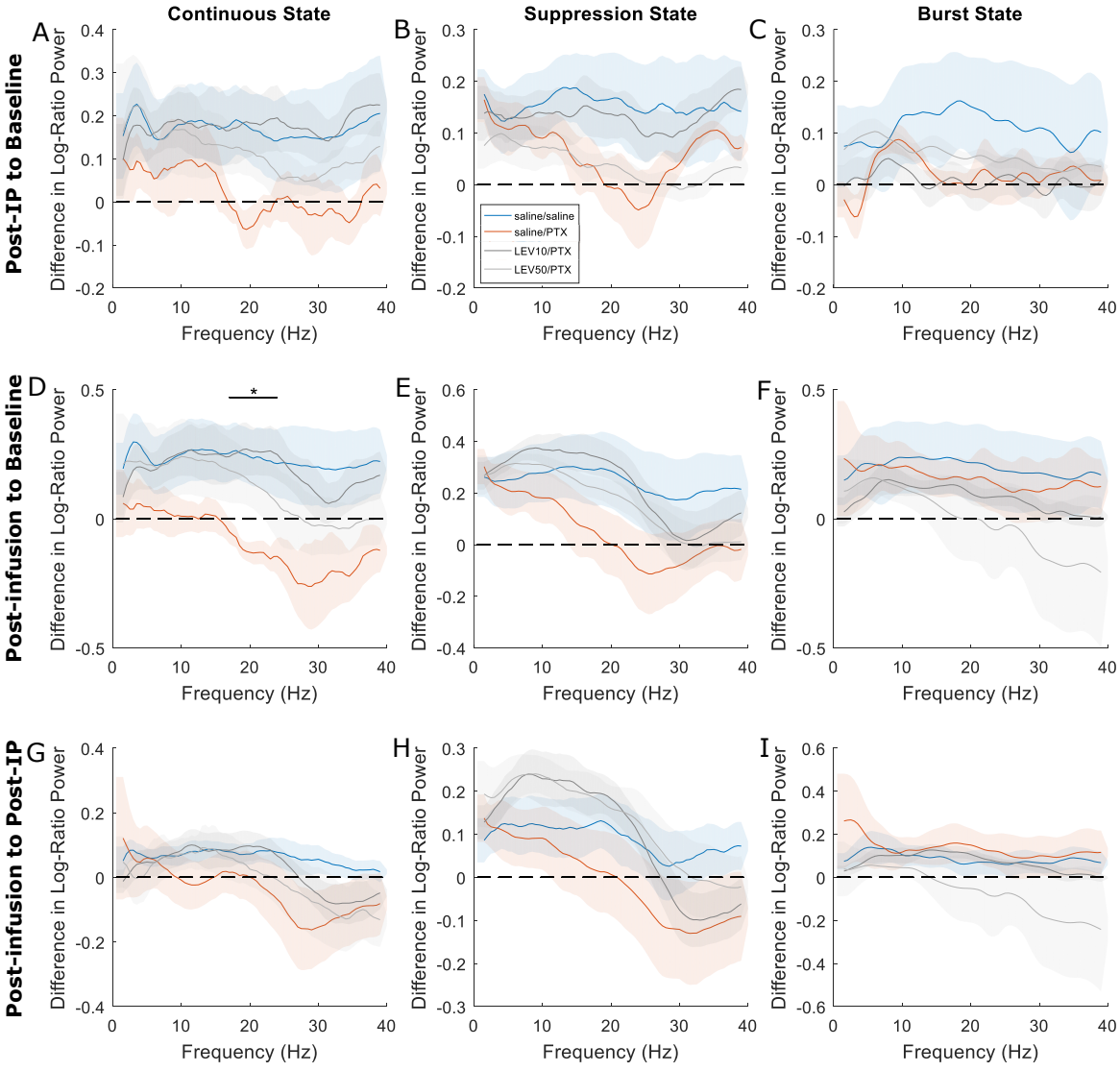


Figure 5.2: Frequency-dependent impact of drug treatment on power in the continuous (left), suppression (middle), and burst (right) states; of systemic drug during post-IP compared to baseline (top), of systemic drug and infused drug (post-infusion) compared to baseline (middle), and compared to post-IP (bottom). The logarithm of the ratio between post-condition (levetiracetam or saline IP/saline or picrotoxin infusion) and pre-condition (baseline or post-IP) power is shown as a measure of their respective "difference" for all infusion groups across frequencies and separately for each state. All values are shown as mean ± SEM. The dotted line (value of 0) represents no change from the pre- to the post-condition period, while positive numbers indicate an increase from baseline and negative numbers a decrease from pre to post. The frequency ranges showing significant ($p < .05$) differences between all the groups based on cluster permutation statistics are indicated by an asterisk (*) and a solid line

there appears to be little difference from post-IP period in the post-infusion period across all drug groups and all frequencies. However, in the suppression state it appears there is a further increase in the lower frequencies from the post-IP period to the post-infusion period, with the change appearing to be more pronounced in the two levetiracetam groups, although this is not supported statistically. Similarly to all the previous evidence, there appears to be no change in the burst state in power across all frequencies and drug groups.

Connectivity

The post-IP period in the connectivity analysis appears to show more changes than was seen in the post-IP period of the power analysis. Most notably is an apparent decrease in the saline/PTX group compared to the other groups at around 11Hz in the burst state. While in the continuous state there appears to be a slight decrease in the saline/PTX group compared to the others in the delta range, although none of the visible differences in the post-IP period were significant. There appear to be no distinguishable differences in higher frequencies in any of the states during this post-IP period, and no change in the lower frequencies in the suppression state. The post-infusion period, when normalised to the baseline period, appears more or less identical to the post-IP normalised to baseline period; the decrease in theta-frequency connectivity in the burst state reaches significance with a significant cluster from 10-14.5Hz (cluster $p = 0.032$) over all drug groups with further comparisons revealing significant clusters between the saline/picrotoxin group and both the saline/saline (10-13.5Hz, cluster $p = 0.028$) and the LEV50/PTX groups (9.5-13.5Hz, cluster $p = 0.009$). Furthermore, there was a significant cluster between the saline/saline and LEV50/picrotoxin groups from 5.5-8.5Hz, during this post-infusion period. However, unlike in the post-IP period an increase in delta frequencies in the saline/picrotoxin is seen while the saline/saline and LEV10/PTX groups are seen to be decreased, although this is not significant. As in the post-IP period there are no differences in the suppression state, or in the higher frequencies of both the burst and the continuous states. There appears to be an increase in the connectivity in the theta frequencies in

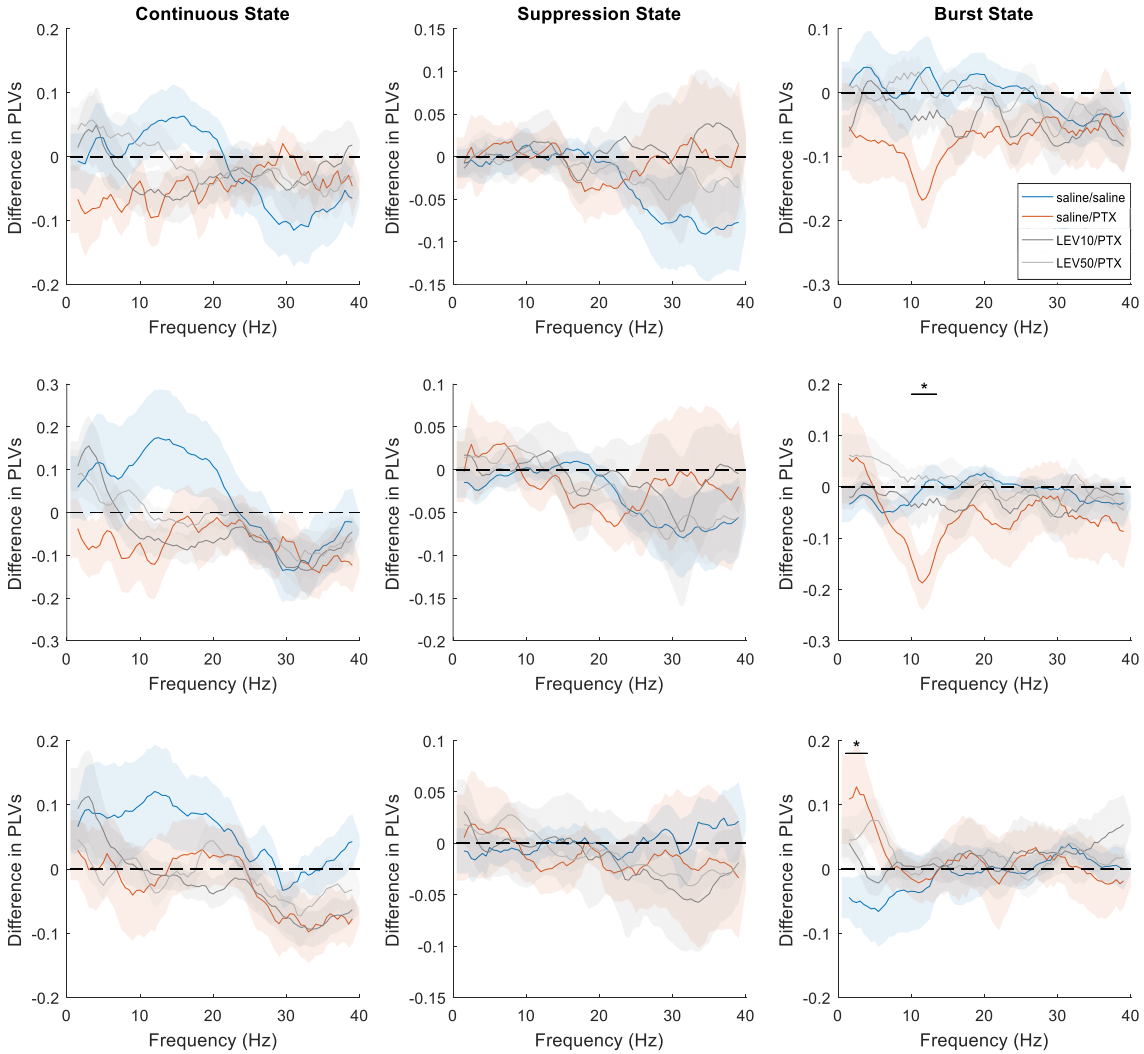


Figure 5.3: Frequency-dependent impact of drug treatment on connectivity in the continuous (left), suppression (middle), and burst (right) states; of systemic drug during post-IP compared to baseline (top), of systemic drug and infused drug (post-infusion) compared to baseline (middle), and compared to post-IP (bottom). The difference between post-condition and pre-condition phase-locking values (PLVs) as a measure of aggregate functional connectivity is shown for all infusion groups across frequencies and separately for each state. All values are shown as mean ± SEM. The dotted line (value of 0) represents no change from the pre- to the post-condition period, while positive numbers indicate an increase from baseline and negative numbers a decrease from pre to post. The frequency ranges showing significant ($p < .05$) differences between all the groups based on cluster permutation statistics are indicated by an asterisk (*) and a solid line.

the continuous state saline/saline group, which is not matched by any of the other groups. Interestingly in the post-infusion normalised to the post-IP period we see a different picture than when either is normalised to the baseline, most notably is the increase in delta frequencies in the burst state in the saline/PTX group, with the two

levetiracetam/PTX groups sitting in-between that and the saline/saline group. This change is supported by a significant cluster from 1 and 4 Hz (cluster p = 0.047) over all drug groups, however further pairwise comparisons did not find any significant clusters; there was a cluster from 1-4Hz between the saline/saline and saline/picrotoxin groups which had a cluster with a p value of 0.0569. For the rest of the frequencies during the burst state and for all frequencies in the suppression state there appears to be no discernible differences. In the continuous state the overall effect looks largely similar as it does in the post-infusion normalised to baseline data, with no real differences shining through.

Discussion

In accordance with our previous study we have successfully separated out the three distinct states under isoflurane anaesthesia; the burst, suppression and continuous states. Our data show, as before, that the burst state has higher raw power than either other state over all frequencies, while the continuous state is generally higher in power than the suppression state. Furthermore, the burst state had greater relative power in the lower frequencies, but lower relative power at higher frequencies compared to both other states. Finally, differently from previously, we see a significantly higher overall connectivity within the continuous state overall frequencies than either other state, and a higher overall connectivity at lower frequencies in the burst state compared to the suppression state. Notably, the overall PLV values are lower within this data set than within the previous set.

We observed no significant differences between the groups that received different systemic injections in the frequency-specific power during the post-IP baseline, whereas in the post-infusion period in the continuous state alone, we see a significant decrease in the saline/picrotoxin group at mid-to-high frequencies compared to the saline/saline and LEV10/picrotoxin groups, indicating an effect of picrotoxin that LEV10mg/kg can ameliorate. There were no further power effects of any drug group.

As with the power, there were no significant differences in the frequency-specific connectivity measures of each drug group during the post-IP period. There was, however, a decrease in low-frequency connectivity in the saline/picrotoxin group during the burst-state compared to the saline/saline and LEV50/picrotoxin groups, and an increase in the LEV50/picrotoxin group compared to both the saline/picrotoxin and saline/saline groups. Furthermore, there was a significant difference between drug groups at the very low frequencies when the post-infusion period was normalised to the pre-infusion period, indicating a possible baseline drift.

Replicated LFP state-separation

We have replicated the raw-power findings from our initial work separating the states, with the burst state showing in both cases (this and previously – chapter 2) that the burst state has significantly higher LFP over all frequencies compared to the suppression state. Furthermore, we replicated the significantly higher burst state power compared to continuous state power from 1-22.5Hz, while finding further significance in the higher frequencies. Similarly, the previous lower frequency significant differences between the burst and both other states in the relative power are replicated in this study, with new significance seen in the higher frequencies where only numerical differences were seen previously.

Overall, the values for the baseline PLVs are quite a bit lower in the present study (axis max 0.35) than the previous study (axis max 1.2). Despite this, the overall pattern of the continuous PLV's across the frequency range remains more or less the same as previously. In contrast to previously, the burst and suppression state patterns appear differently; where previously they tended to increase as the frequency also increased, here they appear relatively steady over all frequencies. A key difference is that here we see the suppression state sitting a lot lower at all frequencies, compared to the continuous state, than it did previously. Where previously there was a significant difference between the suppression and burst states across the whole frequency range (2.5-13 and 17-38), in the current data we see only a significant difference in the lower frequencies (4.5-14.5Hz) with not even a visual difference seen

between the two at higher frequencies. Another stark difference between the connectivity profiles is seen between the suppression and continuous states, where previously there were no detectable differences between the two, now we see that the suppression state has distinctively and significantly lower overall connectivity than the continuous state. Furthermore, previously the only significant difference between burst and continuous states was in lower frequencies (1.5-9Hz), we see now a significant difference not only in the lower frequencies (2.5-7.5Hz) but also in higher frequencies (17-22.5 and 24-39.5Hz).

In all, it appears that the power analysis of baseline states further supports the previous findings, while revealing further significance in differences that could only previously be noted numerically. This is likely due to the increased statistical power in this study, due to an increased number of rats, due in part to four drug groups. Previously there were eight rats in the continuous state and 13 rats in the burst and suppression states for baseline analysis, whereas here we have 26 rats in each of the groups. Interestingly, although there are more significant differences observed in the current connectivity analysis, these do not correspond to patterns seen previously, and are therefore unlikely due to result entirely from an increased number in each group. One main difference between these recordings and the previous recordings is the electrode array used; previously an 8-electrode array that spanned approximately 2mm in the hippocampus was used, whereas in this study we used a 4-electrode array that spanned approximately 1mm in the hippocampus. Therefore, not only have we reduced the number of electrodes that we can measure the connectivity between, but we have also drastically reduced the overall area that the connectivity can be assessed. It has previously been seen and suggested that the connectivity in the hippocampus is seen more strongly at distances greater than 1.5mm. We attributed the weak effects we saw previously to this explanation. While this supports the decrease in overall sizes of PLVs we see in our data (<1mm), the distinct differences we see between these states is quite interesting at such low overall connectivity.

Replication of previous state-dependent picrotoxin effects

Previously we saw a general pattern of picrotoxin increasing the power in lower frequencies and decreasing the power in higher frequencies compared to baseline and saline, in the burst and suppression states, with these effects being statistically significant in the lower frequencies in the burst state. However, in our current data there are little differences seen between the saline and picrotoxin groups in the burst and suppression states during the post-infusion period. In line with previously, during the suppression state the picrotoxin appears to induce a decrease in higher frequency power, albeit non-significant, compared to both the saline group and to baseline; the increase from baseline seen in the lower frequencies with picrotoxin is matched by the saline group. Meanwhile, quite differently to previously, the burst state shows no difference between the saline and picrotoxin groups, despite them both increasing from baseline. However, we do see a significant decrease in power when comparing the picrotoxin to the saline group in mid-frequencies in the continuous state, with visible decreases at higher frequencies, where previously there was no distinguishable effect.

One thing that becomes more pronounced due to the extended recording time is the baseline drift. Previously, we observed an increase from baseline to post infusion in the saline group during the burst state (60 min after baseline). Here we see a similar phenomenon in post-IP period (60 min after baseline) where the saline, and other groups, sit around the 0.1 mark, indicating a similar baseline drift. However, in this data set we then recorded for another 60min (the post-infusion period), and here we can see that there is an even greater increase from baseline in the saline/saline group (sitting around 0.25), which is similar to the saline/picrotoxin group. Further cementing this baseline drift is the overall increase from post-IP to post-infusion period where again the groups sit at around 0.1. It is therefore possible that the reason we do not see the increase in lower frequency power induced by picrotoxin in the burst state as we did previously, is due to a ceiling effect. The overall baseline in this study in the post-infusion period appears to be at the same level of increase (about 0.22) as the

effect in the previous data. While the effect seen in the suppression state was less pronounced previously, it is possible a similar baseline drift prevented us seeing any effect there either.

In terms of the connectivity, the pattern of picrotoxin and saline effects on continuous state PLVs looks largely similar in both our previous and current data, with the picrotoxin numerically decreasing the lower frequency connectivity in comparison to the saline infusion, with no difference between the two drug groups in the higher frequencies. In both cases, no significant clusters were detected when comparing between the picrotoxin and saline infusions. However, in this study, this pattern is also seen in the post-IP period before any drugs have been infused, indicating it is not necessarily a result of the infusion itself. Contrastingly, previously we saw that in the burst and suppression states there was no discernible difference between the saline and picrotoxin groups in the lower frequencies, but we saw a decrease in connectivity in the picrotoxin group at higher frequencies, which was significant in the burst state. In the current data set we see little difference in the suppression state between the two infusion conditions, while in the burst state we see a significant decrease at lower frequencies, and no difference between the groups at the higher frequencies. However, similarly to in the continuous state, this change also appears in the post-IP period, indicating it is not a drug-induced effect.

In terms of the differences we see in the profile of connectivity over the frequency range here compared to previously, this is likely due to a combined result of a marginally different recording area and decreased area of recording. Firstly, reducing the recording area leads to not only a decrease of functional connections, but also a large reduction in the average time-lag of such connections. The method of functional connectivity assessment that we employ, that of the imaginary part of the PLV, is sensitive only to time-lagged interactions thereby meaning the imaginary PLV's diminish if there is a small time-lag between signals (Nolte et al. 2004). This,

therefore, accounts for the decreased values that we see in this data set compared to the previous data set.

Secondly, while we used the same coordinates, the overall decreased spread of electrodes in this study (1mm compared to 2mm previously) excludes some of the previously recorded regions contributing to the connectivity, furthermore, the slight difference in average electrode placement (see figure 4.1 in chapter 4 and figure 2.2A in chapter 2) means we may be assessing connectivity in marginally different areas. For instance, the arrays in the current study tended to sit more anterior than the arrays in the previous study (see figure 2.2a in chapter 2) which means there is a slight difference in hippocampal subregions recorded from. While we cannot pin-point the exact sub-region or cell layer that each one of our electrodes sit in, we can see the overall make-up of the sub-regions in the area recorded from.

In the more posterior regions, where most of the McGarrity et al. (2017) electrodes sat there is no CA2 or CA3 but a large proportion of dentate gyrus and subiculum, whereas in the most anterior regions, where most of our electrodes sat, there is a large proportion of CA3, some CA2 but a lack of subiculum and a diminishing dentate gyrus. There is evidence which suggests that the slow gamma (~25-55Hz) in the CA3 is entrained by generated slow gamma in the dentate gyrus (Hsiao et al. 2016); thereby explaining the significant reduction of slow gamma frequency connectivity from picrotoxin in the previous study where dentate gyrus dominated, but a lack of such effect in the current study. Although the significance found in the theta range in this data set is of questionable origin, that is to say it does not appear to be through any drug-induced effect, there is more of an affect here than there was in the previous study. In parallel to the slow gamma activity, the main generators of hippocampal theta, and therefore its coherence/pace-making, are located in the CA3, entorhinal cortex and other extra-hippocampal areas (Buzsaki 2001). Therefore, the decrease in theta frequency connectivity that we observe in this experiment but not in the previous may well be because of the higher dominance of CA3 in our recording areas, whereby we disrupt a theta generator and not just a propagator, which would have a stronger global effect on connectivity.

Can levetiracetam ameliorate any of the picrotoxin-induced changes?

The significant decrease in power induced by picrotoxin in the continuous state appears to be ameliorated by both doses of levetiracetam. The graph shows that the levetiracetam 10mg/kg group lies at the same level at the saline/saline group, and the levetiracetam 50mg/kg group sits closer to the saline group than to the picrotoxin group. The difference between the saline/picrotoxin group and the LEV10/picrotoxin groups is supported by a significant difference, mimicking that of the saline/saline and saline/picrotoxin. The lack of significant difference between the LEV50/picrotoxin group and all other groups suggests there is some, although not a complete, amelioration of effect. Although no significance is found in the suppression state, a similar effect of levetiracetam can be seen there.

Due to the questioning origin (i.e. the effect being present in the post-IP period negating the possibility of it being picrotoxin-induced) of the decreased low-frequency connectivity in the burst state post-infusion, the apparent amelioration by levetiracetam does not provide us any meaningful information towards our aim.

Our results support the current evidence suggesting that levetiracetam is able to ameliorate condition-induced changes in hippocampal oscillatory activity (see introduction). Furthermore, this adds further support to the mulit-unit findings of levetiracetam ameliorating picrotoxin-induced effects. It also adds weight to the hypothesis, moving forward, that this dose (specifically the lower dose of 10mg/kg) can have ameliorative effects in our awake picrotoxin model of cognition. Interestingly, our findings of significantly decreased hippocampal high beta/low gamma power from picrotoxin disinhibition in unanesthetised rats (chapter 3) corroborates the effect seen here. We would assume that this impact of picrotoxin in freely moving rats would be ameliorated by this dose of levetiracetam, but this would have to be investigated.

In conclusion, we have confirmed that our state separation method is easily replicable, producing very similar results, with the overall frequency make-up of each state closely resembling those of previous. Although we did not completely replicate the

picrotoxin-induced changes as seen previously in anaesthesia, we observed somewhat similar patterns in the high beta/low gamma power as seen numerically in the anaesthetised recordings (chapter 2), and statistically in unanaesthetised recordings (chapter 3). Additionally, we demonstrated that levetiracetam 10mg/kg, and to some extent, 50mg/kg can ameliorate the picrotoxin-induced changes in frequency specific power within the ventral hippocampus, adding further support to our hypothesis of levetiracetam ameliorating cognitive impairments induced through picrotoxin-induced disinhibition.

Chapter 6: Can levetiracetam ameliorate the behavioural changes induced by hippocampal disinhibition?

Introduction

Locomotor hyperactivity is used as a behavioural correlate to positive symptoms of schizophrenia in rodent models of the disease (Koh et al. 2018; Bast et al. 2001). In rats, hippocampal stimulation, including by picrotoxin-induced neural disinhibition (McGarrity et al. 2017), has been shown to increase locomotor activity (Bast and Feldon, 2003). In particular, independent of its relation to symptoms, increased locomotor activity in rats from picrotoxin infusion into the hippocampus is a robust finding (Bast et al., 2001; McGarrity et al., 2017) and, therefore, acts as a positive control for picrotoxin's effect in our model.

Clinically there is little knowledge of the effect of levetiracetam on locomotor hyperactivity, as it is licenced as an anti-epileptic and epilepsy is not known to cause hyperactivity (besides some indication of comorbidities between ADHD, with hyperactivity as a key symptom, in adolescents – Williams et al. 2016). There are a few studies indicating that levetiracetam can reduce the hyperactivity (as measured using various tests from the Connors Diagnostic and Statistical Manual of Mental Disorders) in children with autism (Rugino and Samsock 2002), while data from tourettes syndrome patients indicated levetiracetam has no effect on the locomotor activity as measured using an ADHD scale (Smith-Hicks et al. 2007).

While the information surrounding levetiracetam's effect on locomotor activity in clinic is limited, there are various animal models of disease where levetiracetam has been used and the locomotor activity assessed. The animal models largely show that levetiracetam has limited effect on baseline spontaneous locomotor activity (Gower et al. 2003; Zimicikova et al. 2017; Robinson et al. 2013), but reduces drug-induced locomotor hyperactivity (Robinson et al. 2013 *alcohol*; Koh et al. 2018 *ketamine*; Shannon et al. 2005 *formalin*; Lamberty et al. 2001 *dexamphetamine–chlordiazepoxide mixture*).

As discussed within the introduction (see chapter 1), hippocampal over-activity and disinhibition has been suggested to disrupt various cognitive functions, including memory, in clinical disorders, as well as in rodent models. Low doses of levetiracetam have shown promise to alleviate some of the memory dysfunctions in rodent models of age-related cognitive decline and schizophrenia, which are associated with hippocampal disinhibition (Koh et al. 2010, 2018). Additionally, low doses of levetiracetam have been shown to ameliorate memory in mild cognitive impairment patients alongside normalisation of hippocampal activity as determined through fMRI (Bakker et al. 2012, 2015). This indicates that levetiracetam can ameliorate memory impairments caused by over-activity within the hippocampus in both humans and rodents.

Aims and Hypothesis

We aimed to assess whether 10mg/kg levetiracetam was able to alleviate the increased locomotor activity induced by hippocampal picrotoxin infusion, while leaving the baseline activity level unchanged. Following this, we aimed to assess whether levetiracetam 10mg/kg was able to ameliorate the memory impairments induced by hippocampal disinhibition in the delayed-matching to place (DMP) watermaze task (McGarrity et al., 2017).

We expected to replicate the previous findings of increased locomotor activity and an impairment of memory in the DMP watermaze task due to hippocampal disinhibition via picrotoxin microinfusion (McGarrity et al., 2017). Moreover, we predicted, based on previous evidence and our electrophysiological studies, that baseline locomotor activity will be unaffected by levetiracetam, whereas the increased locomotor activity and impaired memory in the watermaze DMP task will be alleviated by levetiracetam.

Methods

Rats

Adult male Lister-hooded rats (Charles River, UK) (n = 16 for LMA 280-350g and n = 16 for watermaze 270-330g) were housed four per cage in double-decker individually

ventilated cages in a 12h light-dark cycle (lights on at 7am) in a humidity and temperature controlled room (21 ± 1.5°C; 50 ± 8%). They had ad libitum access to food (Teklad 18% protein rodent diet, Envigo, UK) and water throughout the experiment. All procedures were conducted in accordance with the requirements of the United Kingdom (UK) Animals (Scientific Procedures) Act 1986.

Cannulae implantation

Rats were anaesthetised with isoflurane (5% induction and 1-2% maintenance), dosed with Rimadyl (1:9 dilution; 0.1ml/kg) as a peri-operative analgesic, 0.02ml/kg of the antibiotic synulox (140mg amoxicillin, 35mg clavulanic acid/ml Pfizer), then secured into a stereotactic frame with the local anaesthetic EMLA cream (5%, AstraZeneca) on the ear bars to minimise the risk of pain. Surgery was conducted under completely aseptic conditions. Bilateral cannulae (stainless steel, 26-gauge, 8.5mm below pedestal – PlasticsOne, US) with a dummy cap-cannulae combination where the stylet protruded 0.5mm from the base of the cannula, were implanted into the ventral hippocampus (AP: 5.2mm, ML: ±4.8mm, DV: -6.5mm from dura), using the same coordinates as in our previous studies (McGarrity et al. 2017). Four metal screws were then inserted into the skull, two posterior and two anterior to the cannulae, to ensure maximum adhesion of the cement to the skull. Ultraviolet light-curing dental cement (flowable composite; Henry Schein, Germany) was used to seal the cannulae into the hole, completely covering the drilled hole. Dental acrylic was then used to cover this cement, the screws, and the rest of the skull to create a secure pedestal to hold the cannulae in place. The wound was sutured loosely around the pedestal. Rats were left to recover for a minimum of 9 days before undergoing any testing. Throughout the duration of the experiments rats received 0.02ml/kg synulox daily to minimise the risk of meningitis.

Drug administration

Systemic drugs were administered via intraperitoneal-injection and were either of 10mg/1ml/kg levetiracetam or 1ml/kg saline. Having confirmed the lack of ameliorative

effect of 50mg/kg levetiracetam in the electrophysiology (50mg/kg) we did not test this dose in behavioural studies to reduce the number of rats used. Rats were then infused with either 150ng/0.5ul/side picrotoxin or 0.5ul/side saline, as in our previous study (McGarrity et al., 2017). The infusion was delivered using an electric micro-pump holding two 5ul syringes (SLS) attached to polyethene tubing with a 33-gauge injector stylet on the end that was inserted through the cannula to protrude 0.5mm from the end. The infusion of 0.5ul was completed within 1 min, and the injector was left in place for an additional minute after completion of the infusion to allow for the liquid to be absorbed by the brain tissue; the success of infusion was verified by observing the movement of a marker bubble that was included in the infusion tubing.

Open-Field locomotor activity

Locomotor activity was measured as previously (McGarrity et al. 2017). Rats were placed into the centre of 1 of 12 Perspex boxes (29.5x23.5x24.5cm) with metal grid lids, to start a session. Each box had two levels of photobeams in a 4 by 8 configuration (Photobeam Activity System; San Diego Instruments, US). Locomotion was detected as two consecutive beam breaks in the bottom level of photobeams. Rats received intraperitoneal injections 5 min prior to entry into the open-field for the 30 min baseline recording, before being removed for the intracerebral infusion and returned for a 60 min post-infusion session.

This study was run in a within-subjects latin square design, with each rat receiving all four combinations of intraperitoneal condition and infusion conditions (that is: saline-saline, saline-picrotoxin, levetiracetam-saline, and levetiracetam-picrotoxin) over four test sessions, in a counter-balanced design. We started with n=16, however due to the loss of animals due to illness, we have n=13 for the completed study. A sum of all locomotor activity was created for 10min bins, in line with previous analysis (McGarrity et al. 2017). A three-way repeated measures ANOVA was run with time, systemic drug, and infusion drug as the within-subject variables. Mauchly's test was conducted to test for violation of the sphericity assumption. If the result was $p<0.05$, then the assumption of sphericity was rejected and the Greenhouse-Geisser correction was

employed if the Greenhouse-Geisser epsilon was <0.75, otherwise the Huynh-Feldt correction was applied.

DMP Watermaze

Apparatus

The delayed-matching to place (DMP) watermaze task and apparatus was mostly identical to that used previously (McGarrity et al. 2017). In brief, the watermaze itself measured 2m in diameter and 60cm in height and was placed in the middle of a well-lit (200lux) room, with unique three-dimensional cues around the edges of the room. The pool was filled with water and made opaque with non-toxic white children's paint; the water was partially changed each morning and the temperature kept between 24 and 26°C. The escape platform was an Atlantis platform (Noldus Technology, Netherlands) with a diameter of 12cm and a height of 36cm, the water level sat 1-3cm above the surface of the platform so the location was not visible for the rats. The platform had a computer-controlled electromagnetic base (Med associates inc.) that allowed the platform to be manually pushed down and automatically released 60s after the beginning of the probe trial. Rats activity during the watermaze was recorded with overhead video tracking, and were tracked via ethovision software (Version XT 8.5, Noldus Technology, Netherlands) where pathlength, search preference and velocity were calculated. Latency to reach the platform were noted manually.

Procedure

Three arrangements of platforms were used; one for the eight days of pretraining, one for the first series, and one for the second series. In each arrangement there were eight platform locations in two concentric rings with four locations each; one in an inner ring and one in an outer ring (see figure 6.1). To counterbalance between platform locations the rats were split into two groups with each group having a different platform location on any given day. Four trials were run per day, with the rats receiving a consistent platform location, on each trial the rats were released from four different, equally distanced, locations around the outside of the pool (arbitrarily named

N, E, S, W; see figure 6.1) with all rats receiving the same release location sequence each day. Rats were released against the edge of the pool, facing away from the centre of the pool. On each trial, the rat was given a maximum of 120 s to locate the hidden platform, if it was not located during this time they were guided to the platform; once the rat was on the platform they were left for 30 s before being removed. Probe trials were run to establish search preference, in these trials the platform was lowered and held in place by the electromagnet, so that it was absent for the rats, 60 s after the rat was placed into the pool for the trial the platform automatically released and rose into place for the rat to find. There were eight days of pretraining, the first four days all trials were run with minimal inter-trial-interval (ITI, approximately 15 s, i.e. the minimum amount of time required to get the rat and program ready between two successive trials), the other four days had a 20 min ITI between trials 1 and 2, with minimal ITI between trials 2,3 and 4. Days six and eight of pretraining were run with a probe trial in trial 2 and involved mock injections and infusions, with a saline i.p.

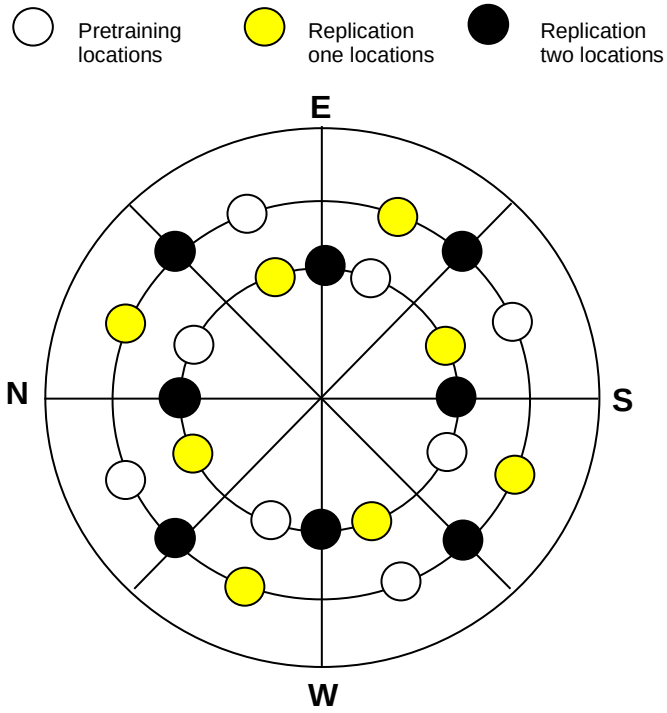


Figure 6.1 – Platform locations used for the DMP Watermaze task

A visual representation of the watermaze arena where there are two concentric rings, one an inner and one an outer, with various platform locations. Three sets of platform arrangements are shown, as used for the pretraining and the first and second replications. Each set of platform arrangements has eight locations, four in the inner ring and four in the outer ring, evenly spaced throughout the arena. The arbituary release locations, N E S W, are indicated evenly spaced around the edge of the pool.

njection and the restraining, stylet insertion and running of the infusions machines without the stylet actually being connected (aka no actual infusion); half of the rats received the mock on day six and half on day eight.

DMP Watermaze - Study Design

As in the previous study (McGarrity et al. 2017) we ran two series of infusions for the watermaze study, in a counter-balanced within subjects design with three drug groups. The first infusion series was completed by all 16 rats, however only 12 rats completed the second series because 3 rats had to be terminated early due to seizures and 1 further rat had to be excluded due to a seizure during the final probe trial. The three drug conditions were: saline i.p. injection with saline microinfusion, saline i.p. injection with picrotoxin microinfusion, and levetiracetam 10mg/kg i.p. injection with picrotoxin microinfusion. The levetiracetam 10mg/kg i.p. and saline microinfusion condition was not included in this study as microinfusion drug effects become unreliable after 6 infusions, presumably due to damage and gliosis around the infusion site (Bast et al. 2001), therefore with two series and a within-subjects design we were only able to run a maximum of 3 drug conditions. As the locomotor study showed no difference between the levetiracetam-saline and saline-saline conditions, the levetiracetam-saline condition was not included for the watermaze.

Each test day was preceded by a non-infusion day where all trials were run with the minimal ITI. On test days rats were injected with i.p. saline or i.p. levetiracetam 40 minutes prior to infusion, the infusions took approximately 5 minutes and the rats were placed immediately from infusion into trial 1 in the watermaze. There was a 20-min ITI between trials 1 and 2, and trial 2 was run as a probe, the ITI between trials 2, 3 and 4 were ~15 s.

If a rat completed all three test sessions in both infusion series, an average of their two performance measures in each condition was used for the analysis. If a rat completed only one infusion series the values from series one were included in the analysis. Therefore, there was one single value for each performance measure in

each infusion condition for each rat, either averaged across the two infusion series or only including the first series, in keeping with our previous study (McGarrity et al. 2017), with a final n = 16. In probe trials search preference was measured as a percentage of time spent in the correct zone, compared to the time spent in all eight other zones of that platform arrangement, and statistical significance for search preference and velocity were assessed using a repeated measures one-way ANOVA with drug treatment (i.p. and infusion) as the condition. The pathlength and latency were calculated for all four trials on the test day, a two-way repeated measures ANOVA with drug treatment and trial as the conditions was used to assess the statistical significance in these measures. Mauchly's test was conducted to test for violation of the sphericity assumption. If the result was $p<0.05$, then the assumption of sphericity was rejected and the Greenhouse-Geisser correction was employed if the Greenhouse-Geisser epsilon was <0.75, otherwise the Huynh-Feldt correction was applied. In all cases Fisher's LSD was used as post-hoc testing.

Results

Locomotor Activity Study

All cannulae placements in the rats who completed the locomotor study sat within the ventral hippocampus, as verified through histology (Figure 6.2A).

Rats in all drug-conditions showed very similar locomotor activity during the baseline 30 minutes, and, as expected, there was a decrease in locomotor activity over this period, reflecting locomotor habituation (figure 6.2B, left). ANOVA revealed a main effect of 10 min block ($F_{1,11} = 155$, $p < 0.0001$), there was also a i.p. drug*infusion drug interaction ($F_{1,12} = 5.12$, $p = 0.043$) which was likely a sampling error or carry over effect as there was no main effect of either i.p. or infusion drug ($F < 0.81$, $p > 0.38$).

After infusion (Fig. 6.2B, right), both of the picrotoxin conditions (with and without LEV) showed an enhancement of locomotor activity compared to the saline conditions, especially before locomotor habituation led to similarly low locomotor activity levels in all four conditions. This was supported by a significant interaction of infusion drug and time ($F_{2.43,29.2} = 11.50$, $p < 0.0001$, with Greenhouse-Geisser correction, Mauchly's $p < 0.0001$). The two picrotoxin conditions showed very similar locomotor hyperactivity, compared to the conditions involving hippocampal saline infusion, for the first 20 minutes, after which locomotor hyperactivity in the LEV*PTX condition was numerically attenuated compared to the saline*PTX condition. However, ANOVA only provided very limited support for such a time-dependent impact of LEV injection on the picrotoxin-induced hyperactivity. There was no significant i.p. drug * infusion drug * time interaction ($F_{5,60} = 1.18$, $p = 0.33$), but the interaction of ip drug and hippocampal infusion drug was just above trend level ($F_{1,12} = 2.83$, $p = 0.12$, no correction). There was no significant interaction of ip drug * time ($F_{1.61,19.3} = 1.93$, $p = 0.18$, with greenhouse-geisser correction, Mauchly's $p < 0.0001$).

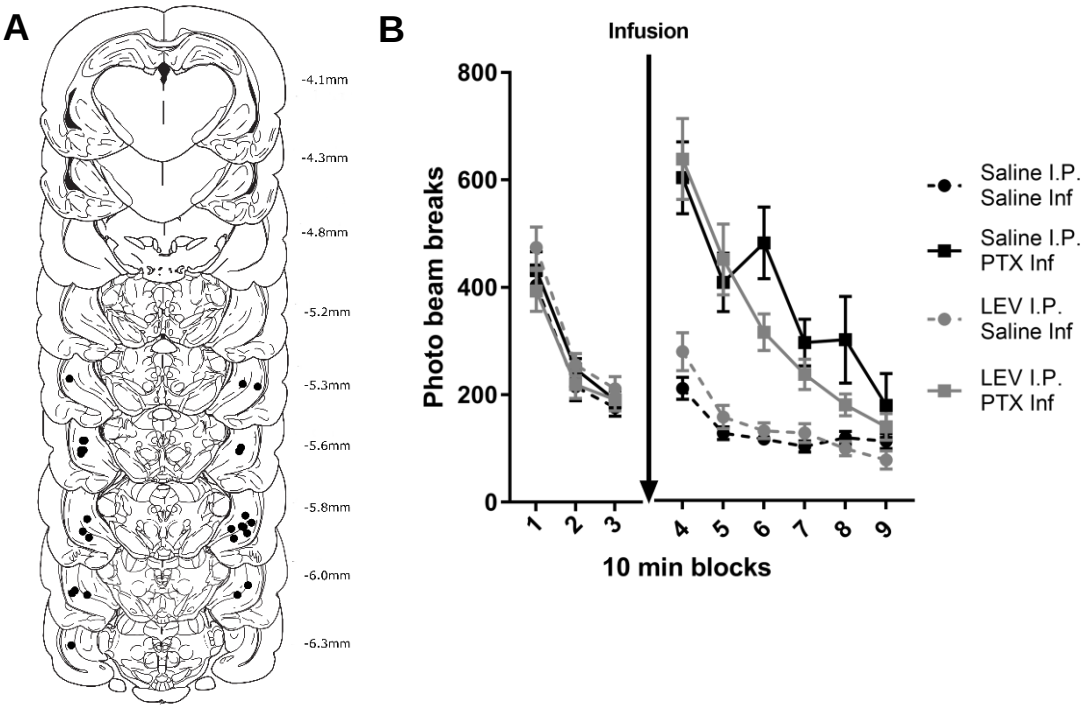


Figure 6.2 – Levetiracetam somewhat attenuates locomotor hyperactivity caused by hippocampal disinhibition

A – Locations of the cannula within the ventral hippocampus determined through histology

B – Locomotor activity within the four drug conditions, as a sum of photobeam breaks per 10 minutes. Data show mean ± SEM with N = 13

Additional behavioural changes that we noted during the course of the experiment are summarised in table 6.1. Wriggly referred to rats who, when handled, were more active and resistant than normal. Neither the saline-saline condition nor the levetiracetam-saline condition experienced any of these changes, while the levetiracetam-picrotoxin condition only showed wet-dog shakes and lethargy, with the saline-picrotoxin group showing all but lethargy.

Table 6.1 – Behavioural Changes noted by visual inspection in the different drug conditions during the locomotor experiment

The numbers represent the number of rats in which the behaviours occurred, not the total number of incidences, during that drug group (i.e. each count has a maximum of 13 due to n = 13).

	Jumpy	Wet Dog Shakes	Popcorning	Seizures	Wriggly	Lethargic
Saline-saline	0	0	0	0	0	0
Saline-picrotoxin	1	5	4	2	1	0
Levetiracetam-saline	0	0	0	0	0	0
Levetiracetam-picrotoxin	0	6	0	0	0	1

Delayed-Matching-to-Place Watermaze study

Replicating our previous findings (McGarrity et al., 2017), search preference was reduced in the saline-picrotoxin condition (13 ± 2.9 %) compared to the saline-saline condition (31 ± 4.9%) and more or less at chance (12.5%) (figure 6.3A). Search preference in the levetiracetam-picrotoxin condition (17 ± 5.2%) was between the two other conditions, with higher preference for the correct zone than the saline-picrotoxin, but impaired preference compared to the saline-saline group. A one-way repeated measures ANOVA revealed an overall significant effect of drug condition ($F_{2,30} = 4.03$, $p = 0.028$). In post-hoc testing using Fisher's LSD multiple comparisons a significant effect was found between the saline-saline condition and the saline-picrotoxin condition ($p = 0.009$), with no significant effect between the levetiracetam-saline condition and either the saline-saline ($p = 0.074$) or the saline-picrotoxin conditions (p

= 0.49). Planned comparisons of each group to chance, using one-sample unpaired tests revealed only the saline-saline group significantly differed from chance (t(30) = 3.67, p = 0.001) with the saline-picrotoxin (t(30) = 0.28, p = 0.78) and levetiracetam-picrotoxin (t(30) = 0.91, p = 0.37).

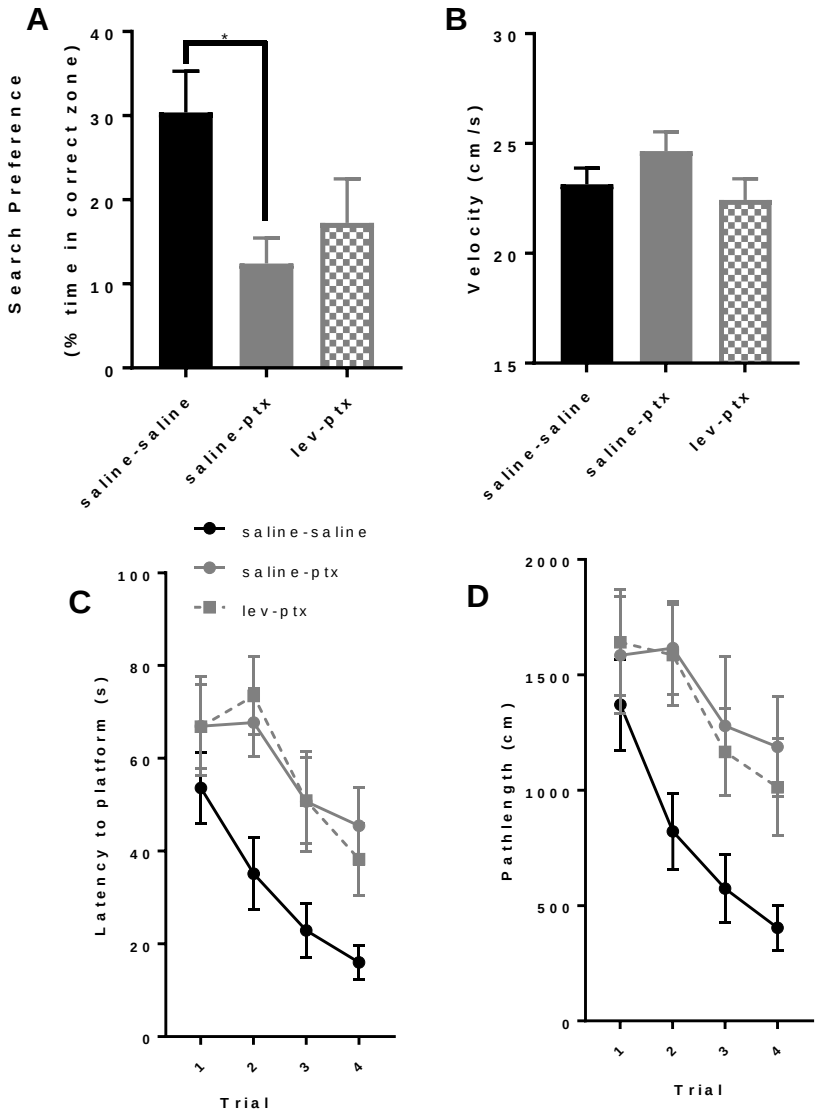


Figure 6.3 – DMP Watermaze impairment in hippocampal disinhibition is partially ameliorated with levetiracetam

A – Search preference for the correct platform location as a percentage of the time spent in that zone compared to the other 8 zones in the platform arrangement, during the probe trial. Bars are the mean ± SEM. * = p<0.05 in post-hoc tests between the pair of conditions.

B – Velocity of rats in the watermaze during the first 60 s of the probe trial. Bars are the mean ± SEM.

C - D – Shows the latency for the rats to find the platform (C) the pathlength to platform (D), in the probe trial the first time the rat crossed the platform location was counted as finding the platform, over all trials on test

The velocity of rats during the first 60 s of the probe trial (figure 6.3B) shows an increased swim speed in the saline-picrotoxin rats, and a numerically decreased swim speed in the levetiracetam-picrotoxin group. The ANOVA revealed a trend towards an effect of drug condition ($F_{1.87,28.1} = 2.79$, $p = 0.081$), with post-hoc tests revealing a trend between saline-picrotoxin and levetiracetam-picrotoxin ($p = 0.06$), with no difference between other combinations ($p > 0.25$).

The patterns of latency to find platform and pathlength are mostly identical; in both cases the saline-saline condition shows a marked decrease over the four trials, and this decrease is substantially impaired in the two conditions involving hippocampal picrotoxin infusions (figure 6.3C&D). Although the differences in latencies and path lengths between the saline infused and the picrotoxin infused conditions was most evident from trial 2 to 4, ANOVAs of both measures did not reveal a significant trial*drug-condition interaction (latency: $F_{6,90} = 0.538$, $p = 0.78$; pathlength $F_{6,90} = 0.50$, $p = 0.81$). There were only significant overall main effects of trial (latency: $F_{3,45} = 0.02$, $p < 0.0001$; pathlength $F_{3,45} = 6.59$, $p = 0.0009$) and of treatment (latency: $F_{2,30} = 11.9$, $p = 0.0002$; pathlength $F_{2,30} = 10.4$, $p = 0.0004$).

Additional behavioural and search-strategy changes were noted during the experiment and are recorded in table 6.2. Behavioural changes included wet dog shakes, which were noticeably distinct from normal drying behaviours seen during the watermaze, jumpy behaviour, and convulsive seizures noted by loss of postural control. Changes in search strategy noted were sinking, where rats would bob under the water briefly before resurfacing and continuing to swim, circling where the rats would rotate in tight circles in a different manner from circling around where they assume the platform is, and stopping where the rats would cease swimming for any amount of time without sinking. As would be expected, these behavioural and search strategy changes were never seen in the saline-saline condition, were generally more often seen in the saline-picrotoxin condition than the lev-picrotoxin condition, except

for wet dog shakes which were more often noted in the lev-picrotoxin condition than the saline-picrotoxin condition.

Table 6.2 – Behavioural and Search Strategy Changes noted during the DMP watermaze

The numbers represent the number of incidences of each behaviour noted in each drug group. For each drug-condition a value is shown for series 1 and series 2 with a total over both series. These counts are not individual incidences, but rather the count of rats who experienced it (i.e. for series one there was a maxiumum of 16).

		Behavioural						Search-Strategy					
		Jumpy		Wet-Dog shakes		Seizures		Circles		Stopping		Sinking	
Saline - saline	Series 1	0	*0*	0	*0*	0	*0*	0	*0*	0	0	0	*0*
	Series 2	0		0		0		0		0		0	
Saline - picrotoxin	Series 1	3	*3*	5	*10*	1	*5*	3	*7*	1	9	3	*6*
	Series 2	0		5		4		4		8		3	
Levetiracetam - picrotoxin	Series 1	0	*0*	7	*13*	0	*1*	2	*4*	1	3	3	*4*
	Series 2	0		6		1		2		2		1	

Discussion

We showed that hippocampal disinhibition through picrotoxin microinfusion increased locomotor activity and decreased rapid place learning performance on the delayed-matching to place watermaze task, replicating previous findings (McGarrity et al. 2017). There was some evidence for levetiracetam (10mg/kg) to attenuate these behavioural effects of hippocampal disinhibition, with the levetiracetam-picrotoxin condition showing intermediate locomotor and DMP watermaze performance measures between the saline-saline and saline-picrotoxin conditions although statistical support for these effects of LEV were very limited.

Seizure-related changes caused by hippocampal disinhibition

In both the locomotor and the DMP watermaze study, visual inspection revealed some seizure-related behavioural changes in the rats after hippocampal picrotoxin, but not saline, microinfusion. In both studies we noted three common behavioural changes: wet dog shakes, jumpiness, and seizures (convulsions with loss of postural control). In the locomotor activity study, we also noted incidences of popcorning, wriggling and lethargy. Distinct changes in the swim behaviour of some rats in the watermaze were

noted, specifically circling, stopping and sinking. Apart from lethargy and wet dog shakes, the occurrence of these behavioural changes was greater in the saline-picrotoxin group than the levetiracetam-picrotoxin group. The wet dog shakes were noted more often, in both studies, in the levetiracetam-picrotoxin group than the saline-picrotoxin group. While we do not often see seizures, we commonly see the seizure-precursor wet-dog shakes in our hippocampal picrotoxin model, with jumpiness and popcorning being less common and later-stage precursors observed. The shift backwards from later-stage precursors, towards wet-dog shakes, in the levetiracetam-picrotoxin condition compared to the saline-picrotoxin condition is expected considering levetiracetam's antiepileptic properties. Changes in swim behaviour in all picrotoxin infused rats may be because of behavioural changes induced by picrotoxin; for example, stopping was sometimes accompanied by wet dog shakes, where rats were unable to continue swimming forward while enacting the behaviour.

Locomotor activity study

The significant increase in locomotor activity after picrotoxin infusion compared to saline infusion is a replication of our previous findings (McGarrity et al. 2016). Although there was no significant alleviation of this effect by levetiracetam 10mg/kg, there was in indication of a decrease from 30 minutes onwards, compared to the saline-picrotoxin, although this was not significant. A ceiling effect likely prevented us from seeing any ameliorative effect of levetiracetam during the first 20 minutes following hippocampal picrotoxin infusion, and, numerically, the impact of levetiracetam was only apparent during the last 40 min of the locomotor session when activity levels were declining in both picrotoxin conditions, but levetiracetam facilitated the reduction in locomotor activity.

Similar to the electrophysiological data, we see some indication of levetiracetam ameliorating the locomotor hyperactivity, although it is limited. Interestingly, the attenuation by levetiracetam (10 mg/kg) of ketamine-induced locomotor hyperactivity reported by Koh and colleagues (2018) was of similar magnitude to the effect we

observed and was also only at trend level (drug*time p = 0.09), whereas there was a significant amelioration of place memory on the radial arm maze task.

Watermaze DMP study

Firstly, we were able to replicate the impairment of one-trial place-memory following picrotoxin infusion as seen previously, where picrotoxin infused rats showed search preference for the correct location at chance level, and saline infused rats performed significantly better than chance (McGarrity et al. 2017). Additionally, the pathlengths show similar patterns to previously where from trial 2 onwards the saline-saline groups decrease their pathlengths at a faster rate than the saline-picrotoxin rats.

There was some indication that levetiracetam (10mg/kg) slightly ameliorated the memory-impairment induced by hippocampal picrotoxin microinfusion. More specifically, although there was a statistically significant difference between the saline-saline and saline-picrotoxin conditions in search preference for the correct zone, there was no statistical significance between saline-saline and levetiracetam-picrotoxin, nor saline-picrotoxin and levetiracetam-picrotoxin conditions. However, when each group is compared to chance, only the saline-saline condition performs significantly better than chance level, which indicates that levetiracetam 10mg/kg does not significantly restore memory above chance. Interestingly, there is no such effect in the pathlength or latency to platform in the probe trial; both the saline-picrotoxin and levetiracetam-picrotoxin groups are statistically increased from the saline-saline group and statistically indistinguishable from one-another.

Koh and colleagues (2010) have previously assessed the impact of an acute dose of 10mg/kg levetiracetam in a watermaze task. They found that, with levetiracetam administered prior to trial 1, memory in the probe trial was significantly increased, as measured by the percentage of time in the correct quadrant. However, the trial 1 to trial 2 delay was 24 hours, not 20 minutes as in ours. Further studies using acute, low doses of levetiracetam (<10mg/kg) have shown restoration of memory deficits,

however this was shown in both the hippocampal dependent memory task, the radial arm maze (Koh et al. 2010, 2018), and in a contextual fear task (Devi and Ohno, 2013). We could not find any reports of low doses of levetiracetam (<10mg/kg) failing to significantly ameliorate memory impairments.

Studies using acute higher doses of levetiracetam in memory tasks have, however, reported lack of ameliorative effect (Sanon et al. 2018 *300mg/kg in kainic acid epileptogenesis*; Sanchez et al. 2012 *200mg/kg in AD mice*; Lamberty et al. 2001 *54mg/kg and 170mg/kg kindled rats*). Whereas, chronic mid-to-high doses show varied results, with some successfully ameliorating memory impairments in water maze and elevated plus maze tasks (Sanchez et al. 2012 *75mg/kg/day in AD mice*; Ge et al. 2016 *50mg/kg 2 times daily for 2 weeks in status epilepticus rats)* and some showing no effect (Brandt et al. 2007 *200mg/kg in status epilepticus rats*; Zhou et al. 2006 *50mg/kg 2 times daily for 2 weeks in status epilepticus rats).*

Overall, the current literature suggests that acute low-doses of levetiracetam can ameliorate non-epilepsy related memory impairments, while higher acute-doses are ineffective at restoring memory impairments, and mid-to-high chronic doses show variation in the efficacy of memory restoration. To our knowledge, our findings of limited effect of acute-low doses of levetiracetam in memory restoration are the first. Non-specific effects of picrotoxin in our model may be a confounding factor within our data limiting the observation of levetiracetam's effect; however, the variability of levetiracetam's effectiveness at higher chronic doses brings into question the consistency and nuances of levetiracetam's ameliorative effect.

Conclusions

These behavioural studies have confirmed the effects seen previously from hippocampal disinhibition (McGarrity et al, 2017), specifically an increase in locomotor activity and a decrease of search preference and increased pathlength in the DMP watermaze task. There is little support within this data-set for levetiracetam to

ameliorate either picrotoxin-induced locomotor activity nor decreased DMP watermaze performance after picrotoxin infusion.

Chapter 7: General Discussion

Main Findings

Impact of hippocampal disinhibition on neural oscillations

Firstly, within this thesis we extended the previous findings in our rat model of hippocampal disinhibition by analysing the impact of hippocampal disinhibition on hippocampal LFP and surface EEG oscillations. We started, in chapter 2, by analysing hippocampal LFP data recorded in conjunction with the previously published multi-unit data, in the vicinity of the hippocampal infusion site, in anaesthetised rats (McGarrity et al. 2017). We created a semi-automated method for separating out the clearly distinct LFP states so that we could then analyse them robustly. We demonstrated that these states: the 'burst', 'suppression', and 'continuous', have distinct and unique power and connectivity profiles, emphasising the importance of separating out the states prior to analysis to disentangle any state-specific effects. Overall, in the anaesthetised recordings we found a general increase in theta power and a decrease in beta/gamma connectivity, with an indication of a decrease in beta/gamma power with hippocampal disinhibition, which was most evident in the burst state.

In Chapter 3, to examine how these findings under anaesthesia may relate to electrophysiological recordings made in clinic, i.e. surface EEG recordings, and thereby provide greater translatability for our model, we conducted a telemetric LFP/EEG study in unanaesthetised rats with hippocampal disinhibition. This allowed us examine the impact of hippocampal disinhibition on LFP oscillations in the hippocampus of unanaesthetised rats, in parallel to surface EEG recordings above the frontal cortex, and to measurements of heart-rate variability as a further translational measure. Our data revealed that, in contrast to the anaesthetised recordings, hippocampal disinhibition did not affect hippocampal theta power but significantly decreased beta/gamma power, confirming the trend seen previously in the anaesthetised rats. The impact of hippocampal disinhibition on surface EEG recordings over the frontal cortex and on heart-rate variability was limited.

These studies combined confirmed and extended previous findings of GABA-A receptor mediated mechanisms regulating hippocampal LFP oscillations by positively modulating power and connectivity at higher frequencies (Buzsaki & Wang, 2012; Traub et al., 2004; Whittington et al., 2000), independent of anaesthesia. Whereas our anaesthetised recordings confirmed and extended previous evidence of GABA-A receptor mechanisms negatively modulating power at lower frequencies (Kowalczyk et al., 2013), our ability to detect such changes under anesthersia was likely due to already decreased theta from anaesthesia (MacIver and Bland 2014); a ceiling effect likely prevents such an increase in theta power being seen in our unanaesthetised recordings.

Impact of levetiracetam on neuro-behavioural effects of hippocampal disinhibition

Secondly, we applied the same electrophysiological and behavioural approaches as previously (McGarrity et al. 2017), as well as the anaesthetised LFP analysis we developed (Gwilt et al. 2020; chapter 2) to establish if low doses of the second-generation anti-epileptic levetiracetam could ameliorate the effect of our hippocampal neural disinhibition model. Initially, in chapter 4, we assessed the electrophysiological effects under anaesthesia as previously this showed a robust change from picrotoxin infusion in the hippocampus. We replicated the finding that hippocampal disinhibition increases burst parameters (McGarrity et al., 2017). However, we only found an amelioration of the burst duration from the low-dose (10mg/kg) of levetiracetam, with no effect on other parameters. Furthermore, there was a significant decrease in the baseline peak frequency in burst at the higher-dose (50mg/kg; used to compare to seizure studies), indicating higher doses of levetiracetam can affect baseline activity. The LFP recordings under anaesthesia, presented in chapter 5, once again showed a decrease in power from picrotoxin in the high beta/low gamma range, however this was seen during the continuous state not the burst state as previously. This picrotoxin-induced decrease in high beta/low gamma power was significantly ameliorated by the 10mg/kg levetiracetam but not 50mg/kg. Considering the indication of ameliorative effects of 10mg/kg, but not 50mg/kg, and the evidence that 50 mg/kg

may affect baseline hippocampal activity, behavioural studies that are presented in chapter 6, focused on the dose of 10mg/kg. First, locomotor activity was tested using a 2x2 design with saline and 10mg/kg levetiracetam as i.p. conditions and saline and picrotoxin as infusion conditions, all rats received all four combinations. This locomotor test confirmed the increased locomotor activity from hippocampal picrotoxin infusion (Bast et al., 2001; McGarrity et al., 2017) and revealed a slight numerical attenuation of this locomotor hyperactivity with 10mg/kg levetiracetam. We further confirmed that 10mg/kg levetiracetam has no effect on the baseline activity, considering the lack of difference between the saline-saline and levetiracetam-saline groups. Second, we assessed whether levetiracetam could ameliorate the memory-impairments induced by hippocampal disinhibition and measured through the DMP watermaze task (McGarrity et al., 2017). This study was run in a within-subjects design with three treatment conditions (saline i.p. and saline infusion, saline i.p. and picrotoxin infusion, and levetiracetam 10mg/kg i.p. and picrotoxin infusion) in two infusion series. Once again, the findings from McGarrity et al. (2017) were replicated, in that hippocampal picrotoxin microinfusion significantly impaired memory for the correct platform location compared to saline microinfusion. As with the electrophysiological and locomotor studies, levetiracetam had limited effect on the hippocampal disinhibition-induced impairments in memory. A slight amelioration of memory impairment was seen with levetiracetam pretreatment, in that unlike the saline-saline and saline-picrotoxin search preferences that were statistically independent of one another, the levetiracetam-picrotoxin group sat between the two with no statistical difference from either. However, neither the saline-picrotoxin nor the levetiracetam-picrotoxin group showed a significant difference from chance in the search preference, indicating a limited impact of levetiracetam.

Clinical Implications

Overall, this thesis has shown that our hippocampal disinhibition model results in local oscillatory changes in the hippocampus both under anaesthesia and in natural wake and sleep. The most robust oscillatory change induced by our model is a decrease in

the beta/gamma power and connectivity. This is also a common clinical finding, albeit in surface EEG recordings in various regions, in both schizophrenia (Moran and Hong 2011; Schnitzler and Gross 2005) and mild cognitive decline and early stages of Alzheimer's disease (Rossini et al. 2007; McBride et al. 2014; Benwell 2020; Schnitzler and Gross 2005). Furthermore, we have demonstrated that low doses of levetiracetam have a limited effect on hippocampal disinhibition, where it is unable to completely ameliorate many induced changes. We do show, however, an amelioration in the multi-unit burst duration that is supported by the proposed mechanism of action of levetiracetam (Meehan et al. 2011), an amelioration of the beta/gamma oscillatory changes, and a decrease in seizure-precursor behaviours, all of which act as positive controls of levetiracetam's effect. Our findings of limited effects of low-doses of levetiracetam are in contrast to findings by others in rodent models of age-related cognitive decline, and schizophrenia models (Koh et al. 2010, 2018). One consideration is that we have a more severe hippocampal disinhibition and over-activity in our model, than the more subtle hippocampal disinhibition likely involved both in the animal models used by Koh and colleagues, and in clinical conditions. This may lead to non-specific effects in our model, such as the behavioural changes discussed, which impair our ability to detect amelioration of memory. On the other hand, the increased severity of our hippocampal disinhibition may be too great for levetiracetam to ameliorate. Therefore, while we are unable to show a distinct ameliorative effect of levetiracetam in our model, the indication towards such an effect combined with the more severe hippocampal disinhibition we induce, does not disprove any potential clinical benefits of levetiracetam.

Limitations of studies

Multi-unit Recordings

The signals that we record during our electrophysiological studies are not sufficient to reliably separate out the spikes into single-unit recordings, therefore to prevent over-interpretation or over-manipulation of unit-data we solely analyse the multi-unit data. While the burst-analysis we apply to such multi-unit data is mostly used for single-

units where the bursting can be attributed to firing of individual neurons, here we apply it in a cruder manner to determine if there is an increase or decrease in overall population activity. The use of the bursting methods for our multi-unit data is supported by our previous study where a picrotoxin-induced increase in population bursting parameters, but not overall firing rate was seen (McGarrity et al. 2017). Therefore, while such burst-analysis should be viewed cautiously within this work, the overall changes of such multi-unit 'bursting' in our data informs whether the manipulations are causing a general change within the system.

tEEG study

As mentioned in chapter 3, one main limitation of the evaluation of prefrontal activity via surface recordings is the depth of the area in rodents and the confounding signal from areas sitting between the prefrontal cortex and the recording electrode. Perhaps a more appropriate step before implementation of a frontal surface recording would have been to record prefrontal activity with a depth electrode to ascertain the direct impact of hippocampal disinhibition on prefrontal activity. If we had such a dataset it may be easier to interpret if effects in the frontal EEG recordings after picrotoxin infusion may be from prefrontal cortex.

Furthermore, the implantation tEEG transmitters and leads caused more problems within the Lister-hooded rats used in this study than in the albino rats, which had been used previously. This added complication limited data collection as many rats had to be culled early to prevent severity-limit breaches. If the surgery were not so hard on the rats data collection such as the impact of levetiracetam on non-anaesthetised recordings, and even anaesthesed recordings in the same animals as non-anaesthetised recordings for greater translation within the studies would have been able to be considered.

Anaesthetised recording differences

As discussed in chapter 5, slight differences in the recording in the experiments detailed in chapters 4 and 5, and of those from McGarrity et al. (2017) may lead to

differences in effects seen and potentially confound any comparison between the two. While a smaller array (4-wire) was used than previously (8-wire), the electrodes actually recorded from previously was on average 6-electrodes, due to many sitting outside the hippocampus. The 4-wire array was thus selected for the later experiments as there would be a fairly consistent number of electrodes recorded from each time, and all four wires (1mm) would fit within the hippocampus. Another significant difference between the two datasets is the area of the hippocampus where they sat: previously the bulk were located more anterior than in the recent study despite the same coordinates being used, which is likely an inter-experimenter effect. Overall, these differences likely contribute to the decreased firing we saw in the levetiracetam experiment. Nevertheless, we saw comparable patterns of MUA in both studies following picrotoxin infusion, which allows us relative confidence of comparison between studies especially the ameliorative effect of levetiracetam. Similarly, the patterns seen in the LFP power at baseline and after picrotoxin infusion are comparable to those previously (notwithstanding the time spent in different LFP anaesthetic states), once again justifying comparison between datasets. In contrast to these two, these differences between recordings appear to impact on the local LFP connectivity (see chapter 5 discussion) which prevented us being able to draw comparisons.

Conclusions

This thesis has demonstrated that hippocampal disinhibition causes a local decrease in high beta/low gamma power and connectivity, in both anaesthetised and unanesthetised rats. Furthermore, we showed that only anaesthetised rats showed marked increases in theta frequencies following hippocampal disinhibition. Importantly, we also showed the value of separating out anaesthetic and vigilance states, prior to analysis, and highlighted the semi-automated method we developed for anaesthetic state separation.

Low doses of levetiracetam show limited effectiveness in ameliorating picrotoxin-induced hippocampal disinhibition. Electrophysiological findings show a slight amelioration of the burst duration multi-unit parameter, and of the beta/gamma power in the LFP, but no effect in the other multi-unit parameters. Furthermore, although a slight numerical amelioration is seen in both the locomotor activity and the delayed matching to place watermaze task, levetiracetam was unable to completely restore normal activity. Overall, low doses of levetiracetam have some ameliorative effects in our hippocampal disinhibition model, but these are not sufficient to restore normal cognitive function.

References

Abramov, E., Dolev, I., Fogel, H., Ciccotosto, G. D., Ruff, E., & Slutsky, I. (2009). Amyloid-beta as a positive endogenous regulator of release probability at hippocampal synapses. *Nat Neurosci, 12*(12), 1567-1576. doi:10.1038/nn.2433

Adamantidis, A. R., Gutierrez Herrera, C., & Gent, T. C. (2019). Oscillating circuitries in the sleeping brain. *Nat Rev Neurosci, 20*(12), 746-762. doi:10.1038/s41583-019-0223-4

Alvares, G. A., Quintana, D. S., Hickie, I. B., & Guastella, A. J. (2016). Autonomic nervous system dysfunction in psychiatric disorders and the impact of psychotropic medications: a systematic review and meta-analysis. *J Psychiatry Neurosci, 41*(2), 89-104. doi:10.1503/jpn.140217

Amilhon, B., Huh, C. Y., Manseau, F., Ducharme, G., Nichol, H., Adamantidis, A., & Williams, S. (2015). Parvalbumin Interneurons of Hippocampus Tune Population Activity at Theta Frequency. *Neuron, 86*(5), 1277-1289. doi:10.1016/j.neuron.2015.05.027

Angehagen, M., Margineanu, D. G., Ben-Menachem, E., Ronnback, L., Hansson, E., & Klitgaard, H. (2003). Levetiracetam reduces caffeine-induced Ca2+ transients and epileptiform potentials in hippocampal neurons. *Neuroreport, 14*(3), 471-475. doi:10.1097/00001756-200303030-00035

Arai, J., & Natsume, K. (2006). The properties of carbachol-induced beta oscillation in rat hippocampal slices. *Neurosci Res, 54*(2), 95-103. doi:10.1016/j.neures.2005.10.011

Aydore, S., Pantazis, D., & Leahy, R. M. (2013). A note on the phase locking value and its properties. *Neuroimage, 74*, 231-244. doi:10.1016/j.neuroimage.2013.02.008

Bai, D., Zhu, G., Pennefather, P., Jackson, M. F., MacDonald, J. F., & Orser, B. A. (2001). Distinct functional and pharmacological properties of tonic and quantal inhibitory postsynaptic currents mediated by gamma-aminobutyric acid(A)

receptors in hippocampal neurons. *Mol Pharmacol, 59*(4), 814-824. doi:10.1124/mol.59.4.814

Bakker, A., Albert, M. S., Krauss, G., Speck, C. L., & Gallagher, M. (2015). Response of the medial temporal lobe network in amnestic mild cognitive impairment to therapeutic intervention assessed by fMRI and memory task performance. *Neuroimage Clin, 7*, 688-698. doi:10.1016/j.nicl.2015.02.009

Bakker, A., Krauss, G. L., Albert, M. S., Speck, C. L., Jones, L. R., Stark, C. E., . . . Gallagher, M. (2012). Reduction of hippocampal hyperactivity improves cognition in amnestic mild cognitive impairment. *Neuron, 74*(3), 467-474. doi:10.1016/j.neuron.2012.03.023

Bar, K. J., Letzsch, A., Jochum, T., Wagner, G., Greiner, W., & Sauer, H. (2005). Loss of efferent vagal activity in acute schizophrenia. *J Psychiatr Res, 39*(5), 519-527. doi:10.1016/j.jpsychires.2004.12.007

Bast, T. (2007). Toward an integrative perspective on hippocampal function: from the rapid encoding of experience to adaptive behavior. *Rev Neurosci, 18*(3-4), 253-281. doi:10.1515/revneuro.2007.18.3-4.253

Bast, T. (2011). The hippocampal learning-behavior translation and the functional significance of hippocampal dysfunction in schizophrenia. *Curr Opin Neurobiol, 21*(3), 492-501. doi:10.1016/j.conb.2011.01.003

Bast, T., Pezze, M., & McGarrity, S. (2017). Cognitive deficits caused by prefrontal cortical and hippocampal neural disinhibition. *Br J Pharmacol, 174*(19), 3211-3225. doi:10.1111/bph.13850

Bast, T., Zhang, W. N., Heidbreder, C., & Feldon, J. (2001). Hyperactivity and disruption of prepulse inhibition induced by N-methyl-D-aspartate stimulation of the ventral hippocampus and the effects of pretreatment with haloperidol and clozapine. *Neuroscience, 103*(2), 325-335. doi:10.1016/s0306-4522(00)00589-3

Bastos, A. M., & Schoffelen, J. M. (2015). A Tutorial Review of Functional Connectivity Analysis Methods and Their Interpretational Pitfalls. *Front Syst Neurosci, 9*, 175. doi:10.3389/fnsys.2015.00175

Belluscio, M. A., Mizuseki, K., Schmidt, R., Kempter, R., & Buzsaki, G. (2012). Cross-frequency phase-phase coupling between theta and gamma oscillations in the hippocampus. *J Neurosci, 32*(2), 423-435. doi:10.1523/JNEUROSCI.4122-11.2012

Benes, F. M., & Berretta, S. (2001). GABAergic interneurons: implications for understanding schizophrenia and bipolar disorder. *Neuropsychopharmacology, 25*(1), 1-27. doi:10.1016/S0893-133X(01)00225-1

Benwell, C. S. Y., Davila-Perez, P., Fried, P. J., Jones, R. N., Travison, T. G., Santarnecchi, E., . . . Shafi, M. M. (2020). EEG spectral power abnormalities and their relationship with cognitive dysfunction in patients with Alzheimer's disease and type 2 diabetes. *Neurobiol Aging, 85*, 83-95. doi:10.1016/j.neurobiolaging.2019.10.004

Bieda, M. C., Su, H., & Maciver, M. B. (2009). Anesthetics discriminate between tonic and phasic gamma-aminobutyric acid receptors on hippocampal CA1 neurons. *Anesth Analg, 108*(2), 484-490. doi:10.1213/ane.0b013e3181904571

Billman, G. E. (2013). The effect of heart rate on the heart rate variability response to autonomic interventions. *Front Physiol, 4*, 222. doi:10.3389/fphys.2013.00222

Birnstiel, S., Wulfert, E., & Beck, S. G. (1997). Levetiracetam (ucb LO59) affects in vitro models of epilepsy in CA3 pyramidal neurons without altering normal synaptic transmission. *Naunyn Schmiedebergs Arch Pharmacol, 356*(5), 611-618. doi:10.1007/pl00005097

Boddeke, H. W., Best, R., & Boeijinga, P. H. (1997). Synchronous 20 Hz rhythmic activity in hippocampal networks induced by activation of metabotropic glutamate receptors in vitro. *Neuroscience, 76*(3), 653-658.

Boido, D., Farisello, P., Cesca, F., Ferrea, E., Valtorta, F., Benfenati, F., & Baldelli, P. (2010). Cortico-hippocampal hyperexcitability in synapsin I/II/III knockout mice: age-dependency and response to the antiepileptic drug levetiracetam. *Neuroscience, 171*(1), 268-283. doi:10.1016/j.neuroscience.2010.08.046

Borhegyi, Z., Varga, V., Szilagyi, N., Fabo, D., & Freund, T. F. (2004). Phase segregation of medial septal GABAergic neurons during hippocampal theta activity. *J Neurosci, 24*(39), 8470-8479. doi:10.1523/JNEUROSCI.1413-04.2004

Boutros, N. N. (2008). P300 amplitude reduction in schizophrenia: an endophenotype or an illness indicator? *Clin Neurophysiol, 119*(12), 2669-2670. doi:10.1016/j.clinph.2008.09.012

Bouwman, B. M., & van Rijn, C. M. (2004). Effects of levetiracetam on spike and wave discharges in WAG/Rij rats. *Seizure, 13*(8), 591-594. doi:10.1016/j.seizure.2004.02.001

Bragin, A., Azizyan, A., Almajano, J., & Engel, J., Jr. (2009). The cause of the imbalance in the neuronal network leading to seizure activity can be predicted by the electrographic pattern of the seizure onset. *J Neurosci, 29*(11), 3660-3671. doi:10.1523/JNEUROSCI.5309-08.2009

Brandon, M. P., Bogaard, A. R., Libby, C. P., Connerney, M. A., Gupta, K., & Hasselmo, M. E. (2011). Reduction of theta rhythm dissociates grid cell spatial periodicity from directional tuning. *Science, 332*(6029), 595-599. doi:10.1126/science.1201652

Brandt, C., Glien, M., Gastens, A. M., Fedrowitz, M., Bethmann, K., Volk, H. A., . . . Loscher, W. (2007). Prophylactic treatment with levetiracetam after status epilepticus: lack of effect on epileptogenesis, neuronal damage, and behavioral alterations in rats. *Neuropharmacology, 53*(2), 207-221. doi:10.1016/j.neuropharm.2007.05.001

Breier, A. (2005). Developing drugs for cognitive impairment in schizophrenia. *Schizophr Bull, 31*(4), 816-822. doi:10.1093/schbul/sbi051

Brown, R. E., Basheer, R., McKenna, J. T., Strecker, R. E., & McCarley, R. W. (2012). Control of sleep and wakefulness. *Physiol Rev, 92*(3), 1087-1187. doi:10.1152/physrev.00032.2011

Busche, M. A., Chen, X., Henning, H. A., Reichwald, J., Staufenbiel, M., Sakmann, B., & Konnerth, A. (2012). Critical role of soluble amyloid-beta for early

hippocampal hyperactivity in a mouse model of Alzheimer's disease. *Proc Natl Acad Sci U S A, 109*(22), 8740-8745. doi:10.1073/pnas.1206171109

Busche, M. A., Eichhoff, G., Adelsberger, H., Abramowski, D., Wiederhold, K. H., Haass, C., . . . Garaschuk, O. (2008). Clusters of hyperactive neurons near amyloid plaques in a mouse model of Alzheimer's disease. *Science, 321*(5896), 1686-1689. doi:10.1126/science.1162844

Buzsaki, G. (2001). Hippocampal GABAergic interneurons: a physiological perspective. *Neurochem Res, 26*(8-9), 899-905. doi:10.1023/a:1012324231897

Buzsaki, G., Anastassiou, C. A., & Koch, C. (2012). The origin of extracellular fields and currents--EEG, ECoG, LFP and spikes. *Nat Rev Neurosci, 13*(6), 407-420. doi:10.1038/nrn3241

Buzsaki, G., & Draguhn, A. (2004). Neuronal oscillations in cortical networks. *Science, 304*(5679), 1926-1929. doi:10.1126/science.1099745

Castle, M., Comoli, E., & Loewy, A. D. (2005). Autonomic brainstem nuclei are linked to the hippocampus. *Neuroscience, 134*(2), 657-669. doi:10.1016/j.neuroscience.2005.04.031

Cataldi, M., Lariccia, V., Secondo, A., di Renzo, G., & Annunziato, L. (2005). The antiepileptic drug levetiracetam decreases the inositol 1,4,5-trisphosphate-dependent [Ca2+]I increase induced by ATP and bradykinin in PC12 cells. *J Pharmacol Exp Ther, 313*(2), 720-730. doi:10.1124/jpet.104.079327

Chang, J. S., Yoo, C. S., Yi, S. H., Hong, K. H., Lee, Y. S., Oh, H. S., . . . Ahn, Y. M. (2010). Changes in heart rate dynamics of patients with schizophrenia treated with risperidone. *Prog Neuropsychopharmacol Biol Psychiatry, 34*(6), 924-929. doi:10.1016/j.pnpbp.2010.04.017

Chang, J. S., Yoo, C. S., Yi, S. H., Hong, K. H., Oh, H. S., Hwang, J. Y., . . . Kim, Y. S. (2009). Differential pattern of heart rate variability in patients with schizophrenia. *Prog Neuropsychopharmacol Biol Psychiatry, 33*(6), 991-995. doi:10.1016/j.pnpbp.2009.05.004

Cho, J. R., Koo, D. L., Joo, E. Y., Yoon, S. M., Ju, E., Lee, J., . . . Hong, S. B. (2012). Effect of levetiracetam monotherapy on background EEG activity and cognition in drug-naive epilepsy patients. *Clin Neurophysiol, 123*(5), 883-891. doi:10.1016/j.clinph.2011.09.012

Clamor, A., Lincoln, T. M., Thayer, J. F., & Koenig, J. (2016). Resting vagal activity in schizophrenia: meta-analysis of heart rate variability as a potential endophenotype. *Br J Psychiatry, 208*(1), 9-16. doi:10.1192/bjp.bp.114.160762

Clement, E. A., Richard, A., Thwaites, M., Ailon, J., Peters, S., & Dickson, C. T. (2008). Cyclic and sleep-like spontaneous alternations of brain state under urethane anaesthesia. *PLoS One, 3*(4), e2004. doi:10.1371/journal.pone.0002004

Cohen, M. X. (2015). Effects of time lag and frequency matching on phase-based connectivity. *J Neurosci Methods, 250*, 137-146. doi:10.1016/j.jneumeth.2014.09.005

Colgin, L. L. (2011). Oscillations and hippocampal-prefrontal synchrony. *Curr Opin Neurobiol, 21*(3), 467-474. doi:10.1016/j.conb.2011.04.006

Colgin, L. L. (2016). Rhythms of the hippocampal network. *Nat Rev Neurosci, 17*(4), 239-249. doi:10.1038/nrn.2016.21

Colgin, L. L., Denninger, T., Fyhn, M., Hafting, T., Bonnevie, T., Jensen, O., . . . Moser, E. I. (2009). Frequency of gamma oscillations routes flow of information in the hippocampus. *Nature, 462*(7271), 353-357. doi:10.1038/nature08573

Coyle, J. T. (2012). NMDA receptor and schizophrenia: a brief history. *Schizophr Bull, 38*(5), 920-926. doi:10.1093/schbul/sbs076

Cuomo, O., Rispoli, V., Leo, A., Politi, G. B., Vinciguerra, A., di Renzo, G., & Cataldi, M. (2013). The antiepileptic drug levetiracetam suppresses non-convulsive seizure activity and reduces ischemic brain damage in rats subjected to permanent middle cerebral artery occlusion. *PLoS One, 8*(11), e80852. doi:10.1371/journal.pone.0080852

Daniels, V., Wood, M., Leclercq, K., Kaminski, R. M., & Gillard, M. (2013). Modulation of the conformational state of the SV2A protein by an allosteric mechanism as evidenced by ligand binding assays. *Br J Pharmacol, 169*(5), 1091-1101. doi:10.1111/bph.12192

Das, P., & Dillon, G. H. (2005). Molecular determinants of picrotoxin inhibition of 5-hydroxytryptamine type 3 receptors. *J Pharmacol Exp Ther, 314*(1), 320-328. doi:10.1124/jpet.104.080325

De Smedt, T., Raedt, R., Vonck, K., & Boon, P. (2007a). Levetiracetam: part II, the clinical profile of a novel anticonvulsant drug. *CNS Drug Rev, 13*(1), 57-78. doi:10.1111/j.1527-3458.2007.00005.x

De Smedt, T., Raedt, R., Vonck, K., & Boon, P. (2007b). Levetiracetam: the profile of a novel anticonvulsant drug-part I: preclinical data. *CNS Drug Rev, 13*(1), 43-56. doi:10.1111/j.1527-3458.2007.00004.x

De Smedt, T., Vonck, K., Raedt, R., Dedeurwaerdere, S., Claeys, P., Legros, B., . . . Boon, P. (2005). Rapid kindling in preclinical anti-epileptic drug development: the effect of levetiracetam. *Epilepsy Res, 67*(3), 109-116. doi:10.1016/j.eplepsyres.2005.09.004

Degenetais, E., Thierry, A. M., Glowinski, J., & Gioanni, Y. (2003). Synaptic influence of hippocampus on pyramidal cells of the rat prefrontal cortex: an in vivo intracellular recording study. *Cereb Cortex, 13*(7), 782-792. doi:10.1093/cercor/13.7.782

Devi, L., & Ohno, M. (2013). Effects of levetiracetam, an antiepileptic drug, on memory impairments associated with aging and Alzheimer's disease in mice. *Neurobiol Learn Mem, 102*, 7-11. doi:10.1016/j.nlm.2013.02.001

Doheny, H. C., Ratnaraj, N., Whittington, M. A., Jefferys, J. G., & Patsalos, P. N. (1999). Blood and cerebrospinal fluid pharmacokinetics of the novel anticonvulsant levetiracetam (ucb L059) in the rat. *Epilepsy Res, 34*(2-3), 161-168. doi:10.1016/s0920-1211(98)00104-1

Eichenbaum, H. (2017). Prefrontal-hippocampal interactions in episodic memory. *Nat Rev Neurosci, 18*(9), 547-558. doi:10.1038/nrn.2017.74

Engel, A. K., Moll, C. K., Fried, I., & Ojemann, G. A. (2005). Invasive recordings from the human brain: clinical insights and beyond. *Nat Rev Neurosci, 6*(1), 35-47. doi:10.1038/nrn1585

Fauchier, L., Melin, A., Eder, V., Antier, D., & Bonnet, P. (2006). Heart rate variability in rats with chronic hypoxic pulmonary hypertension. *Ann Cardiol Angeiol (Paris), 55*(5), 249-254. doi:10.1016/j.ancard.2006.01.005

Faulkner, H. J., Traub, R. D., & Whittington, M. A. (1998). Disruption of synchronous gamma oscillations in the rat hippocampal slice: a common mechanism of anaesthetic drug action. *Br J Pharmacol, 125*(3), 483-492. doi:10.1038/sj.bjp.0702113

Ferron, J. F., Kroeger, D., Chever, O., & Amzica, F. (2009). Cortical inhibition during burst suppression induced with isoflurane anesthesia. *J Neurosci, 29*(31), 9850-9860. doi:10.1523/JNEUROSCI.5176-08.2009

Fisahn, A., Contractor, A., Traub, R. D., Buhl, E. H., Heinemann, S. F., & McBain, C. J. (2004). Distinct roles for the kainate receptor subunits GluR5 and GluR6 in kainate-induced hippocampal gamma oscillations. *J Neurosci, 24*(43), 9658-9668. doi:10.1523/JNEUROSCI.2973-04.2004

Foss-Feig, J. H., Adkinson, B. D., Ji, J. L., Yang, G., Srihari, V. H., McPartland, J. C., . . . Anticevic, A. (2017). Searching for Cross-Diagnostic Convergence: Neural Mechanisms Governing Excitation and Inhibition Balance in Schizophrenia and Autism Spectrum Disorders. *Biol Psychiatry, 81*(10), 848-861. doi:10.1016/j.biopsych.2017.03.005

Freund, T. F., & Antal, M. (1988). GABA-containing neurons in the septum control inhibitory interneurons in the hippocampus. *Nature, 336*(6195), 170-173. doi:10.1038/336170a0

Gao, X. M., Sakai, K., Roberts, R. C., Conley, R. R., Dean, B., & Tamminga, C. A. (2000). Ionotropic glutamate receptors and expression of N-methyl-D-aspartate receptor subunits in subregions of human hippocampus: effects of schizophrenia. *Am J Psychiatry, 157*(7), 1141-1149. doi:10.1176/appi.ajp.157.7.1141

Garcia-Perez, E., Mahfooz, K., Covita, J., Zandueta, A., & Wesseling, J. F. (2015). Levetiracetam accelerates the onset of supply rate depression in synaptic vesicle trafficking. *Epilepsia, 56*(4), 535-545. doi:10.1111/epi.12930

Garcia, P. S., Kolesky, S. E., & Jenkins, A. (2010). General anesthetic actions on GABA(A) receptors. *Curr Neuropharmacol, 8*(1), 2-9. doi:10.2174/157015910790909502

Ge, Y. X., Tian, X. Z., Lin, Y. Y., & Liu, X. Y. (2016). Chronic treatment with levetiracetam reverses deficits in hippocampal LTP in vivo in experimental temporal lobe epilepsy rats. *Neurosci Lett, 628*, 194-200. doi:10.1016/j.neulet.2016.06.043

Gillard, M., Chatelain, P., & Fuks, B. (2006). Binding characteristics of levetiracetam to synaptic vesicle protein 2A (SV2A) in human brain and in CHO cells expressing the human recombinant protein. *Eur J Pharmacol, 536*(1-2), 102-108. doi:10.1016/j.ejphar.2006.02.022

Golebiewski, H., Eckersdorf, B., & Konopacki, J. (1996). Cholinergic/GABAergic interaction in the production of EEG theta oscillations in rat hippocampal formation in vitro. *Acta Neurobiol Exp (Wars), 56*(1), 147-153.

Gordon, J. A. (2011). Oscillations and hippocampal-prefrontal synchrony. *Curr Opin Neurobiol, 21*(3), 486-491. doi:10.1016/j.conb.2011.02.012

Goutagny, R., Manseau, F., Jackson, J., Danik, M., & Williams, S. (2008). In vitro activation of the medial septum-diagonal band complex generates atropine-sensitive and atropine-resistant hippocampal theta rhythm: an investigation using a complete septohippocampal preparation. *Hippocampus, 18*(6), 531-535. doi:10.1002/hipo.20418

Gower, A. J., Falter, U., & Lamberty, Y. (2003). Anxiolytic effects of the novel anti-epileptic drug levetiracetam in the elevated plus-maze test in the rat. *Eur J Pharmacol, 481*(1), 67-74. doi:10.1016/j.ejphar.2003.09.004

Gower, A. J., Hirsch, E., Boehrer, A., Noyer, M., & Marescaux, C. (1995). Effects of levetiracetam, a novel antiepileptic drug, on convulsant activity in two genetic

rat models of epilepsy. *Epilepsy Res, 22*(3), 207-213. doi:10.1016/0920-1211(95)00077-1

Grunze, H. C., Rainnie, D. G., Hasselmo, M. E., Barkai, E., Hearn, E. F., McCarley, R. W., & Greene, R. W. (1996). NMDA-dependent modulation of CA1 local circuit inhibition. *J Neurosci, 16*(6), 2034-2043.

Gwilt, M., Bauer, M., & Bast, T. (2020). Frequency- and state-dependent effects of hippocampal neural disinhibition on hippocampal local field potential oscillations in anesthetized rats. *Hippocampus, 30*(10), 1021-1043. doi:10.1002/hipo.23212

Haberman, R. P., Koh, M. T., & Gallagher, M. (2017). Heightened cortical excitability in aged rodents with memory impairment. *Neurobiol Aging, 54*, 144-151. doi:10.1016/j.neurobiolaging.2016.12.021

Hangya, B., Borhegyi, Z., Szilagyi, N., Freund, T. F., & Varga, V. (2009). GABAergic neurons of the medial septum lead the hippocampal network during theta activity. *J Neurosci, 29*(25), 8094-8102. doi:10.1523/JNEUROSCI.5665-08.2009

Hara, K., & Harris, R. A. (2002). The anesthetic mechanism of urethane: the effects on neurotransmitter-gated ion channels. *Anesth Analg, 94*(2), 313-318. doi:10.1097/00000539-200202000-00015

Hayasaka, S., Phan, K. L., Liberzon, I., Worsley, K. J., & Nichols, T. E. (2004). Nonstationary cluster-size inference with random field and permutation methods. *Neuroimage, 22*(2), 676-687. doi:10.1016/j.neuroimage.2004.01.041

Hazra, A., Gu, F., Aulakh, A., Berridge, C., Eriksen, J. L., & Ziburkus, J. (2013). Inhibitory neuron and hippocampal circuit dysfunction in an aged mouse model of Alzheimer's disease. *PLoS One, 8*(5), e64318. doi:10.1371/journal.pone.0064318

Headley, D. B., & Pare, D. (2017). Common oscillatory mechanisms across multiple memory systems. *NPJ Sci Learn, 2*. doi:10.1038/s41539-016-0001-2

Heckers, S. (2001). Neuroimaging studies of the hippocampus in schizophrenia. *Hippocampus, 11*(5), 520-528. doi:10.1002/hipo.1068

Heckers, S., & Konradi, C. (2015). GABAergic mechanisms of hippocampal hyperactivity in schizophrenia. *Schizophr Res, 167*(1-3), 4-11. doi:10.1016/j.schres.2014.09.041

Hempel, R. J., Tulen, J. H., van Beveren, N. J., Roder, C. H., & Hengeveld, M. W. (2009). Cardiovascular variability during treatment with haloperidol, olanzapine or risperidone in recent-onset schizophrenia. *J Psychopharmacol, 23*(6), 697-707. doi:10.1177/0269881108091254

Hentschke, H., Benkwitz, C., Banks, M. I., Perkins, M. G., Homanics, G. E., & Pearce, R. A. (2009). Altered GABAA,slow inhibition and network oscillations in mice lacking the GABAA receptor beta3 subunit. *J Neurophysiol, 102*(6), 3643-3655. doi:10.1152/jn.00651.2009

Heynen, A. J., Sainsbury, R. S., & Bilkey, D. K. (1993). Stimulation-induced RSA-like field activity in region CA1 of the hippocampal slice: amplitude maxima and topography. *Brain Res Bull, 32*(2), 113-122. doi:10.1016/0361-9230(93)90065-j

Hong, L. E., Summerfelt, A., Buchanan, R. W., O'Donnell, P., Thaker, G. K., Weiler, M. A., & Lahti, A. C. (2010). Gamma and delta neural oscillations and association with clinical symptoms under subanesthetic ketamine. *Neuropsychopharmacology, 35*(3), 632-640. doi:10.1038/npp.2009.168

Hsiao, Y. T., Zheng, C., & Colgin, L. L. (2016). Slow gamma rhythms in CA3 are entrained by slow gamma activity in the dentate gyrus. *J Neurophysiol, 116*(6), 2594-2603. doi:10.1152/jn.00499.2016

Hunt, M. J., Kopell, N. J., Traub, R. D., & Whittington, M. A. (2017). Aberrant Network Activity in Schizophrenia. *Trends Neurosci, 40*(6), 371-382. doi:10.1016/j.tins.2017.04.003

Husum, H., Bolwig, T. G., Sanchez, C., Mathe, A. A., & Hansen, S. L. (2004). Levetiracetam prevents changes in levels of brain-derived neurotrophic factor and neuropeptide Y mRNA and of Y1- and Y5-like receptors in the

hippocampus of rats undergoing amygdala kindling: implications for antiepileptogenic and mood-stabilizing properties. *Epilepsy Behav, 5*(2), 204-215. doi:10.1016/j.yebeh.2003.12.004

Janz, R., Goda, Y., Geppert, M., Missler, M., & Sudhof, T. C. (1999). SV2A and SV2B function as redundant Ca2+ regulators in neurotransmitter release. *Neuron, 24*(4), 1003-1016. doi:10.1016/s0896-6273(00)81046-6

Jay, T. M., & Witter, M. P. (1991). Distribution of hippocampal CA1 and subicular efferents in the prefrontal cortex of the rat studied by means of anterograde transport of Phaseolus vulgaris-leucoagglutinin. *J Comp Neurol, 313*(4), 574-586. doi:10.1002/cne.903130404

Ji-qun, C., Ishihara, K., Nagayama, T., Serikawa, T., & Sasa, M. (2005). Long-lasting antiepileptic effects of levetiracetam against epileptic seizures in the spontaneously epileptic rat (SER): differentiation of levetiracetam from conventional antiepileptic drugs. *Epilepsia, 46*(9), 1362-1370. doi:10.1111/j.1528-1167.2005.29604.x

Jodo, E., Suzuki, Y., Katayama, T., Hoshino, K. Y., Takeuchi, S., Niwa, S., & Kayama, Y. (2005). Activation of medial prefrontal cortex by phencyclidine is mediated via a hippocampo-prefrontal pathway. *Cereb Cortex, 15*(5), 663-669. doi:10.1093/cercor/bhh168

Kay, K., & Frank, L. M. (2019). Three brain states in the hippocampus and cortex. *Hippocampus, 29*(3), 184-238. doi:10.1002/hipo.22956

Kenny, J. D., Westover, M. B., Ching, S., Brown, E. N., & Solt, K. (2014). Propofol and sevoflurane induce distinct burst suppression patterns in rats. *Front Syst Neurosci, 8*, 237. doi:10.3389/fnsys.2014.00237

Klarer, M., Weber-Stadlbauer, U., Arnold, M., Langhans, W., & Meyer, U. (2017). Cognitive effects of subdiaphragmatic vagal deafferentation in rats. *Neurobiol Learn Mem, 142*(Pt B), 190-199. doi:10.1016/j.nlm.2017.05.006

Klitgaard, H. (2001). Levetiracetam: the preclinical profile of a new class of antiepileptic drugs? *Epilepsia, 42 Suppl 4*, 13-18.

Klitgaard, H., Matagne, A., Grimee, R., Vanneste-Goemaere, J., & Margineanu, D. G. (2003). Electrophysiological, neurochemical and regional effects of levetiracetam in the rat pilocarpine model of temporal lobe epilepsy. *Seizure, 12*(2), 92-100. doi:10.1016/s1059131102001930

Koenig, J., Linder, A. N., Leutgeb, J. K., & Leutgeb, S. (2011). The spatial periodicity of grid cells is not sustained during reduced theta oscillations. *Science, 332*(6029), 592-595. doi:10.1126/science.1201685

Koh, M. T., Haberman, R. P., Foti, S., McCown, T. J., & Gallagher, M. (2010). Treatment strategies targeting excess hippocampal activity benefit aged rats with cognitive impairment. *Neuropsychopharmacology, 35*(4), 1016-1025. doi:10.1038/npp.2009.207

Koh, M. T., Shao, Y., Rosenzweig-Lipson, S., & Gallagher, M. (2018). Treatment with levetiracetam improves cognition in a ketamine rat model of schizophrenia. *Schizophr Res, 193*, 119-125. doi:10.1016/j.schres.2017.06.027

Konopacki, J., Golebiewski, H., Eckersdorf, B., Blaszczyk, M., & Grabowski, R. (1997). Theta-like activity in hippocampal formation slices: the effect of strong disinhibition of GABAA and GABAB receptors. *Brain Res, 775*(1-2), 91-98. doi:10.1016/s0006-8993(97)00919-0

Konradi, C., Yang, C. K., Zimmerman, E. I., Lohmann, K. M., Gresch, P., Pantazopoulos, H., . . . Heckers, S. (2011). Hippocampal interneurons are abnormal in schizophrenia. *Schizophr Res, 131*(1-3), 165-173. doi:10.1016/j.schres.2011.06.007

Kontos, A., Baumert, M., Lushington, K., Kennedy, D., Kohler, M., Cicua-Navarro, D., . . . Martin, J. (2020). The Inconsistent Nature of Heart Rate Variability During Sleep in Normal Children and Adolescents. *Frontiers in Cardiovascular Medicine, 7*, 19.

Kowalczyk, T., Bocian, R., & Konopacki, J. (2013). The generation of theta rhythm in hippocampal formation maintained in vitro. *Eur J Neurosci, 37*(5), 679-699. doi:10.1111/ejn.12091

Kraguljac, N. V., White, D. M., Reid, M. A., & Lahti, A. C. (2013). Increased hippocampal glutamate and volumetric deficits in unmedicated patients with schizophrenia. *JAMA Psychiatry, 70*(12), 1294-1302. doi:10.1001/jamapsychiatry.2013.2437

Kroeger, D., & Amzica, F. (2007). Hypersensitivity of the anesthesia-induced comatose brain. *J Neurosci, 27*(39), 10597-10607. doi:10.1523/JNEUROSCI.3440-07.2007

Krystal, J. H., Anticevic, A., Yang, G. J., Dragoi, G., Driesen, N. R., Wang, X. J., & Murray, J. D. (2017). Impaired Tuning of Neural Ensembles and the Pathophysiology of Schizophrenia: A Translational and Computational Neuroscience Perspective. *Biol Psychiatry, 81*(10), 874-885. doi:10.1016/j.biopsych.2017.01.004

Lamberty, Y., Margineanu, D. G., & Klitgaard, H. (2001). Effect of the New Antiepileptic Drug Levetiracetam in an Animal Model of Mania. *Epilepsy Behav, 2*(5), 454-459. doi:10.1006/ebeh.2001.0254

Land, R., Engler, G., Kral, A., & Engel, A. K. (2012). Auditory evoked bursts in mouse visual cortex during isoflurane anesthesia. *PLoS One, 7*(11), e49855. doi:10.1371/journal.pone.0049855

Laroche, S., Jay, T. M., & Thierry, A. M. (1990). Long-term potentiation in the prefrontal cortex following stimulation of the hippocampal CA1/subicular region. *Neurosci Lett, 114*(2), 184-190. doi:10.1016/0304-3940(90)90069-l

Lawrie, S. M., & Abukmeil, S. S. (1998). Brain abnormality in schizophrenia. A systematic and quantitative review of volumetric magnetic resonance imaging studies. *Br J Psychiatry, 172*, 110-120. doi:10.1192/bjp.172.2.110

Lee, C. Y., Chen, C. C., & Liou, H. H. (2009). Levetiracetam inhibits glutamate transmission through presynaptic P/Q-type calcium channels on the granule cells of the dentate gyrus. *Br J Pharmacol, 158*(7), 1753-1762. doi:10.1111/j.1476-5381.2009.00463.x

Lei, M., Xu, H., Li, Z., Wang, Z., O'Malley, T. T., Zhang, D., . . . Li, S. (2016). Soluble Abeta oligomers impair hippocampal LTP by disrupting

glutamatergic/GABAergic balance. *Neurobiol Dis, 85*, 111-121. doi:10.1016/j.nbd.2015.10.019

Letzkus, J. J., Wolff, S. B., & Luthi, A. (2015). Disinhibition, a Circuit Mechanism for Associative Learning and Memory. *Neuron, 88*(2), 264-276. doi:10.1016/j.neuron.2015.09.024

Levesque, M., Cataldi, M., Chen, L. Y., Hamidi, S., & Avoli, M. (2017). Carbachol-induced network oscillations in an in vitro limbic system brain slice. *Neuroscience, 348*, 153-164. doi:10.1016/j.neuroscience.2017.02.021

Lewis, D. A., Curley, A. A., Glausier, J. R., & Volk, D. W. (2012). Cortical parvalbumin interneurons and cognitive dysfunction in schizophrenia. *Trends Neurosci, 35*(1), 57-67. doi:10.1016/j.tins.2011.10.004

Lewis, D. A., & Moghaddam, B. (2006). Cognitive dysfunction in schizophrenia: convergence of gamma-aminobutyric acid and glutamate alterations. *Arch Neurol, 63*(10), 1372-1376. doi:10.1001/archneur.63.10.1372

Lieberman, J. A., Girgis, R. R., Brucato, G., Moore, H., Provenzano, F., Kegeles, L., . . . Small, S. A. (2018). Hippocampal dysfunction in the pathophysiology of schizophrenia: a selective review and hypothesis for early detection and intervention. *Mol Psychiatry, 23*(8), 1764-1772. doi:10.1038/mp.2017.249

Liu, Y. W., Tzeng, N. S., Yeh, C. B., Kuo, T. B., Huang, S. Y., Chang, C. C., & Chang, H. A. (2016). Reduced cardiac autonomic response to deep breathing: A heritable vulnerability trait in patients with schizophrenia and their healthy first-degree relatives. *Psychiatry Res, 243*, 335-341. doi:10.1016/j.psychres.2016.04.076

Loscher, W., & Honack, D. (2000). Development of tolerance during chronic treatment of kindled rats with the novel antiepileptic drug levetiracetam. *Epilepsia, 41*(12), 1499-1506. doi:10.1111/j.1499-1654.2000.001499.x

Loscher, W., Honack, D., & Bloms-Funke, P. (1996). The novel antiepileptic drug levetiracetam (ucb L059) induces alterations in GABA metabolism and turnover in discrete areas of rat brain and reduces neuronal activity in

substantia nigra pars reticulata. *Brain Res, 735*(2), 208-216. doi:10.1016/0006-8993(96)00587-2

Loscher, W., Honack, D., & Rundfeldt, C. (1998). Antiepileptogenic effects of the novel anticonvulsant levetiracetam (ucb L059) in the kindling model of temporal lobe epilepsy. *J Pharmacol Exp Ther, 284*(2), 474-479.

Lozano-Soldevilla, D., ter Huurne, N., Cools, R., & Jensen, O. (2014). GABAergic modulation of visual gamma and alpha oscillations and its consequences for working memory performance. *Curr Biol, 24*(24), 2878-2887. doi:10.1016/j.cub.2014.10.017

Lu, C. B., & Henderson, Z. (2010). Nicotine induction of theta frequency oscillations in rodent hippocampus in vitro. *Neuroscience, 166*(1), 84-93. doi:10.1016/j.neuroscience.2009.11.072

Lukyanetz, E. A., Shkryl, V. M., & Kostyuk, P. G. (2002). Selective blockade of N-type calcium channels by levetiracetam. *Epilepsia, 43*(1), 9-18. doi:10.1046/j.1528-1157.2002.24501.x

Lustig, B., Wang, Y., & Pastalkova, E. (2016). Oscillatory patterns in hippocampus under light and deep isoflurane anesthesia closely mirror prominent brain states in awake animals. *Hippocampus, 26*(1), 102-109. doi:10.1002/hipo.22494

MacIver, M. B., & Bland, B. H. (2014). Chaos analysis of EEG during isoflurane-induced loss of righting in rats. *Front Syst Neurosci, 8*, 203. doi:10.3389/fnsys.2014.00203

Madeja, M., Margineanu, D. G., Gorji, A., Siep, E., Boerrigter, P., Klitgaard, H., & Speckmann, E. J. (2003). Reduction of voltage-operated potassium currents by levetiracetam: a novel antiepileptic mechanism of action? *Neuropharmacology, 45*(5), 661-671. doi:10.1016/s0028-3908(03)00248-x

Maier, S. U., & Hare, T. A. (2017). Higher Heart-Rate Variability Is Associated with Ventromedial Prefrontal Cortex Activity and Increased Resistance to Temptation in Dietary Self-Control Challenges. *J Neurosci, 37*(2), 446-455. doi:10.1523/JNEUROSCI.2815-16.2016

Mann, E. O., Suckling, J. M., Hajos, N., Greenfield, S. A., & Paulsen, O. (2005). Perisomatic feedback inhibition underlies cholinergically induced fast network oscillations in the rat hippocampus in vitro. *Neuron, 45*(1), 105-117. doi:10.1016/j.neuron.2004.12.016

Margineanu, D. G., & Wulfert, E. (1997). Inhibition by levetiracetam of a non-GABAA receptor-associated epileptiform effect of bicuculline in rat hippocampus. *Br J Pharmacol, 122*(6), 1146-1150. doi:10.1038/sj.bjp.0701476

Maric, N. P., Jovicic, M. J., Mihaljevic, M., & Miljevic, C. (2016). Improving Current Treatments for Schizophrenia. *Drug Dev Res, 77*(7), 357-367. doi:10.1002/ddr.21337

Marín, O. (2012). Interneuron dysfunction in psychiatric disorders. *Nature Reviews Neuroscience, 13*(2), 107-120.

Maris, E., & Oostenveld, R. (2007). Nonparametric statistical testing of EEG- and MEG-data. *J Neurosci Methods, 164*(1), 177-190. doi:10.1016/j.jneumeth.2007.03.024

McBride, J. C., Zhao, X., Munro, N. B., Smith, C. D., Jicha, G. A., Hively, L., . . . Jiang, Y. (2014). Spectral and complexity analysis of scalp EEG characteristics for mild cognitive impairment and early Alzheimer's disease. *Comput Methods Programs Biomed, 114*(2), 153-163. doi:10.1016/j.cmpb.2014.01.019

McGarrity, S., Mason, R., Fone, K. C., Pezze, M., & Bast, T. (2017). Hippocampal Neural Disinhibition Causes Attentional and Memory Deficits. *Cereb Cortex, 27*(9), 4447-4462. doi:10.1093/cercor/bhw247

Meehan, A. L., Yang, X., McAdams, B. D., Yuan, L., & Rothman, S. M. (2011). A new mechanism for antiepileptic drug action: vesicular entry may mediate the effects of levetiracetam. *J Neurophysiol, 106*(3), 1227-1239. doi:10.1152/jn.00279.2011

Meister, A. L., Doheny, K. K., & Travagli, R. A. (2019). Necrotizing enterocolitis attenuates developmental heart rate variability increases in newborn rats. *Neurogastroenterol Motil, 31*(3), e13484. doi:10.1111/nmo.13484

Mendoza-Torreblanca, J. G., Vanoye-Carlo, A., Phillips-Farfan, B. V., Carmona-Aparicio, L., & Gomez-Lira, G. (2013). Synaptic vesicle protein 2A: basic facts and role in synaptic function. *Eur J Neurosci, 38*(11), 3529-3539. doi:10.1111/ejn.12360

Moran, L. V., & Hong, L. E. (2011). High vs low frequency neural oscillations in schizophrenia. *Schizophr Bull, 37*(4), 659-663. doi:10.1093/schbul/sbr056

Mujica-Parodi, L. R., Yeragani, V., & Malaspina, D. (2005). Nonlinear complexity and spectral analyses of heart rate variability in medicated and unmedicated patients with schizophrenia. *Neuropsychobiology, 51*(1), 10-15. doi:10.1159/000082850

Murray, J. D., Anticevic, A., Gancsos, M., Ichinose, M., Corlett, P. R., Krystal, J. H., & Wang, X. J. (2014). Linking microcircuit dysfunction to cognitive impairment: effects of disinhibition associated with schizophrenia in a cortical working memory model. *Cereb Cortex, 24*(4), 859-872. doi:10.1093/cercor/bhs370

Napadow, V., Dhond, R., Conti, G., Makris, N., Brown, E. N., & Barbieri, R. (2008). Brain correlates of autonomic modulation: combining heart rate variability with fMRI. *Neuroimage, 42*(1), 169-177. doi:10.1016/j.neuroimage.2008.04.238

Nava-Mesa, M. O., Jimenez-Diaz, L., Yajeya, J., & Navarro-Lopez, J. D. (2014). GABAergic neurotransmission and new strategies of neuromodulation to compensate synaptic dysfunction in early stages of Alzheimer's disease. *Front Cell Neurosci, 8*, 167. doi:10.3389/fncel.2014.00167

Niespodziany, I., Klitgaard, H., & Margineanu, D. G. (2001). Levetiracetam inhibits the high-voltage-activated Ca(2+) current in pyramidal neurones of rat hippocampal slices. *Neurosci Lett, 306*(1-2), 5-8. doi:10.1016/s0304-3940(01)01884-5

Nolte, G., Bai, O., Wheaton, L., Mari, Z., Vorbach, S., & Hallett, M. (2004). Identifying true brain interaction from EEG data using the imaginary part of coherency. *Clin Neurophysiol, 115*(10), 2292-2307. doi:10.1016/j.clinph.2004.04.029

Noyer, M., Gillard, M., Matagne, A., Henichart, J. P., & Wulfert, E. (1995). The novel antiepileptic drug levetiracetam (ucb L059) appears to act via a specific

binding site in CNS membranes. *Eur J Pharmacol, 286*(2), 137-146. doi:10.1016/0014-2999(95)00436-o

O'Donnell, P. (2011). Adolescent onset of cortical disinhibition in schizophrenia: insights from animal models. *Schizophr Bull, 37*(3), 484-492. doi:10.1093/schbul/sbr028

Olney, J. W., Newcomer, J. W., & Farber, N. B. (1999). NMDA receptor hypofunction model of schizophrenia. *J Psychiatr Res, 33*(6), 523-533. doi:10.1016/s0022-3956(99)00029-1

Olsen, R. W. (2006). Picrotoxin-like channel blockers of GABAA receptors. *Proc Natl Acad Sci U S A, 103*(16), 6081-6082. doi:10.1073/pnas.0601121103

Oostenveld, R., Fries, P., Maris, E., & Schoffelen, J. M. (2011). FieldTrip: Open source software for advanced analysis of MEG, EEG, and invasive electrophysiological data. *Comput Intell Neurosci, 2011*, 156869. doi:10.1155/2011/156869

Oostenveld, R., & Praamstra, P. (2001). The five percent electrode system for high-resolution EEG and ERP measurements. *Clin Neurophysiol, 112*(4), 713-719. doi:10.1016/s1388-2457(00)00527-7

Pagliardini, S., Gosgnach, S., & Dickson, C. T. (2013). Spontaneous sleep-like brain state alternations and breathing characteristics in urethane anesthetized mice. *PLoS One, 8*(7), e70411. doi:10.1371/journal.pone.0070411

Palop, J. J., & Mucke, L. (2016). Network abnormalities and interneuron dysfunction in Alzheimer disease. *Nat Rev Neurosci, 17*(12), 777-792. doi:10.1038/nrn.2016.141

Patel, J., Fujisawa, S., Berenyi, A., Royer, S., & Buzsaki, G. (2012). Traveling theta waves along the entire septotemporal axis of the hippocampus. *Neuron, 75*(3), 410-417. doi:10.1016/j.neuron.2012.07.015

Paxinos, G., & Watson, C. (1998). A stereotaxic atlas of the rat brain. *New York: Academic*.

Peleg-Raibstein, D., Pezze, M. A., Ferger, B., Zhang, W. N., Murphy, C. A., Feldon, J., & Bast, T. (2005). Activation of dopaminergic neurotransmission in the

medial prefrontal cortex by N-methyl-d-aspartate stimulation of the ventral hippocampus in rats. *Neuroscience, 132*(1), 219-232. doi:10.1016/j.neuroscience.2004.12.016

Penttonen, M., Kamondi, A., Acsady, L., & Buzsaki, G. (1998). Gamma frequency oscillation in the hippocampus of the rat: intracellular analysis in vivo. *Eur J Neurosci, 10*(2), 718-728. doi:10.1046/j.1460-9568.1998.00096.x

Pezze, M., McGarrity, S., Mason, R., Fone, K. C., & Bast, T. (2014). Too little and too much: hypoactivation and disinhibition of medial prefrontal cortex cause attentional deficits. *J Neurosci, 34*(23), 7931-7946. doi:10.1523/JNEUROSCI.3450-13.2014

Poulain, P., & Margineanu, D. G. (2002). Levetiracetam opposes the action of GABAA antagonists in hypothalamic neurones. *Neuropharmacology, 42*(3), 346-352. doi:10.1016/s0028-3908(01)00185-x

Raith, H., Schuelert, N., Duveau, V., Roucard, C., Plano, A., Dorner-Ciossek, C., & Ferger, B. (2020). Differential effects of traxoprodil and S-ketamine on quantitative EEG and auditory event-related potentials as translational biomarkers in preclinical trials in rats and mice. *Neuropharmacology, 171*, 108072. doi:10.1016/j.neuropharm.2020.108072

Reynolds, G. P., Czudek, C., & Andrews, H. B. (1990). Deficit and hemispheric asymmetry of GABA uptake sites in the hippocampus in schizophrenia. *Biol Psychiatry, 27*(9), 1038-1044. doi:10.1016/0006-3223(90)90039-5

Robinson, J. E., Chen, M., Stamatakis, A. M., Krouse, M. C., Howard, E. C., Faccidomo, S., . . . Malanga, C. J. (2013). Levetiracetam has opposite effects on alcohol- and cocaine-related behaviors in C57BL/6J mice. *Neuropsychopharmacology, 38*(7), 1322-1333. doi:10.1038/npp.2013.30

Robitsek, J., Ratner, M. H., Stewart, T., Eichenbaum, H., & Farb, D. H. (2015). Combined administration of levetiracetam and valproic acid attenuates age-related hyperactivity of CA3 place cells, reduces place field area, and increases spatial information content in aged rat hippocampus. *Hippocampus, 25*(12), 1541-1555. doi:10.1002/hipo.22474

Rossini, P. M., Rossi, S., Babiloni, C., & Polich, J. (2007). Clinical neurophysiology of aging brain: from normal aging to neurodegeneration. *Prog Neurobiol, 83*(6), 375-400. doi:10.1016/j.pneurobio.2007.07.010

Royer, S., Sirota, A., Patel, J., & Buzsaki, G. (2010). Distinct representations and theta dynamics in dorsal and ventral hippocampus. *J Neurosci, 30*(5), 1777-1787. doi:10.1523/JNEUROSCI.4681-09.2010

Rugino, T. A., & Samsock, T. C. (2002). Levetiracetam in autistic children: an open-label study. *J Dev Behav Pediatr, 23*(4), 225-230. doi:10.1097/00004703-200208000-00006

Ruit, K. G., & Neafsey, E. J. (1988). Cardiovascular and respiratory responses to electrical and chemical stimulation of the hippocampus in anesthetized and awake rats. *Brain Res, 457*(2), 310-321. doi:10.1016/0006-8993(88)90701-9

Ruzicka, W. B., Subburaju, S., & Benes, F. M. (2015). Circuit- and Diagnosis-Specific DNA Methylation Changes at gamma-Aminobutyric Acid-Related Genes in Postmortem Human Hippocampus in Schizophrenia and Bipolar Disorder. *JAMA Psychiatry, 72*(6), 541-551. doi:10.1001/jamapsychiatry.2015.49

Sanchez, P. E., Zhu, L., Verret, L., Vossel, K. A., Orr, A. G., Cirrito, J. R., . . . Mucke, L. (2012). Levetiracetam suppresses neuronal network dysfunction and reverses synaptic and cognitive deficits in an Alzheimer's disease model. *Proc Natl Acad Sci U S A, 109*(42), E2895-2903. doi:10.1073/pnas.1121081109

Sanon, N. T., Gagne, J., Wolf, D. C., Aboulamer, S., Bosoi, C. M., Simard, A., . . . Carmant, L. (2018). Favorable adverse effect profile of brivaracetam vs levetiracetam in a preclinical model. *Epilepsy Behav, 79*, 117-125. doi:10.1016/j.yebeh.2017.11.019

Santana-Gomez, C. E., Valle-Dorado, M. G., Dominguez-Valentin, A. E., Hernandez-Moreno, A., Orozco-Suarez, S., & Rocha, L. (2018). Neuroprotective effects of levetiracetam, both alone and combined with propylparaben, in the long-term consequences induced by lithium-pilocarpine status epilepticus. *Neurochem Int, 120*, 224-232. doi:10.1016/j.neuint.2018.09.004

Scharfman, H. E. (2012). "Untangling" Alzheimer's disease and epilepsy. *Epilepsy Curr, 12*(5), 178-183. doi:10.5698/1535-7511-12.5.178

Schnitzler, A., & Gross, J. (2005). Normal and pathological oscillatory communication in the brain. *Nat Rev Neurosci, 6*(4), 285-296. doi:10.1038/nrn1650

Schobel, S. A., Chaudhury, N. H., Khan, U. A., Paniagua, B., Styner, M. A., Asllani, I., . . . Small, S. A. (2013). Imaging patients with psychosis and a mouse model establishes a spreading pattern of hippocampal dysfunction and implicates glutamate as a driver. *Neuron, 78*(1), 81-93. doi:10.1016/j.neuron.2013.02.011

Schobel, S. A., Kelly, M. A., Corcoran, C. M., Van Heertum, K., Seckinger, R., Goetz, R., . . . Malaspina, D. (2009). Anterior hippocampal and orbitofrontal cortical structural brain abnormalities in association with cognitive deficits in schizophrenia. *Schizophr Res, 114*(1-3), 110-118. doi:10.1016/j.schres.2009.07.016

Seeber, M., Cantonas, L. M., Hoevels, M., Sesia, T., Visser-Vandewalle, V., & Michel, C. M. (2019). Subcortical electrophysiological activity is detectable with high-density EEG source imaging. *Nat Commun, 10*(1), 753. doi:10.1038/s41467-019-08725-w

Shaffer, F., & Ginsberg, J. P. (2017). An Overview of Heart Rate Variability Metrics and Norms. *Front Public Health, 5*, 258. doi:10.3389/fpubh.2017.00258

Shannon, H. E., Eberle, E. L., & Peters, S. C. (2005). Comparison of the effects of anticonvulsant drugs with diverse mechanisms of action in the formalin test in rats. *Neuropharmacology, 48*(7), 1012-1020. doi:10.1016/j.neuropharm.2005.01.013

Shimono, K., Brucher, F., Granger, R., Lynch, G., & Taketani, M. (2000). Origins and distribution of cholinergically induced beta rhythms in hippocampal slices. *J Neurosci, 20*(22), 8462-8473. doi:10.1523/JNEUROSCI.20-22-08462.2000

Sigurdsson, T., & Duvarci, S. (2015). Hippocampal-Prefrontal Interactions in Cognition, Behavior and Psychiatric Disease. *Front Syst Neurosci, 9*, 190. doi:10.3389/fnsys.2015.00190

Smith-Hicks, C. L., Bridges, D. D., Paynter, N. P., & Singer, H. S. (2007). A double blind randomized placebo control trial of levetiracetam in Tourette syndrome. *Mov Disord, 22*(12), 1764-1770. doi:10.1002/mds.21615

Smythe, J. W., Colom, L. V., & Bland, B. H. (1992). The extrinsic modulation of hippocampal theta depends on the coactivation of cholinergic and GABA-ergic medial septal inputs. *Neurosci Biobehav Rev, 16*(3), 289-308. doi:10.1016/s0149-7634(05)80203-9

Snyder, M. A., & Gao, W. J. (2013). NMDA hypofunction as a convergence point for progression and symptoms of schizophrenia. *Front Cell Neurosci, 7*, 31. doi:10.3389/fncel.2013.00031

Soltesz, I., & Deschenes, M. (1993). Low- and high-frequency membrane potential oscillations during theta activity in CA1 and CA3 pyramidal neurons of the rat hippocampus under ketamine-xylazine anesthesia. *J Neurophysiol, 70*(1), 97-116. doi:10.1152/jn.1993.70.1.97

Srinivasan, R., Winter, W. R., Ding, J., & Nunez, P. L. (2007). EEG and MEG coherence: measures of functional connectivity at distinct spatial scales of neocortical dynamics. *J Neurosci Methods, 166*(1), 41-52. doi:10.1016/j.jneumeth.2007.06.026

Stanley, E. M., Fadel, J. R., & Mott, D. D. (2012). Interneuron loss reduces dendritic inhibition and GABA release in hippocampus of aged rats. *Neurobiol Aging, 33*(2), 431 e431-413. doi:10.1016/j.neurobiolaging.2010.12.014

Stephenson, R., Caron, A. M., Cassel, D. B., & Kostela, J. C. (2009). Automated analysis of sleep-wake state in rats. *J Neurosci Methods, 184*(2), 263-274. doi:10.1016/j.jneumeth.2009.08.014

Steriade, M., Amzica, F., & Contreras, D. (1994). Cortical and thalamic cellular correlates of electroencephalographic burst-suppression. *Electroencephalogr Clin Neurophysiol, 90*(1), 1-16. doi:10.1016/0013-4694(94)90108-2

Stratton, S. C., Large, C. H., Cox, B., Davies, G., & Hagan, R. M. (2003). Effects of lamotrigine and levetiracetam on seizure development in a rat amygdala

kindling model. *Epilepsy Res, 53*(1-2), 95-106. doi:10.1016/s0920-1211(02)00254-1

Surges, R., Volynski, K. E., & Walker, M. C. (2008). Is levetiracetam different from other antiepileptic drugs? Levetiracetam and its cellular mechanism of action in epilepsy revisited. *Ther Adv Neurol Disord, 1*(1), 13-24. doi:10.1177/1756285608094212

Svetlana, A. L., Tatyana, A. V., Lubov, N. N., Inga, S. K., Georgii, G. A., & Gagik, N. A. (2019). Levetiracetam effect and electrophysiological mechanism of action in rats with cobalt-induced chronic epilepsy. *European journal of pharmacology, 854*, 380-386. doi:10.1016/j.ejphar.2019.04.041

Thome, A., Gray, D. T., Erickson, C. A., Lipa, P., & Barnes, C. A. (2016). Memory impairment in aged primates is associated with region-specific network dysfunction. *Mol Psychiatry, 21*(9), 1257-1262. doi:10.1038/mp.2015.160

Thompson, J. A., Lanctin, D., Ince, N. F., & Abosch, A. (2014). Clinical implications of local field potentials for understanding and treating movement disorders. *Stereotact Funct Neurosurg, 92*(4), 251-263. doi:10.1159/000364913

Tierney, P. L., Degenetais, E., Thierry, A. M., Glowinski, J., & Gioanni, Y. (2004). Influence of the hippocampus on interneurons of the rat prefrontal cortex. *Eur J Neurosci, 20*(2), 514-524. doi:10.1111/j.1460-9568.2004.03501.x

Tiesinga, P. H., Fellous, J. M., Jose, J. V., & Sejnowski, T. J. (2001). Computational model of carbachol-induced delta, theta, and gamma oscillations in the hippocampus. *Hippocampus, 11*(3), 251-274. doi:10.1002/hipo.1041

Tokuda, S., Sofue, N., Ohno, Y., Sasa, M., & Serikawa, T. (2010). Inhibitory effects of levetiracetam on absence seizures in a novel absence-like epilepsy animal model, Groggy rat. *Brain Res, 1359*, 298-303. doi:10.1016/j.brainres.2010.08.084

Tong, X., & Patsalos, P. N. (2001). A microdialysis study of the novel antiepileptic drug levetiracetam: extracellular pharmacokinetics and effect on taurine in rat brain. *Br J Pharmacol, 133*(6), 867-874. doi:10.1038/sj.bjp.0704141

Toth, K., Freund, T. F., & Miles, R. (1997). Disinhibition of rat hippocampal pyramidal cells by GABAergic afferents from the septum. *J Physiol, 500 (Pt 2)*, 463-474. doi:10.1113/jphysiol.1997.sp022033

Traub, R. D., Bibbig, A., Fisahn, A., LeBeau, F. E., Whittington, M. A., & Buhl, E. H. (2000). A model of gamma-frequency network oscillations induced in the rat CA3 region by carbachol in vitro. *Eur J Neurosci, 12*(11), 4093-4106. doi:10.1046/j.1460-9568.2000.00300.x

Traub, R. D., Bibbig, A., LeBeau, F. E., Buhl, E. H., & Whittington, M. A. (2004). Cellular mechanisms of neuronal population oscillations in the hippocampus in vitro. *Annu Rev Neurosci, 27*, 247-278. doi:10.1146/annurev.neuro.27.070203.144303

Trevino, M., Vivar, C., & Gutierrez, R. (2007). Beta/gamma oscillatory activity in the CA3 hippocampal area is depressed by aberrant GABAergic transmission from the dentate gyrus after seizures. *J Neurosci, 27*(1), 251-259. doi:10.1523/JNEUROSCI.3815-06.2007

Tukker, J. J., Fuentealba, P., Hartwich, K., Somogyi, P., & Klausberger, T. (2007). Cell type-specific tuning of hippocampal interneuron firing during gamma oscillations in vivo. *J Neurosci, 27*(31), 8184-8189. doi:10.1523/JNEUROSCI.1685-07.2007

Uhlhaas, P. J., & Singer, W. (2006). Neural synchrony in brain disorders: relevance for cognitive dysfunctions and pathophysiology. *Neuron, 52*(1), 155-168. doi:10.1016/j.neuron.2006.09.020

Uhlhaas, P. J., & Singer, W. (2010). Abnormal neural oscillations and synchrony in schizophrenia. *Nat Rev Neurosci, 11*(2), 100-113. doi:10.1038/nrn2774

Uhlhaas, P. J., & Singer, W. (2015). Oscillations and neuronal dynamics in schizophrenia: the search for basic symptoms and translational opportunities. *Biol Psychiatry, 77*(12), 1001-1009. doi:10.1016/j.biopsych.2014.11.019

Vanoli, E., Adamson, P. B., Ba, L., Pinna, G. D., Lazzara, R., & Orr, W. C. (1995). Heart rate variability during specific sleep stages. A comparison of healthy

subjects with patients after myocardial infarction. *Circulation, 91*(7), 1918-1922. doi:10.1161/01.cir.91.7.1918

Verberne, A. J. (1996). Medullary sympathoexcitatory neurons are inhibited by activation of the medial prefrontal cortex in the rat. *Am J Physiol, 270*(4 Pt 2), R713-719. doi:10.1152/ajpregu.1996.270.4.R713

Vogl, C., Mochida, S., Wolff, C., Whalley, B. J., & Stephens, G. J. (2012). The synaptic vesicle glycoprotein 2A ligand levetiracetam inhibits presynaptic Ca2+ channels through an intracellular pathway. *Mol Pharmacol, 82*(2), 199-208. doi:10.1124/mol.111.076687

Vossel, K. A., Beagle, A. J., Rabinovici, G. D., Shu, H., Lee, S. E., Naasan, G., . . . Mucke, L. (2013). Seizures and epileptiform activity in the early stages of Alzheimer disease. *JAMA Neurol, 70*(9), 1158-1166. doi:10.1001/jamaneurol.2013.136

Westerhaus, M. J., & Loewy, A. D. (2001). Central representation of the sympathetic nervous system in the cerebral cortex. *Brain Res, 903*(1-2), 117-127. doi:10.1016/s0006-8993(01)02453-2

Whittington, M. A., Traub, R. D., & Adams, N. E. (2018). A future for neuronal oscillation research. *Brain Neurosci Adv, 2*, 2398212818794827. doi:10.1177/2398212818794827

Whittington, M. A., Traub, R. D., Faulkner, H. J., Jefferys, J. G., & Chettiar, K. (1998). Morphine disrupts long-range synchrony of gamma oscillations in hippocampal slices. *Proc Natl Acad Sci U S A, 95*(10), 5807-5811. doi:10.1073/pnas.95.10.5807

Whittington, M. A., Traub, R. D., Kopell, N., Ermentrout, B., & Buhl, E. H. (2000). Inhibition-based rhythms: experimental and mathematical observations on network dynamics. *Int J Psychophysiol, 38*(3), 315-336. doi:10.1016/s0167-8760(00)00173-2

Williams, A. E., Giust, J. M., Kronenberger, W. G., & Dunn, D. W. (2016). Epilepsy and attention-deficit hyperactivity disorder: links, risks, and challenges. *Neuropsychiatr Dis Treat, 12*, 287-296. doi:10.2147/NDT.S81549

Wolansky, T., Clement, E. A., Peters, S. R., Palczak, M. A., & Dickson, C. T. (2006). Hippocampal slow oscillation: a novel EEG state and its coordination with ongoing neocortical activity. *J Neurosci, 26*(23), 6213-6229. doi:10.1523/JNEUROSCI.5594-05.2006

Wright, C., Downing, J., Mungall, D., Khan, O., Williams, A., Fonkem, E., . . . Kirmani, B. (2013). Clinical pharmacology and pharmacokinetics of levetiracetam. *Front Neurol, 4*, 192. doi:10.3389/fneur.2013.00192

Wulff, P., Ponomarenko, A. A., Bartos, M., Korotkova, T. M., Fuchs, E. C., Bahner, F., . . . Monyer, H. (2009). Hippocampal theta rhythm and its coupling with gamma oscillations require fast inhibition onto parvalbumin-positive interneurons. *Proc Natl Acad Sci U S A, 106*(9), 3561-3566. doi:10.1073/pnas.0813176106

Ylinen, A., Bragin, A., Nadasdy, Z., Jando, G., Szabo, I., Sik, A., & Buzsaki, G. (1995). Sharp wave-associated high-frequency oscillation (200 Hz) in the intact hippocampus: network and intracellular mechanisms. *J Neurosci, 15*(1 Pt 1), 30-46.

Yoon, K. W., Covey, D. F., & Rothman, S. M. (1993). Multiple mechanisms of picrotoxin block of GABA-induced currents in rat hippocampal neurons. *J Physiol, 464*, 423-439. doi:10.1113/jphysiol.1993.sp019643

Zhang, X. B., Sun, G. C., Liu, L. Y., Yu, F., & Xu, T. L. (2008). Alpha2 subunit specificity of cyclothiazide inhibition on glycine receptors. *Mol Pharmacol, 73*(4), 1195-1202. doi:10.1124/mol.107.042655

Zhang, Y., Llinas, R. R., & Lisman, J. E. (2009). Inhibition of NMDARs in the Nucleus Reticularis of the Thalamus Produces Delta Frequency Bursting. *Front Neural Circuits, 3*, 20. doi:10.3389/neuro.04.020.2009

Zhou, J. L., Zhao, Q., & Holmes, G. L. (2007). Effect of levetiracetam on visual-spatial memory following status epilepticus. *Epilepsy Res, 73*(1), 65-74. doi:10.1016/j.eplepsyres.2006.08.007

Zimcikova, E., Simko, J., Karesova, I., Kremlacek, J., & Malakova, J. (2017). Behavioral effects of antiepileptic drugs in rats: Are the effects on mood and

behavior detectable in open-field test? *Seizure, 52*, 35-40. doi:10.1016/j.seizure.2017.09.015

Zona, C., Niespodziany, I., Marchetti, C., Klitgaard, H., Bernardi, G., & Margineanu, D. G. (2001). Levetiracetam does not modulate neuronal voltage-gated Na+ and T-type Ca2+ currents. *Seizure, 10*(4), 279-286. doi:10.1053/seiz.2000.0504

Appendix 1: Published Work

Peer Reviewed

Gwilt, M., Bauer, M., & Bast, T. (2020). Frequency-and state-dependent effects of hippocampal neural disinhibition on hippocampal local field potential oscillations in anesthetized rats. *Hippocampus*.

Published Poster Abstracts

FENS Forum 2020: Can levetiracetam ameliorate neurocognitive effects of hippocampal disinhibition? In vivo electrophysiological and behavioural studies *Miriam Gwilt, Adam Seaton, Stuart Williams, Marie Pezze, Charlie Taylor, Joanna Loayza, Boris Ferger, Tobias Bast*

BNA 2019 Festival of Neuroscience: Three distinct hippocampal LFP states in anaesthetised rats: state-dependent LFP changes caused by hippocampal neural disinhibition *Miriam Gwilt, Markus Bauer, Tobias Bast*

FENS Forum 2018: Frequency- and state- specific effects of hippocampal neural disinhibition on local LFP oscillations in anaesthetised rats *Miriam Gwilt, Markus Bauer, Tobias Bast*

Appendix 2: Additional Work

BNA 2017 Abstracts

Poster number: P-W100

Theme: Learning & memory

A role for the nucleus accumbens in the hippocampal learning-behaviour translation?

Authors: *Adam Seaton, Rebecca Hock, Charles Greenspon, Miriam Gwilt, Robert Mason, Tobias Bast*

The role of the hippocampus in important types of rapid everyday learning, such as place learning, is well established. However, the mechanisms via which rapidly-acquired place memory may be translated into behaviour are yet to be determined. The intermediate hippocampus, which has been shown to be critical for the hippocampal learning-behaviour translation, combines neural substrates of accurate place encoding with links to prefrontal and subcortical behavioural control sites. This supports that these sites, including the nucleus accumbens (NAc), may be critical for this translation (Bast et al., 2009, PLoS Biol; Bast, 2011, Curr Opin Neurobiol). The NAc is a main candidate due to strong hippocampo-NAc projections that have been implicated in behaviour based on place memory (van der Meer et al., 2014, In: Space, Time and Memory in the Hippocampal Formation, ed. Derdikman & Knierim). To examine the role of the NAc in the hippocampal learning-behaviour translation, we combined functional inhibition of the NAc (via microinfusion of the GABA agonist muscimol) with measurements of behavioural performance based on hippocampusdependent rapid place learning using the watermaze delayed-matching-to-place test (DMTP) (Bast et al., 2009). In preparation for these studies, we conducted in vivo electrophysiological and sensorimotor experiments (locomotor activity, LMA and startle response/prepulse inhibition, PPI) to establish suitable muscimol doses to reduce NAc neuronal activity without causing gross sensorimotor side effects. Muscimol infusions into the NAc (125-250 ng/0.5 µl/side) reduced neuronal firing in the infusion site vicinity by 40-50% and, if at all, only moderately reduced LMA and PPI; the latter is consistent with findings that these sensorimotor

functions mainly depend on the NAc core (Pothuizen et al., 2005, Neuropsychopharmacology), whereas our infusions targeted the NAc shell, which is the main recipient of hippocampo-NAc projections (Humphreys & Preston, 2010, Prog Neurobiol). Preliminary findings from our studies combining functional inhibition of the NAc with DMTP testing support that the NAc is required for performance based on hippocampus-dependent rapid place learning. Additional experiments to confirm and extend these findings are on the way.

FENS 2018 abstracts

Poster number: F106

Theme: Animal studies: Pharmacology of learning and memory - part I

A role for the nucleus accumbens in the hippocampal learning-behaviour translation

Adam Seaton1, Rebecca Hock1, Miriam Gwilt1, Stuart Williams1, Charles Greenspon2, Robert Mason2, Tobias Bast1

1University of Nottingham, Psychology, Nottingham, United Kingdom

2University of Nottingham, Life Sciences, Nottingham, United Kingdom

The hippocampus is required for important types of rapid everyday learning, including place learning. However, the pathways via which hippocampal place learning is translated into behaviour remain to be determined. The intermediate hippocampus is critical for the hippocampal learning-behaviour translation and combines neural substrates of accurate place encoding with links to prefrontal and subcortical behavioural control sites, which may contribute to this translation(Bast et al.,2009,PLoSBiol; Bast,2011,CurrOpinNeurobiol). The nucleus accumbens (NAc) is a main candidate due to strong hippocampo-NAc projections that have been implicated in behaviour based on place memory (Humphries & Prescott, 2010, Prog Neurobiol). To examine the role of the NAc, we combined functional inhibition (via microinfusion of the GABA agonist muscimol) with measurements of behavioural performance based on hippocampus-dependent rapid place learning using the watermaze delayed-matching-to-place (DMP) test (Bast et al., 2009). Electrophysiological and

sensorimotor experiments (locomotor activity, startle response/prepulse inhibition) showed that muscimol (125-250ng/0.5 µl/side) reduced NAc neuron firing around the infusion site by about 50% and caused, if at all, only moderate sensorimotor effects. Watermaze Experiment 1, testing the impact of NAc muscimol within-subjects, supported that the NAc is required for DMP performance; however, there appeared to be a carry-over effect, with NAc muscimol eroding the typical DMP search strategy on subsequent test days, possibly reflecting that NAc is required to reinforce the strategy. Watermaze Experiment 2, using a between-subjects design, confirmed that NAc muscimol impairs expression of hippocampus-dependent rapid place learning on the DMP test. Overall, these findings support that the NAc contributes to the hippocampal learning-behaviour translation.

Poster number: P105

Theme: Animal studies: Pharmacology of learning and memory - part I

Too little and too much: impact of functional inhibition and disinhibition of the medial prefrontal cortex on cognitive flexibility assessed using an operant strategy-shifting task

Rebecca Hock1, Adam Seaton1, Stuart Williams1, Miriam Gwilt1, Stan Floresco2, Paula Moran1, Tobias Bast1

1University of Nottingham UK, School of Psychology, Nottingham, United Kingdom

2University of British Columbia, Department of Psychology, Vancouver, Canada

Attentional performance requires balanced medial prefrontal cortex (mPFC) activity, with functional inhibition or disinhibition (by micro-infusion of GABA agonist muscimol or antagonist picrotoxin, respectively) causing impairments (Pezze et al., 2014, J Neurosci). Cognitive flexibility has also been suggested to require balanced mPFC activity (Brady & Floresco, 2016, JoVE). To confirm this, we examined how mPFC muscimol and picrotoxin affect cognitive flexibility in Lister-hooded rats, using an operant strategy-shifting task involving shifts from egocentric-spatial to cue light-based responses or vice versa (Brady&Floresco,2016). Remarkably, Lister-hooded rats (irrespective of infusion) required three times as many trials compared to previous

studies in other strains to shift from egocentric to cue light-based responses (Brady & Floresco, 2016). These slow shifts were unaffected by the prefrontal manipulations. However, disinhibition, but not inhibition, impaired egocentric-response expression and increased trial omissions, showing that regional neural disinhibition can disrupt functions not normally requiring the disinhibited region (Bast et al., 2017, BrJPharmacol). Additional behavioural studies showed that although Lister-hooded rats struggled to shift from egocentric to cue-based responses, they readily acquired cue-based responses when they had not first been trained the egocentric strategy. Moreover, they then readily shifted from cue-based to egocentric strategy, and could perform egocentric-response reversals. However, there was always a higher shift-cost for egocentric-to-cue than for cue-to-egocentric shifting. Overall, although Lister hooded rats readily acquired both strategies, they overcame the egocentric strategy very slowly, and this slow strategy change was not mPFC dependent. Contrastingly, rats readily performed cue-to-egocentric-strategy shifts; we are currently examining the impact of mPFC functional inhibition and disinhibition on such flexible shifts.

BNA 2019 abstracts

Poster number: PM028

Theme: Learning and memory

Too little and too much: impact of functional inhibition and disinhibition of the medial prefrontal cortex on behavioural flexibility assessed using an operant strategy-shifting task

Rebecca Hock1, Stuart Williams1, Miriam Gwilt1, Mr Adam Seaton1, Sara Gonçalves2, Stan B. Floresco3, Paula M. Moran1, Tobias Bast1

1School of Psychology, The University Of Nottingham, Nottingham, United Kingdom, 2School of Life Sciences, The University Of Nottingham, Nottingham, United Kingdom, 3Department of Psychology, University of British Columbia, Vancouver, Canada

Attentional performance requires balanced medial prefrontal cortex (mPFC) activity, with functional inhibition or disinhibition by micro-infusion of the GABA agonist

muscimol or antagonist picrotoxin, respectively, causing impairments (Pezze etal.,2014,JNeurosci). Aspects of behavioural flexibility, linked to the mPFC and local GABA transmission (Brady&Floresco,2016,JoVE), may also require balanced mPFC activity. We examined how mPFC muscimol (62.5ng/side) and picrotoxin (300ng/side), as compared to saline control infusions, affect behavioural flexibility in male Lister Hooded rats, using an operant strategy-shifting task. The task involved 'shifts' (across three sessions) from a spatial-response condition, where food reward was associated with left or right lever responses, to a cue light-based response condition, where food reward was associated with panel light illumination, or vice versa (Brady&Floresco,2016)(see Figure). Trials to criterion and percentage of correct responses, omissions and errors (perseverative or never reinforced) were analysed by ANOVA using infusion group as between-subjects factor and, if appropriate, shift session as within-subjects factor. Fisher's LSD test was used for post-hoc comparisons. Remarkably, irrespective of infusion, to shift from spatial-response to cue light-based responses, Lister hooded rats required three times as many trials as reported in previous studies in other strains (e.g. Brady&Floresco,2016). These slow shifts were not impaired by mPFC inhibition or disinhibition. However, in addition to increasing trial omissions, disinhibition impaired spatial-response expression and, during shifts, reduced perseveration of the spatial-response condition. Although Lister-Hooded rats struggled with spatial-response-to-cue-response shifts, they readily acquired cue-based responses when they had not first been trained in the spatial-response condition. Moreover, they then readily performed cue-to-spatial-response-strategy shifts. Interestingly, there was a strong trend for mPFC disinhibition to slow down the cue-to-spatial-response-shift, with picrotoxin infused rats showing a lower percentage of correct responses than saline-infused rats during shift session 2. In conclusion, although Lister hooded rats readily acquired both spatial-response and cue strategies they were slow to shift from the spatial-response strategy. This was unaffected by mPFC inhibition or disinhibition. In contrast, they readily performed a cue-to-spatial-response-strategy shift, and prefrontal functional disinhibition, but not inhibition, tended to disrupt this shift.

Poster number: PS045

Theme: Learning and memory

A role for the nucleus accumbens in the hippocampal learning-behaviour translation

Adam Seaton1, Miriam Gwilt1, Rebecca Hock1, Stuart Williams1, Charles Greenspon1, Rob Mason1, Tobias Bast1

1University of Nottingham, Nottingham, United Kingdom

The hippocampus is required for rapid place learning, but the pathways via which hippocampal place learning is translated into behaviour remain to be determined. The intermediate hippocampus is critical for the hippocampal learning-behaviour translation and combines neural substrates of accurate place encoding with links to prefrontal and subcortical behavioural control sites, which may contribute to this translation (Bast et al.,2009,PLoSBiol; Bast,2011,CurrOpinNeurobiol). The nucleus accumbens (NAc) is a main candidate due to strong hippocampo-NAc projections that have been implicated in behaviour based on place memory (Humphries&Prescott,2010,ProgNeurobiol). We combined NAc functional inhibition in Lister Hooded rats by microinfusion of the GABA agonist muscimol with in vivo electrophysiological measurements around the infusion site to verify neural effects and with locomotor and startle/prepulse-inhibition (PPI) assays to rule out gross sensorimotor impairments (adapting methods from Pezze et al.,2014,JNeurosc). We then tested the impact of NAc muscimol on behavioural performance based on hippocampus-dependent 1-trial place learning using the watermaze delayed-matching-to-place (DMP) test (Bast et al.,2009), with muscimol infused between trial 1 (learning) and 2 (expression of memory). ANOVA was used whenever the independent variable had more than two levels or to analyse the impact of multiple independent variables. Muscimol (125-250ng/0.5 µl/side) dose-dependently reduced NAc neuronal firing around the infusion site by 30-50% and caused moderate sensorimotor effects. Interestingly, NAc muscimol impaired between-session locomotor habituation. With habituation memory linked to the hippocampus (Fanselow,2000,BehavBrainRes), this is consistent with the idea that NAc is important

for hippocampal memory expression. Our first watermaze experiment, testing the impact of NAc muscimol within-subjects, indicated that the NAc is required for DMP performance. However, there appeared to be a carry-over effect: after repeated testing with muscimol, rats failed to show the typical DMP search strategy (persistent searching in correct location) even on drug-free test days, possibly reflecting that NAc is required to reinforce the strategy. A second watermaze DMP experiment, using a between-subjects design to avoid carry-over effects, confirmed that NAc muscimol impairs expression of hippocampus-dependent rapid place learning. Overall, these findings support that the NAc contributes to translation of rapidly-acquired place memory into behaviour.

Poster number: PM004 (SP)

Theme: Attention, motivation, behaviour

Impact of hippocampal neural disinhibition on latent inhibition in a conditioned emotional response procedure

Authors: *Mr Stuart Williams1 , Ms Miriam Gwilt1 , Ms Rebecca Hock1 , Dr Carl Stevenson2 , Professor Helen Cassaday1 , Dr Tobias Bast1 1School of Psychology, University of Nottingham, Nottingham, United Kingdom, 2School of Biosciences, University of Nottingham, Nottingham, United Kingdom*

Introduction: Hippocampal neural disinhibition, i.e. reduced GABAergic inhibition, is a key feature of schizophrenia pathophysiology (Heckers & Konradi,2015, SchizophrRes). The hippocampus is a crucial component of the fear circuit and positively modulates striatal dopamine (Bast et al, 2011, CurrOpinNeurobiol), which plays a significant role in salience modulation (Kapur, 2003, Am J Psychiatry). Therefore, we examined the contribution of hippocampal neural disinhibition to impairments in fear conditioning and salience modulation associated with schizophrenia (Jensen et al, 2008, Neuropsychopharmacology).

Methods: We examined the effect of ventral hippocampal disinhibition by picrotoxin (GABA-A antagonist) infusion (150ng/side) (McGarrity et al, 2017, Cereb Cortex) on latent inhibition (LI) of fear conditioning, using a conditioned emotional response

paradigm (Nelson et al,2011,Jpsychopharm). Rats received light (CS)-foot shock (US) pairings. Conditioned suppression of the lick response was used as a measure of conditioned fear. Reduced conditioned suppression in rats pre-exposed (PE) to the CS, compared to non-pre-exposed (NPE) rats was used as measure of LI. Picrotoxin or saline was infused prior to both pre-exposure and conditioning. Analysis: Conditioning to the CS was measured using latency to make 50 licks without CS (A) and time taken to complete 50 licks following CS onset (B) to calculate a suppression ratio (A/(A+B). Data was analysed by ANOVA with infusion group and pre-exposure as between-subject factors.

Results and conclusions: In contrast to saline-infused rats, rats that received hippocampal picrotoxin did not express LI, while picrotoxin rats in the PE and NPE groups showing comparable conditioned suppression (Fig.1, left). Abolished LI in picrotoxin-infused animals is explained by reduced conditioned suppression in the NPE group as compared to saline-infused rats, indicating reduced fear conditioning to the light CS. Hippocampal picrotoxin also reduced contextual fear conditioning, indicated by reduced latency to lick compared to the saline group during reexposure to the context after conditioning (Fig.1, right). Overall, rats with ventral hippocampal disinhibition did not express LI, showing similar levels of conditioning regardless of CS pre-exposure. However, this mainly reflected that hippocampal disinhibition impaired fear conditioning to the CS, resembling the reduced aversive cue conditioning in patients with schizophrenia (Jensen et al, 2008), as well as the impaired contextual fear conditioning seen in the present study.

FENS 2020 abstracts

Poster number: 1461

Theme: Animal learning and memory

Too little and too much: impact of functional inhibition and disinhibition of the medial prefrontal cortex on an operant strategy-shifting task of behavioural flexibility

Rebecca Hock1, Miriam Gwilt1, Adam Seaton1, Stuart Williams1, Sara Gonçalves2, Silvia Maggi1, Stan B. Floresco3, Paula M. Moran1, Tobias Bast1

1School of Psychology, University of Nottingham, 2School of Life Sciences, University of Nottingham, 3Department of Psychology, University of British Columbia

Attentional performance requires balanced medial prefrontal cortex (mPFC) activity, with both functional inhibition or disinhibition (by micro-infusion of GABA agonist muscimol or antagonist picrotoxin) causing impairments (Pezze *etal.,*2014,*JNeurosci*). Does this finding extend to behavioural flexibility? We examined effects of mPFC muscimol (62.5ng/side) and picrotoxin (300ng/side), as compared to saline-control infusions, on behavioural flexibility in male Lister-hooded rats, using a food-reinforced operant (lever-press) strategy-shifting task (Brady&Floresco,2016,*JoVE*). The task involved 'shifts' (across three sessions) from a spatial (left/right) response to a cue-light-based response, or vice versa. Irrespective of infusion, shifting from spatial to cue responses required three times as many trials as reported in studies using other rat strains (e.g., Brady&Floresco,2016). These slow shifts were unaffected by mPFC-manipulations. However, mPFC-disinhibition increased trial omissions and impaired spatial-response expression.

However, Lister-hooded rats readily acquired cue responses when they had not first been trained to perform spatial responses; then, they readily shifted from the cue to the spatial response. mPFC disinhibition tended to slow this shift, reducing the percentage of correct responses during shift session 2. If mPFC was disinhibited both during initial-rule acquisition and shift-sessions, this also increased perseveration during shifting. In Lister-hooded rats, prefrontal disinhibition impaired aspects of behavioural flexibility, slowing shifting from cue to spatial responses. Rats were slow to shift from spatial to cue responses, which was unaffected by mPFC inhibition or disinhibition. A Bayesian, trial-by-trial analysis of response strategies is ongoing, which may reveal additional, more subtle, effects of prefrontal manipulations on behavioural flexibility.